INCORPORATION OF PAVEMENT PRESERVATION TREATMENTS IN AASHTOWARE PAVEMENT-ME ANALYSIS AND DESIGN

Final Project Report

By

Muhammad Munum Masud
Syed Waqar Haider
Karim Chatti
Michigan State University

Sponsorship
Center for Highway Pavement Preservation
(CHPP)

For

Center for Highway Pavement Preservation
(CHPP)

In cooperation with US Department of Transportation-Research and Innovative Technology Administration (RITA)

August 2018

Disclaimer

The contents of this report reflect the views of the authors, who are responsible for the facts and the accuracy of the information presented herein. This document is disseminated under the sponsorship of the U.S. Department of Transportation's University Transportation Centers Program, in the interest of information exchange. The Center for Highway Pavement Preservation (CHPP), the U.S. Government and matching sponsor assume no liability for the contents or use thereof.

1. Report No. CHPP Report-MSU#5-2018	2. Government Accession No. N/A	3. Recipient's Catalog No. If applicable
4. Title and Subtitle Incorporation Of Pavement Preservation Treatments in AASHTOWare Pavement-ME Analysis And Design		5. Report Date August 2018
		6. Performing Organization Code N/A
7. Author(s) Muhammad Munum Masud, Syed Waqar Haider, and Karim Chatti		8. Performing Organization Report No. N/A
9. Performing Organization Name and Address Michigan State University Contract & Grant Administration 426 Auditorium Road Room 2 Hannah Administration East Lansing, MI 48824		10. Work Unit No. N/A
		11. Contract or Grant No. ----------
12. Sponsoring Agency Name and Address Center of Highway Pavement Preservation (CHPP) Michigan State University 428 S. Shaw Lane 3562 Engineering Building East Lansing, Michigan 48824		13. Type of Report and Period Covered Final Report, 8/31/2017 to 8/28/2018
		14. Sponsoring Agency Code N/A
15. Supplementary Notes Report uploaded at http:/www.chpp.egr.msu.edu/		

16. Abstract

Moisture increase in pavement subsurface layers has a significant influence on granular material properties that affect the expected pavement performance. In-situ moisture variations in unbound base layer over time significantly depend on water infiltration after precipitation and pavement surface conditions. Consequently, base resilient modulus (MR) is decreased considerably, which leads to premature failure and reduced service life. This study presents Long-term Pavement Performance (LTPP) data analyses for quantifying the effect of moisture infiltration through surface discontinuities (cracks and joint openings) on flexible and rigid pavement performance. Subsurface moisture data obtained through Seasonal Monitoring Program (SMP) time domain reflectometry (TDR) are an excellent source to quantify the moisture-related damage in flexible and rigid pavements located in different climates. The artificial neural network (ANN) models were developed using SMP data for flexible and rigid pavement sections. The results show that higher levels of cracking and joint openings will lead to an increase moisture levels within base layer. Also, the moisture content increases with higher percentage passing # 200 sieve (P200), and higher precipitation levels, especially in wet climates. The MR of the base decreases significantly with an increase in moisture levels. For flexible pavements, the maximum reduction in base MR ranged between 18 to 41% and 153 to 175% for the pavement sections located in dry and wet regions, respectively. In rigid pavements, the maximum reduction in base MR may vary from 10% to 125% for the pavement sections located in dry and wet regions, respectively. The major reasons for higher base moisture variations in wet climates are higher levels of surface cracking and precipitation. The base moisture values do not vary significantly in dryer climates since the amount of precipitation and observed cracking levels were low in these regions. Due to increased moisture and a corresponding reduction in base MR values, the performance of pavement sections located in wet climates is adversely affected. The findings imply that an adequate and timely preservation treatment such as a crack sealing can enhance the pavements service life significantly, especially in wet climates. The results suggest that cracks should be sealed when the extent of fatigue cracking is within 6% and 11% for the flexible pavement sections located in wet and dry climates, respectively. In rigid pavements, the joints should be resealed when the damaged joint sealant length exceeds 150 to 250 feet.

17. Key Words AASHTOWare Pavement-ME, subsurface moisture, artificial neural network, pavement analysis and design	18. Distribution Statement No restrictions. This document is also available to the public through the Michigan Department of Transportation.

19. Security Classification. (of this report) Unclassified	20. Security Classification (of this page) Unclassified	21. No. of Pages 89	22. Price N/A

Form DOT F 1700.7 (8-72) Reproduction of completed page authorized

Table of Contents

LIST OF TABLES

LIST OF FIGURES

CHAPTER 1 INTRODUCTION

1.1 BACKGROUND

The United States highway system is steadily deteriorating and allocating more resources to rebuild new roadways may not be a practical and cost-effective solution. The Nation's highway system is the single largest public investment in history having an estimated initial cost of $3 trillion spread over many years (*1*). Today, the replacement cost could not readily be incurred without severe economic consequences. Therefore, one of the most significant challenges for researchers and engineers is how to minimize life-cycle cost and ensure sound asset management.

Delaying maintenance and repairs until major rehabilitation or replacement is necessary lead to extensive and disruptive work that increases the potential for accidents, injuries, and fatalities among motorists and road workers. An alternative to this scenario is sound planning and implementation of highway preservation practices, which would assure structural integrity and safety of pavement assets. Currently, pavement preservation is an increasingly widespread practice among highway agencies interested in extending the lives of their pavements cost-effectively. One major impediment to widespread implementation of preserving the pavement infrastructure by transportation agencies is lack of knowledge on how to select preservation actions and when and where to apply them to get the most benefit at the least cost. In other words, how to use the right preservation action at the right time to the right pavement (*2-4*). Highway agencies have learned from the practices that if applied at an appropriate time, pavement preservation provides a means for maintaining and improving the functional condition and slowing deterioration of an existing highway system. While pavement preservation is not expected to substantially increase the structural capacity of the existing pavement, it generally leads to improved pavement performance and longer service life. However, still, there are challenges to the success of such practices. These challenges include: (a) identifying good candidate pavements, (b) selecting the best preservation treatments for those pavements, (c) choosing the appropriate treatment application timing, and (d) considering preservation treatments in pavement analysis and design stage. This research specifically addresses the last two challenges, i.e., selection of optimum crack sealing application timings by incorporating preservation treatments in the mechanistic-empirical (ME) pavement analysis and design approach.

The AASHTOWare Mechanistic-Empirical Pavement Design Guide (Pavement-ME) software provide methodologies for the analysis and design of flexible and rigid pavements. However, these methodologies and related performance prediction models focus on new structural design and rehabilitation of existing pavements and do not explicitly consider the contributions of pavement preservation treatments to the overall pavement performance. Thus, research is needed to identify approaches for considering the effects of preservation on pavement performance and developing procedures that facilitate incorporation of pavement preservation treatments in the Pavement-ME analysis process. Such procedures will ensure that the contributions of preservation treatments to expected performance and service life are appropriately considered in the analysis and design processes.

One of the most influential factors affecting pavement performance is the moisture within the pavement system. The infiltration of water from road surface followed by a rainfall event can be

a significant cause of premature pavement deterioration (*5, 6*). The moisture content of the materials near the pavement edges and in the proximity of surface cracks usually shows higher variations due to rainfall events (*7*). Water infiltration through cracks and joints is particularly important in the estimation of sublayer moisture content and its effect on the resilient modulus (MR) (*8, 9*). Accurate predictions of moisture variations can assist in the better estimation of unbound layers MR.

1.2 RESEARCH OBJECTIVES

The main objectives of this study are to (a) (a) evaluate the effect of surface cracking on the aggregate base moisture changes due to infiltration, (b) quantify the impact of moisture change on aggregate base moduli, (c) evaluate the effect of base layer moduli on the predicted long-term pavement performance, and (d) develop guidance for optimum timings of crack sealing for different climates. These objectives were achieved by analyzing the subsurface moisture variations and flexible and rigid pavement performance data in the SMP pavement sections.

1.3 POTENTIAL BENEFITS OF THE STUDY

The results of this research effort will improve and facilitate the implementation of preservation practices in the following manner:

- There are no widely accepted guidelines for incorporating pavement preservation treatment in pavement analysis and design process, mainly because of different practices and experiences in different regions. This research will provide guidelines to facilitate estimation of timing for a pavement preservation treatment at the design stage. The research will also provide examples for different States to demonstrate how to apply the developed guidelines for estimating treatment timings to improve its effectiveness in extending the life of an existing pavement. This will help State Highway Agencies (SHAs) to incorporate preservation treatment practices at the design stage.
- The recommendations developed from this research will be practically-oriented for investment decision making on the highway infrastructure. The recommendations will be specifically designed for application.
- The analysis results from this research can maximize the benefits (both short-term and long-term) accrued from the large investment made in the construction and monitoring of the highway network.

1.4 RESEARCH APPROACH

The following tasks were identified as a general framework for completion of this research:

1. Literature review.
2. Evaluation of infiltration and moisture models.
3. Availability of performance, climatic, and subsurface moisture content data.
4. Analyze subsurface moisture and performance data.
5. Establish impact of moisture change on unbound layers MR.
6. Develop guidelines for incorporating the preservation treatments in the Pavement-ME design process.
7. Demonstrative Examples.

1.5 OUTLINE OF THE REPORT

This thesis contains five (5) chapters. Chapter 1 outlines the problem statement, research objectives, potential benefits, and briefly describes various tasks performed in the study. Chapter 2 documents the thorough literature review, which include sources of water infiltration into pavements, the impact of moisture on pavement performance, mitigation of moisture related damage, and summary of moisture prediction models. The work in this chapter corresponds to Tasks 1 and 2. Chapter 3 describes the SMP LTPP database with a special focus on SMP background. This chapter also discusses the type, extents, and sources of various data types used in this study. The summary of available LTPP SMP sites considered for analysis also presented. The work in this chapter corresponds to Tasks 3. Chapter 4 covers the details of data analysis on flexible and rigid SMP pavement sections, development of moisture content prediction models using Artificial Neural Network (ANN), the impact of moisture on unbound layer stiffness and long-term pavement performance. Last part of this chapter covers pavement preservation guidelines with examples using the Pavement-ME. The work in this chapter corresponds to Task 4 to 7. Chapter 5 documents the conclusions and recommendations based on the analysis.

CHAPTER 2 LITERATURE REVIEW

2.1 SOURCES OF WATER INFILTRATION INTO PAVEMENT LAYERS

Water can enter the pavement-unbound layers through many sources and subsequently affects the in-situ moisture in these materials. The primary sources of moisture variation within a pavement system include external elements such as precipitation, temperature, and the groundwater table. Pavement surface conditions (cracking/discontinuities), drainage, shoulders, edges and pavement cross-section can also facilitate the moisture infiltration (*10*). Figure 2-1 shows the schematic of water ingress sources.

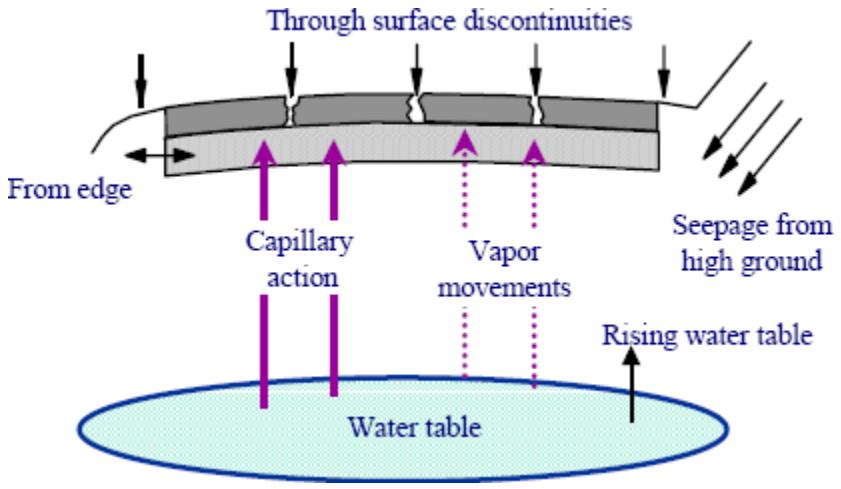

Figure 2-1 Sources of moisture variations in pavement systems (*11*)

2.2 IMPACT OF MOISTURE ON PAVEMENT PERFORMANCE

One of the most influential factors affecting pavement performance is the moisture within the pavement system. As early as 1820, John MacAdam noted that regardless of the strength (thickness) of the pavement structure, many roads in Great Britain prematurely deteriorated due to saturation of pavement subgrade (*12*). Moisture damage in pavements manifests itself in the form of moisture caused, and moisture accelerated distresses. Moisture caused distresses are essentially induced by moisture, such as asphalt stripping in flexible pavements and durability cracking in rigid pavements. Moisture accelerated distresses are those caused by other factors (like traffic loading), but get accelerated with an increase in moisture (*13*).
Many properties of unsaturated soils such as stiffness, permeability and volume vary significantly with change in moisture content. The increase in moisture content affects the durability and stiffness of soils; consequently, the ability of subgrade to support the upper pavement structure (*14, 15*). Variation in moisture content in field conditions depends on the climate of a location and can be difficult to interpret (*16, 17*). It is also known that unsaturated granular material (UGM) exhibits moisture-sensitive and stress-dependent nonlinear behavior in flexible pavements. The in-situ moisture content of unbound pavement materials is significantly affected by weather, groundwater table fluctuations, drainage conditions, soil properties and

pavement surface conditions. It is a well-established fact that with an increase in UGM degree of saturation, the resilient modulus (MR) decreases considerably (*18, 19*).
While investigating the pavement response to the varying levels of moisture, Salour and Erlingsson concluded that increase in moisture content of UGM considerably reduces the back-calculated modulus of base layers (*20*). Various field monitoring studies suggest that change in moisture content can occur after rainfall and it can increase up to 50% in addition to the natural seasonal variation (*21, 22*). This potential increase in moisture content is often neglected while estimating moisture variation in pavement unbound layers. However, such changes in moisture along with axle loads can accelerate pavement deterioration. Therefore, it is essential to develop a moisture prediction model that can capture both seasonal and temporal moistures changes accurately and later incorporate results in the life cycle assessment of infrastructures (*16, 23*).
The infiltration of water from road surface followed by a rainfall event can be a significant cause of premature pavement deterioration (*5, 6*). It was also revealed in the past research that moisture conditions are relatively stable at the bottom of the pavement system. However, depending on climatic events, the moisture condition in the upper pavement section can vary between very dry and fully saturated conditions. The moisture content of the materials near the pavement edges and in the proximity of surface cracks usually shows higher variations due to rainfall events (*7*). Considering water infiltration through cracks and joints is particularly important in the estimation of sublayer moisture content and its effect on the resilient modulus (MR) (*8, 9*). Accurate prediction of moisture content can assist in the better estimation of pavement unbound layers MR. Water movement within pavement system and affiliated moisture change is a complex phenomenon. Problems triggered by prolonged exposure to excess moisture fall into three main categories (*13*):

- Softening of pavement unbound layers as they become saturated and remain saturated for a considerable time.
- Material degradation from interaction with moisture.
- Loss of bonds between pavement layers from saturation with moisture.

2.3 MITIGATION OF MOISTURE RELATED DAMAGE

Despite considerable research in recent years on moisture-related damage in the pavements, there are still several gaps in knowledge and practice. Pavement researchers are still to reach a consensus, whether to design the roads as permeable, impermeable, or combination of the two. One of the primary concern at the pavement design stage is to protect the base, subbase, and subgrade layers from becoming saturated or even being exposed to prolonged high moisture conditions over time. Many pavement engineers would also add hot-mixed asphalt (HMA) and Portland cement concrete (PCC) to this list because excessive moisture coupled with freezing has badly impacted properties of these materials (*13*). Four widely accepted approaches to mitigate moisture damage are listed below:

- Prevent moisture from entering the pavement structure.
- Use of less moisture susceptible materials.
- Incorporate design features to minimize moisture damage.
- Through effective drainage quickly remove moisture that enters the pavement structure.

Many highway agencies use the Pavement-ME for designing and rehabilitating pavements and evaluating their maintenance options. Pavement-ME estimates infiltration through cracks and joints for incorporating the permeable base, separator, and edge-drain design in the design

process. It does not consider the water infiltration in the modeling of moisture content within the pavement layers. Therefore, moisture and material properties of sublayers are not assumed to be affected by water infiltration through discontinuities present at the pavement surface. This study will evaluate the effect of infiltration due to cracks/joints on moisture content and resulting resilient modulus of the unbound materials in a pavement system. The Pavement-ME input material properties can be modified to capture the effect of infiltration on predicted performance. Such incorporation of infiltration in the pavement design process can assist highway agencies to adopt proactive pavement preservation practices.

2.4 EXISTING MOISTURE PREDICTION MODELS

Moisture determination within the pavements layers is a complex task, especially with the varying site and climatic conditions. Researchers have been working to determine field moisture content based on soil properties, field observations and flow theories. In the process of evolution many empirical and analytical solutions were developed to characterize the change in in-situ moisture content. These methods ranged from straightforward empirical equations to very complex computer-based programs (*14*). An integrated model was also developed to predict soil moisture content levels and movements within a pavement structure (*14, 24*). The reliability and application of empirically developed models are limited because most of these models are based on regression analysis with a high standard error. It was also observed by Organization of Economic Corporation and Development (OECD) that the model errors can be very high (i.e., percent of moisture content) (*15, 25*). On the other hand, the analytical solutions available in the literature are complex. Those are based on differential equations with boundary conditions and include variables like hydraulic conductivity, matric suction, porosity and water table depth. Consequently, application of such models is limited for routine use and analysis. Significant limitations of the available models are their universal or regional application and validation with the different site and environmental conditions. Furthermore, most of the available models do not include the effect of surface discontinuities, pavement structure, or temporal changes due to rainfall or subsurface temperature on the sublayer moisture variations. The past research shows that models were developed to measure the change in stiffness properties due to moisture variation. Only a few empirical and analytical models were available in the literature for unbound layers moisture content prediction. Thus, more research is needed for accurate estimation of unbound layers moisture variations due to surface infiltration.

2.4.1 Empirical Models

This section documents the details of empirical moisture prediction models found in the literature.

2.4.1.1 Swanberg and Hansen Model

In Minnesota, where the subgrades were primarily clayey silt soils with plastic limit varying from 15 to 30 and densities between 90 to 105 percent of the modified proctor maximum density, Swanberg, and Hansen (*26*) developed a model to measure the moisture content of highway subgrades using plastic limit. The authors also observed that measured moisture content was about 1 percent higher in spring than in summer. The mathematical form of the relationship is given below:

$$W = 1.16PL - 7.4 \quad (1)$$

where,

w = Moisture content
PL = Plastic limit

2.4.1.2 US Navy Model

US Navy (*15, 27*) developed a model which also relates moisture content with plastic limit. They considered 70 airport sites for investigation of sandy and clay subgrades where the groundwater table was greater than 24 inches below the surface and reached to the conclusion that subgrade moisture content exceeded the plastic limit by approximately 2 percent.

$$W \simeq \quad (2)$$

2.4.1.3 Kersten Model

While investigating subgrade moisture contents in the top 12 inches of subgrade soils below airports pavements in seven states, Kersten (*28*) concluded that water content for sand and clay soils in damp climates could vary between 80 to 120 percent of the plastic limit (PL) (*15*).

$$0.8PL < W < 1.2PL \quad (3)$$

It was also noted that typically clay equilibrium moisture content exceeds the PL, silts are equal to or just under the PL, and sandy soils are less than the PL. Thus, for many subgrade soils, the lower limit of predicted moisture content varies between optimum moisture content (OMC) and the PL and the upper limit between the PL and 100 percent degree of saturation.

2.4.1.4 Arkansas Highway and Transportation Department (AHTD) - Rao, S Moisture Content Prediction Equations

In a study at AHTD, prediction equations were developed to estimate subgrade in-situ moisture content for low-volume pavement design. Data of 18 different sites from 14 counties were collected from 1991 to 1993 (*14*). Data elements including general site information, soil series and profile information, moisture content at 9 different depths (starting from 18 to 90 inches), average monthly temperature and precipitation were obtained for the analysis. At two different depths, (30 and 90 inches) correlation analysis was developed between moisture content and precipitation, also between moisture content and average monthly temperature. Relatively low correlation coefficients were observed for both variables. Also for different sites great variation was observed in correlation coefficients at different depths (*14, 15*). The author observed that correlation of moisture content with precipitation was positive and with average monthly temperature was predominantly negative.

Average monthly precipitation and moisture content at varying depths were plotted as a function of time as shown in Figure 2-2, limited range of values were observed for moisture content at different sites and depths.

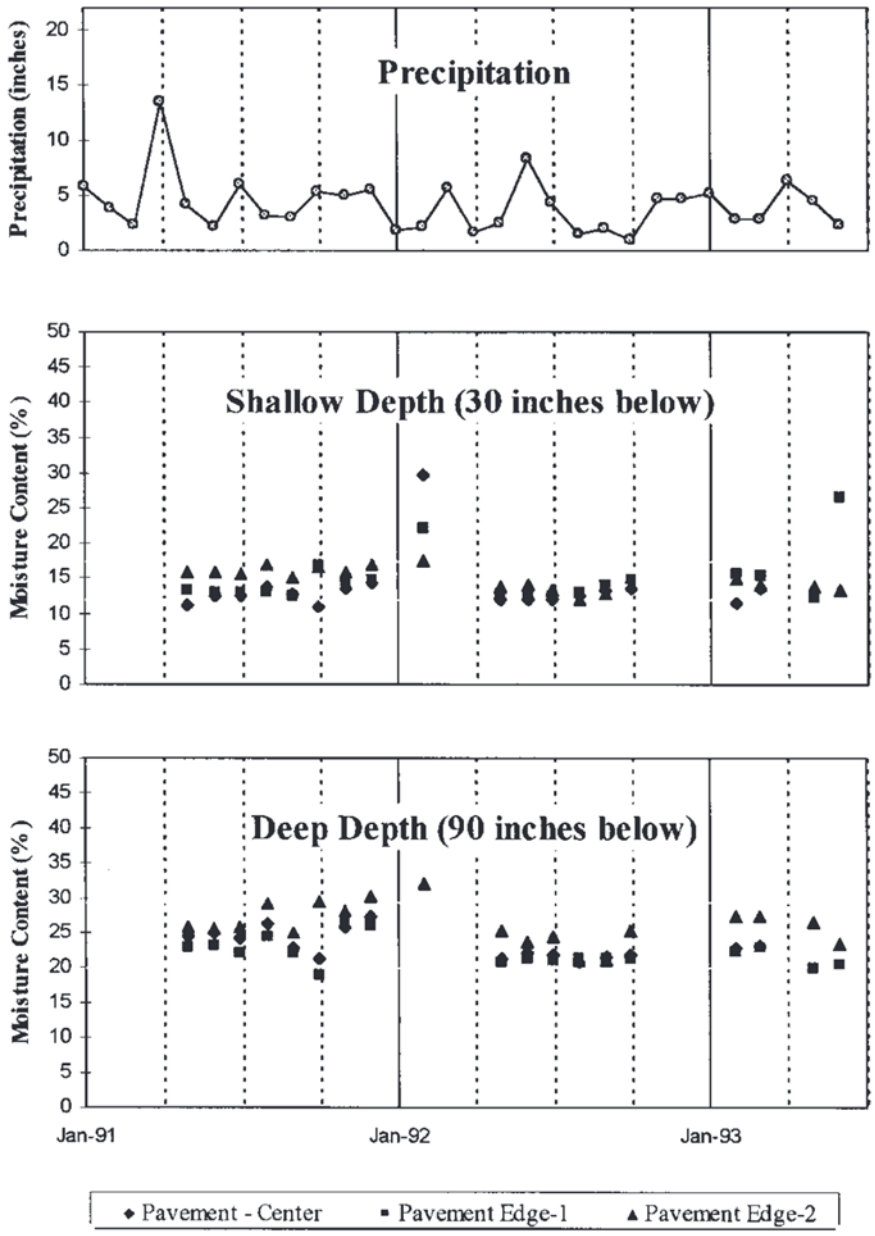

Figure 2-2 Subgrade moisture variations and precipitation for Arkansas Site 2 (*14*)

The author considered upper and lower values of moisture content as the upper and lower equilibrium values for moisture content in the subgrade. It was concluded that upper and lower limits of moisture content in subgrade depend on soil properties and vary with depth. However, temperature and precipitation had not much effect. Based on this observation, to estimate upper and lower equilibrium values for moisture content from soil properties, the following regression equations were developed: -

- For 18 inches below the pavement surface:

$$ELL = 2.86 + 0.174(P200_L)^{1.08} - 0.173(LL_U + 5)^{1.11} + 0.021(PI_L)^{2.12} - 0.089\left[Log(PERM_U)\right]^{-3} \quad (4)$$

$R^2 = 0.79$

$$EUL = 6.45 + 0.221(P200_L)^{1.08} - 0.174(LL_U + 5)^{1.11} + 0.024(PI_L)^{2.12} - 0.071\left[Log(PERM_U)\right]^{-3} \quad (5)$$

$R^2 = 0.80$

- For 30 inches below the pavement surface: -

$$EUL = -1.25 + 0.313(P200_{LA})^{1.08} - 0.292(LL_{UA} + 5)^{1.11} + 0.028(PI_{LA})^{2.13} - 0.075\left[Log(PERM_{UA})\right]^{-3} \quad (6)$$

$R^2 = 0.61$

$$EUL = 9.66 + 0.212(P200_{LA})^{1.08} - 0.118(LL_{UA} + 5)^{1.14} + 0.023(PI_{LA})^{2.13} - 0.059\left[Log(PERM_{UA})\right]^{-3} \quad (7)$$

$R^2 = 0.74$

where,

ELL	=	Equilibrium lower limit
EUL	=	Equilibrium upper limit
P_{200}	=	Percent passing No. 200 sieve
LL	=	Liquid limit
PI	=	Plasticity index
$PERM$	=	Permeability

The subscript L and U are used for upper and lower limits from the county soil reports, whereas subscript A indicates soil properties,12 inches above selected depth.

2.4.1.5 A Systems Approach for Estimating Field Moisture Content

Han, Petry, and Richardson (*29*) developed a system for estimation of moisture content. The system was equipped with five different models, including Swanberg and Hansen (*26*) , Kersten (*28*), US Navy (*27*), Arkansas Highway and Transportation Department moisture predictions equations (*15*), and volumetric moisture content estimation equations from the SMP (*29, 30*). The user is asked to input project site data and material characteristics, then it provides a range of estimated moisture contents with a guide to narrow down choice. Degree of saturation is also an output because few resilient modulus prediction equations use a degree of saturation instead of moisture content (*29*). System structure diagram is shown in Figure 2-3.

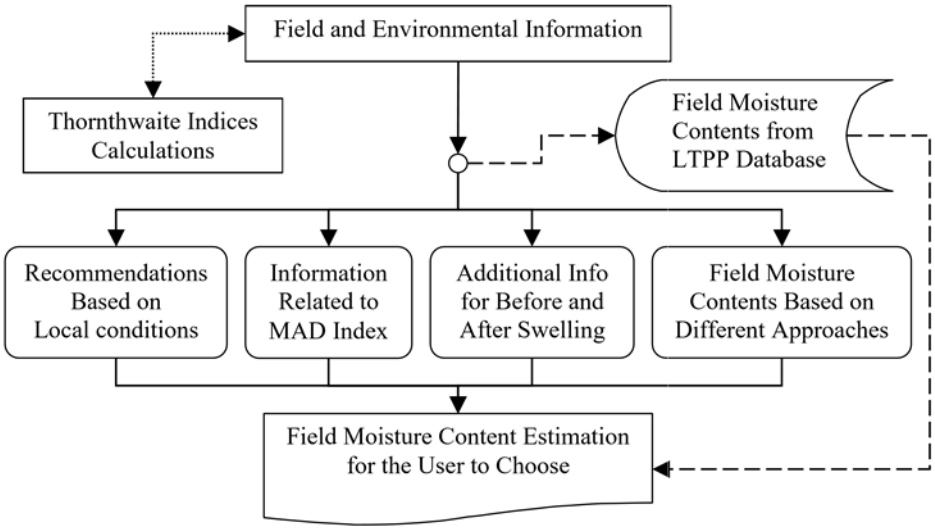

Figure 2-3 Field moisture estimation system diagram (*29*)

2.4.1.6 Hedayati and Hossain Data-Based Model

In North Texas, a study was conducted to estimate moisture variation in pavement subgrade soils due to seasonal and time-dependent changes in climate. A two-lane HMA road was selected for this study. Hourly moisture at varying depth (0 to 4.5 m) and precipitation data were collected over the period of two years. Based on the overall data analysis a model was developed. The model considered the effect of seasonal trends and temporary rainfall in predicting moisture content of different soil layers (*16*).

$$\theta = \theta_0 + \theta_a \sin(\omega t - \frac{z}{d} + C_0) + f(t, rainfall) \tag{8}$$

Where Θ is calculated using following equation: -

$$\theta = [0.39 + 0.053e^{-0.639z} \sin(0.0172t - 0.2z)] + [0.0134 + .00058Rain_t] \tag{9}$$

Finally, authors summarized above two equations using the following equation: -

$$\theta = 0.4104 + 0.053e^{-0.639z} \sin(0.0172t) + .00058Rain_t \tag{10}$$

where,

θ = Volumetric water content at depth z at any time t;

θ_0 = Average soil moisture at depth z over time

θ_a = The domain of moisture variation at any depth over time.Which can be determined as (*16, 31*) using equation 11.

θ_s = The surface volumetric water content

ω = Angular frequency (equal to $2\pi / 365 = 0.0172 day^{-1}$ for a perfect seasonal trend)

t	=	Time from an arbitrary starting point (day)
z	=	Depth(m)
d	=	Damping depth (described below)
C_o	=	Phase correction factor
$Rain_t$	=	Rainfall defined in time series (mm)

$$\theta_a = \theta_s.\exp(-\frac{z}{d}) \tag{11}$$

Damping depth reflects a reduction in soil moisture variation with depth and can be estimated as (*16*):

$$d = \sqrt{\frac{2D}{w}} \cong 4.8m \tag{12}$$

2.4.1.7 Fredlund And Xing Equation

Fredlund and Xing (*32*) proposed a model to calculate equilibrium moisture content based on soil suction, and soil index properties, such as Passing #200 (P_{200}), diameter (D_{60}), and plasticity index. This soil water characterization curve model is also used in Enhanced Integrated Climatic Model (EICM).

$$\theta = C(h)\times\left[\frac{\theta_{sat}}{\left[\ln\left[\exp(1)+\left(\frac{h}{a_f}\right)^{b_f}\right]\right]^{c_f}}\right] \tag{13}$$

$$C(h) = \left[1-\frac{\ln\left(1+\frac{h}{h\varepsilon}\right)}{\ln\left(1+\frac{1.45\times10^5}{h\varepsilon}\right)}\right] \tag{14}$$

where,

θ_w	=	Volumetric moisture content (%)
θ_{sat}	=	Saturated moisture content
a_f, b_f, c_f and h_ε	=	SWCC fitting parameters
θ_s	=	The surface volumetric water content
h	=	Equilibrium suction as defined in equation 15
y	=	Distance from the ground water table

γ_{water} = Unit weight of water

$$h = y.\gamma_{water} \tag{15}$$

2.4.2 Analytical and Mechanistic Models

Moisture content predictions based on empirical equations showed significant variations. Moreover, most of the empirical methods were developed for specific locations, which limited their regional application. Therefore, analytical solutions to predict moisture change were developed. Analytical solutions for moisture infiltration/variation found in the literature were reviewed and summarized in this section.

2.4.2.1 Han-Cheng Dan, Jia-Wei Tan, Zhi Zhang and Lin-Hua He Model for Water Infiltration Rate into Cracked Asphalt Pavement

Using flow theory in porous and cracked medium, Dan et al. (*5*) proposed a model to quantify the water balance between surface and drainage layers in asphalt pavements to estimate pavement infiltration rate (PIR). Since the water can enter into the pavements through linked cracks and connected pores, accordingly it was assumed that the total water inflow infiltrating the pavement structure equals the sum of water flow through surface course and cracks. The total water infiltration quantity can be expressed as:

$$Q_{Total} = Q_1 + Q_2 = \int_0^B (q_1 + q_2)dx \tag{16}$$

where,

Q_1 = Water quantity through the porosity of asphalt layer (L^2/T);
Q_2 = Water quantity through cracks present in asphalt pavements (L^2/T)
q_1 = Water flow through the micro-segmentation of surface course to the drainage layer (L^2/T)
q_2 = Water quantity through the crack per unit length along the longitudinal pavement (L^2/T)

Using hydraulic conductivity of the porous medium and equivalent hydraulic conductivity of cracked asphalt layer, and solving integral for simplification (*5*), final expression obtained by the authors for PIR with full-length transverse cracks is given below:

$$\mathrm{I}_M = (k_1 + k_C)\frac{T_1 + T_2 - \bar{h}^*}{T_1} \tag{17}$$

For no crack on the pavement surface, authors expressed the infiltration as:

$$\mathrm{I}_S = k_1\frac{T_1 + T_2 - \bar{h}^*}{T_1} \tag{18}$$

Also, the difference between *Im* and *Is* is given by the following equation:

$$\mathrm{I}_C = k_C \frac{T_1 + T_2 - \bar{h}^*}{T_1} \tag{19}$$

K_1 and K_C expressed by the authors as:

$$K_1 = \frac{\rho g}{\mu} \frac{\phi}{8} r^2 \tag{20}$$

$$K_C = \rho g \frac{\gamma w^3}{12\mu} \tag{21}$$

where,

I_M = Water Infiltration rate per unit width of the pavement incorporating crack and porosity (L/T)

I_S = Water Infiltration rate per unit width of the pavement due to and porosity only (L/T)

I_C = Difference between I_M and I_S (L/T)

k = Hydraulic conductivity (L/T)

k_C = The equivalent hydraulic conductivity of crack (L/T)

T_1 = The thickness of surface course (L)

T_2 = The thickness of drainage layer (L)

$\bar{h}^*$ = Average water thickness (L)

ρ = Water density (M/L^3)

g = Gravity acceleration (L/T^2)

ϕ = The porosity of porous media

r = Uniform radius of microtubules (L)

γ = Crack density, defined as $\gamma = N / L_C$

N = Crack number with uniform width

L_C = Crack distance

w = Crack opening width (L)

μ = Kinematic viscosity of flow (Pa S)

Finally, the expression for infiltration rate with the random crack length of asphalt pavement was presented with following modification:

$$I_{in} = \xi . I_C + I_S \tag{22}$$

where, ξ is the ratio of crack length to pavement width, expressed as: -

$$\xi = L_C / B \tag{23}$$

where,
B = Pavement width (L)
Authors compared the results of this model with Ridgeway's method (*5, 33*). The general trends noted are presented in Figure 2-4, and briefly discussed below.

- PIR increases with increase in crack width as shown in Figure 2-4(a).
- Amount of water seeping through pores is negligible as compared to the quantity of water infiltrating through surface cracks [see Figure 2-4(a)].
- As the crack interval increases the PIR decreases considerably, and when it becomes very large, the PIR achieves a relatively stable position as shown in Figure 2-4(b).
- PIR significantly increases with increase in transverse crack length as shown in [see Figure 2-4(c)].
- Crack open width has a significant effect on infiltration rate. Infiltration rate increased in quadratic polynomial form with an increase in open crack width as shown in Figure 2-4(d).
- Thicknesses of pavement surface and drainage layers also impact PIR. However, the behavior of both layers is contrary to each other. With the increase in surface layer thickness, PIR decreases. Whereas, with an increase in drainage layer thickness, PIR increases. The reverse trend by both layers is observed, because the change in hydraulic gradient, which decreases with increase in surface course thickness, and increases with increase in drainage layer thickness [see Figure 2-4 (a) and (b)].

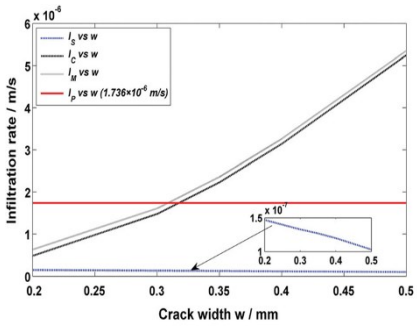

(a) PIR vs. transverse crack width

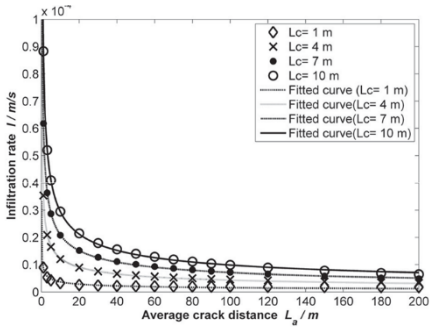

(b) PIR vs. average crack distance for different transverse crack lengths

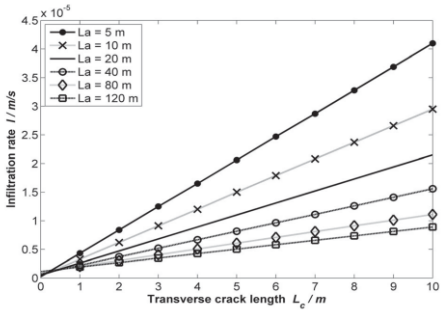

(c) PIR vs. transverse crack length for different average crack distances

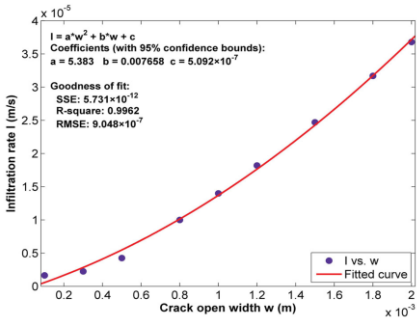

(d) PIR vs. crack open width

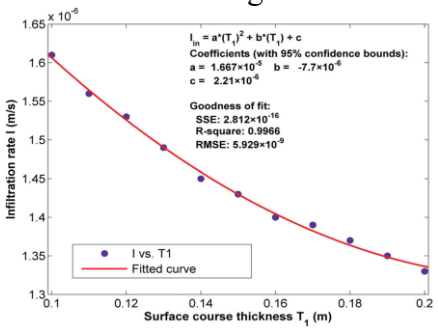

(e) PIR vs. surface course thickness

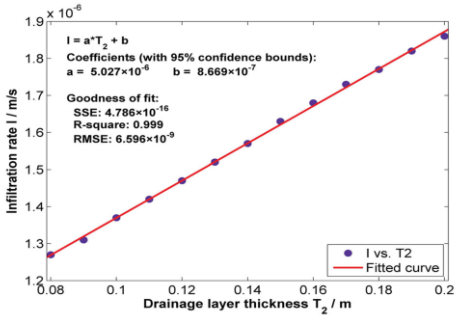

(f) PIR vs. drainage layer thickness

Figure 2-4 Model simulation results (*5*)

2.4.2.2 Hansson, K, Lundin, L. Charister and Simunek, J. Numerical Model Using Hydrus 2D for Modelling for Water Flow Patterns in Flexible Pavements

In this study, proposed by Hansson et al. water flow patterns were simulated in flexible pavements. A numerical code built in Hydrus 2D software to depict simulations of water movement in pavement layers. Primarily, water movement due to rainfall was considered in this study. Special emphasis was given to three processes, the surface runoff followed by an infilterarion through an asphalt fractured zone, the surface runoff with subsequent infilteration in the embankment, and capillary barrier effects between layers within the roads (*34*). The road section simulated is shown in Figure 2-5.

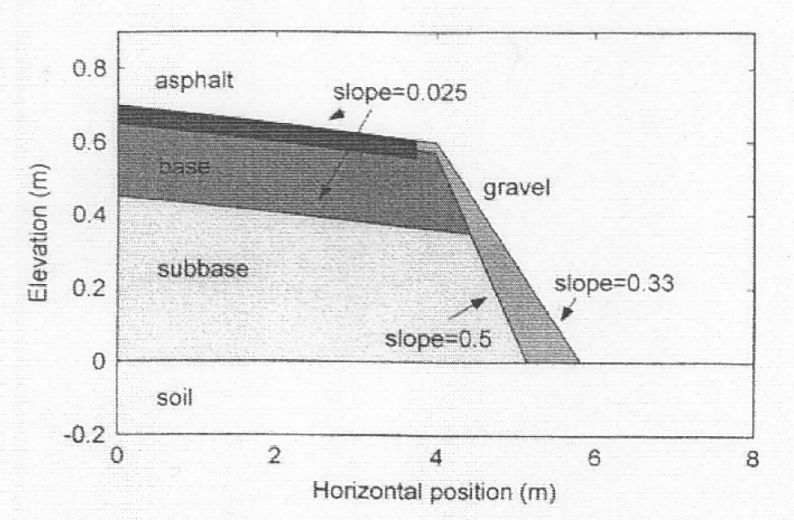

Figure 2-5 Model road construction with material constructions, dimensions, and slopes (*34*)

Authors used Richard's equation to calculate water flow in unsaturated porous medium (*34, 35*). Different equations used for calculation of water flow, effective degree of saturation, retention curves, and effective hydraulic conductivity of a fracture zone are summarized below:

$$\frac{\partial\theta}{\partial t}=\frac{\partial}{\partial x}\left[k(h)\frac{\partial h}{\partial x}\right]+\frac{\partial}{\partial z}\left[k(h)\frac{\partial h}{\partial z}\right]++\frac{\partial k}{\partial z} \tag{24}$$

where,

θ = Volumetric water content
h = Pressure head (L)
k = Hydraulic conductivity ($L.T^{-1}$)
t = Time
x = Horizontal coordinate
z = Vertical coordinate, positive upward

$$S_e=\frac{\theta-\theta_r}{\theta_{sat}-\theta_r} \tag{25}$$

where,

S_e = Effective saturation
θ_r = Residual water content
θ_{sat} = Saturated water content

Authors used Van Genuchten analytical model to characterize retention curve(*34, 35*).

$$S_e=\frac{1}{\left[1+(\alpha h)^n\right]^m} \tag{26}$$

where, $\alpha\left[L^{-1}\right], m, and\ n$ are empirical parameters.

Following relationship by Van-Genuchten-Mualem (*34-36*) was used to describe unsaturated hydraulic conductivity.

$$kS_e = k_s S_e^l \left[\left(1 - S_e^{1/m}\right)^m\right]^2 \tag{27}$$

$$m = 1 - 1/n \tag{28}$$

where,

k_s = Saturated hydraulic conductivity ($L.T^{-1}$)

l = Pore connectivity parameter

Finally, the effective hydraulic conductivity of fractured zone was obtained by Parallel plate model (*34, 37*).

$$k_f = \frac{(2b)^2}{2B}\frac{\rho g}{12\mu} \tag{29}$$

where,

$2b$ = Fracture aperture

$2B$ = Distance between fractures

ρ = The density of water (~ $.m^{-3}$)

g = Gravitational acceleration ($= 9.82 m.s^{-2}$)

μ = Dynamic viscosity ($= 100 * 10^{-3} Kg.m^{-1}.s^{1} at 20^{\circ}$)

To visualize flow pattern, numerical simulations in Hydrus 2D were carried out using the particle tracking. Many hypothetical particles were released at different locations on the road surface, both at the embankment and fractured portion. No particles were released at intact asphalt surface because it was considered impermeable(*34*). Multiple simulations were planned to study the effect of rainfall amount, duration, and fracture conductivity (*34*).

- 30 mm rainfall amount was applied for 1,2,4 and 8 hours duration to visualize the effect of rainfall rate.
- 2.75,7.5 and 30 mm rainfall amounts were applied during 1hour duration to see precipitation amount impact,.
- three fracture sizes were used as 0.5,0.1 and 0.01 mm, while studying the effect of varying fracture hydraulic conductivity. The precipitation for this simulation was 7.5 mm during a one-hour rainfall event.

Following conclusions were made based on the simulations results:

- Varying precipitation rate had little effect on traveled particle distances at the end of simulations (i.e., three days after the rainfall), however, with higher precipitation rate, particles travelled farther (*34*) as shown in Figure 2-6.

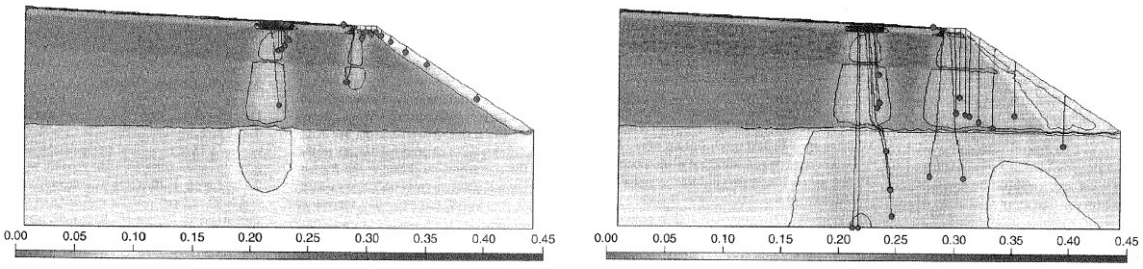

(g) Precipitated amount 3.75 mm (h) Precipitated amount 30 mm

Figure 2-6 Water content distribution 3 days after onset of 1-hour rain event (*34*)

- With small fracture aperture, i.e., 0.01 mm, K_f was considerably decreased and all the infiltration took place through the embankment. Whereas for higher K_f, as in case of 0.5 mm aperture the infiltration and particle movement took place right in the fractured zone as shown in Figure 2-7(*34*).

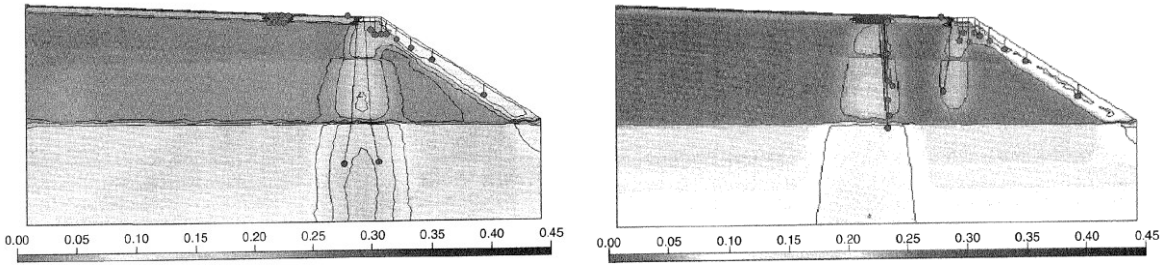

(a) Fracture aperture 0.01 mm (b) Fracture aperture 0.5 mm

Figure 2-7 Water content distribution 3 days after onset of 7.5 mm, 1-hour rain event (*34*)

- It was observed that flow velocities were at peak at the end of a rainfall event, and most of the infiltration took place in initial few hours after the rainfall event. This phenomenon is well explained by particle movement. The particles traveled maximum distance in the first couple of hours after the onset of rain. After three days of rainfall event, the increase in distance traveled was minute [see Figure 2-8].

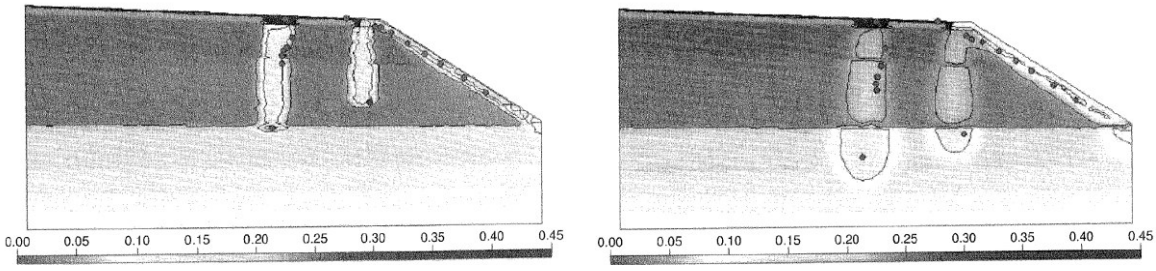

(a) 2-Hours after the rainfall event (b) 3-Days after the rainfall event

Figure 2-8 Water content distribution after the onset of 7.5 mm, 1-hour rain event (*34*)

2.4.2.3 Fan et al. Numerical Modelling of Unsaturated Granular Materials (UGM) in Flexible Pavements

In this study, a new constitutive model for UGM was proposed, which captured both non-linear and moisture-sensitive characteristics of UGM. The proposed model was incorporated into finite element model for the base layer to quantify the influence of moisture content on the pavement performance (*18*). Lytton model was used to capture explanation of this behavior (*18, 38, 39*).

$$E_y = k_1 p_a \left(\frac{I_1 - 3\theta f h_m}{p_a} \right)^{k_2} \left(\frac{\tau_{oct}}{p_a} \right)^{k_3} \quad (30)$$

where,

E_y = Vertical modulus

I_1 = First invariant of the stress tensor

p_a = Atmospheric pressure

θ = Volumetric moisture content

f = Saturation factor, $1 \le f \le \frac{1}{\theta}$

h_m = Matric suction in aggregate base

τ_{oct} = Octahedral shear stress

k_1, k_2 and k_3 = Regression coefficients

For Lytton model validation, repeated load triaxial test lab results for three different materials at different moisture contents (at OMC and ± 1.5 OMC) were compared with predicted modulus. The results amply clarified the moisture sensitive and stress-dependent behavior of UGM, as shown in Figure 2-9.

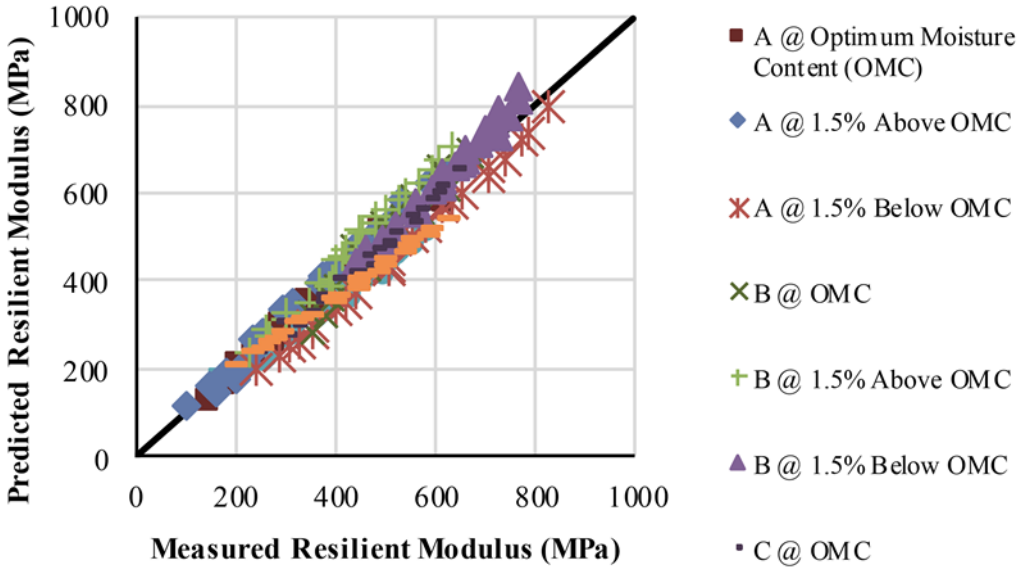

Figure 2-9 Comparison of predicted and measured resilient moduli for selected materials (*18*)

In numerical models, different moisture conditions were simulated to investigate the effect of moisture content of UGM on pavement response. Three cases were considered, a low moisture condition with a degree of saturation 0.7, an optimum moisture condition (OMC) with a degree of saturation 0.85, and a saturated condition with a degree of saturation of 1. The results are shown in Figure 2-10 which indicates moisture content influence on UGM.

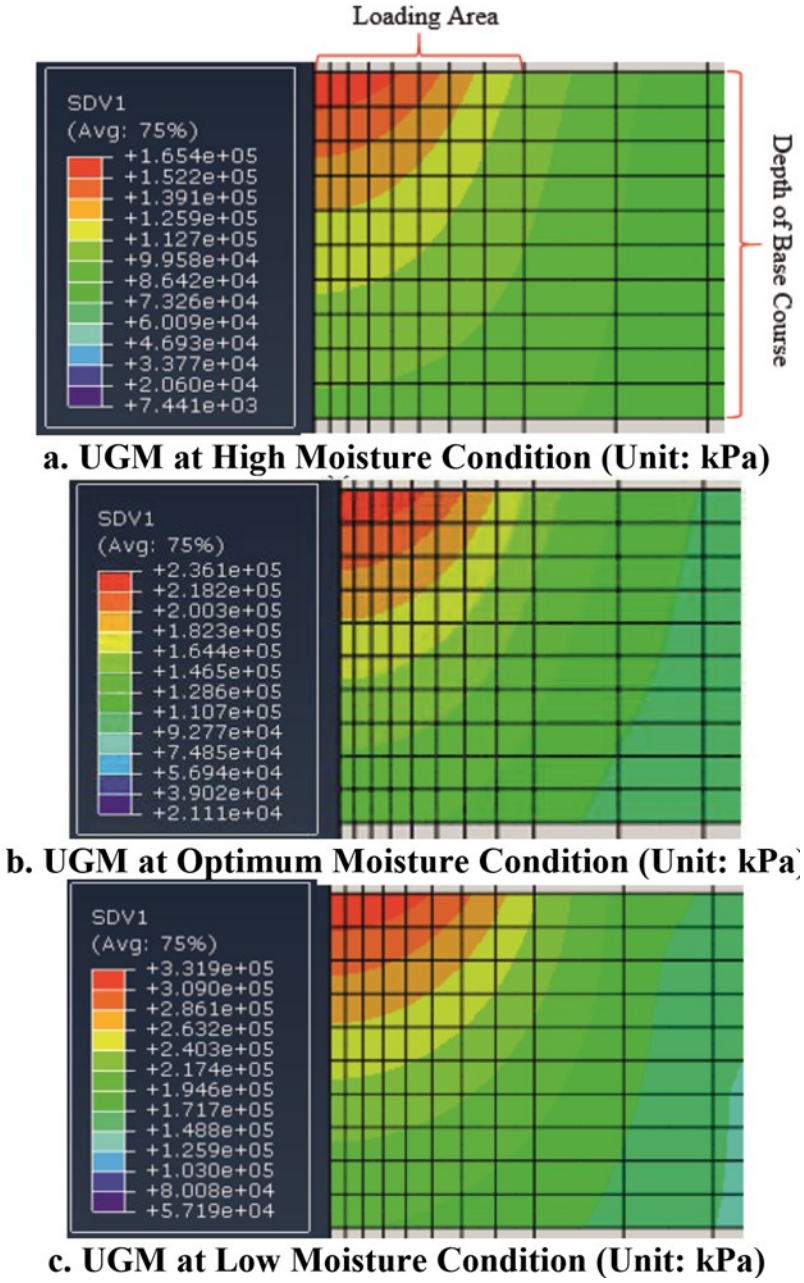

Figure 2-10 Vertical Moduli Distribution Base layer (*18*)

2.4.2.4 Resilient Modulus as a Function of Soil Moisture (EICM)

The unbound base and subbase layers are an integral part of a pavement structure. Change in moisture content of subsurface layers can have an impact on the material properties (i.e., MR) of these layers. Consequently, the difference in material properties will affect the structural capacity

of the whole pavement structure. The Pavement-ME Design Guide uses the moisture-modulus or Witzack model to determine the variation in MR of the unbound layer with moisture change (*40*).

$$\log \frac{M_R}{M_{R(opt)}} = a + \frac{b-a}{1+\exp\left(\ln\frac{-b}{a} + k_m.(S-S_{opt})\right)} \tag{31}$$

where;

M_R	=	Resilient modulus at the degree of saturation S (decimal)
M_{ROPT}	=	Resilient modulus at the maximum dry density and optimum moisture
a	=	Minimum of log (MR/MR_{OPT})
b	=	Maximum of log (MR/MR_{OPT}
$a,\ b,\ and\ k_m$	=	-0.5934, 0.4 and 6.1324 for fine grained materials 0.3123, 0.3, and 6.8157 for coarse grained materials
$S - S_{OPT}$	=	Variation in the degree of saturation expressed in decimal

2.4.3 Summary of Existing Models from Literature

Table 2-1 summarizes features, advantages, and disadvantages of different moisture content/infiltration prediction models found in the literature.

Table 2-1 Summary of existing models from literature

Model	Main Feature	Advantages	Disadvantages	Additional Comments
Swanberg and Hansen (*26*)	Uses PL to calculate moisture content	Single input, simple to use	Only considered soil properties, surface conditions and climatic factors not considered	Developed for SG layer
US Navy (*27*)	Uses PL to calculate moisture content	Single input, simple to use	Only considered soil properties, surface conditions and climatic factors not considered	Developed for SG layer of airfield pavements
Kersten Model (*28*)	Uses PL to calculate moisture content	Single input, simple to use	Large variation in prediction of moisture content for different soils	Empirical solution
Rao's moisture content prediction model (*15*)	Uses index properties like % passing No 200, LL, PI, Permeability	Index properties can be determined readily. Briefly discussed the effect of precipitation and temperature	Climatic loading and surface conditions are not included in the final model	Data from 18 different sites of Arkansas was used to calculate moisture in SG layer
Hedayati and Hossain- data-based model (*16*)	Uses one-dimensional partial differential equations as a function of time and depth and in situ precipitation and moisture data to predict moisture variation	Considered seasonal variations and temporal changes comprehensively. Incorporated depth factor gives the flexibility to calculate moisture content for different pavement layers	No consideration is given to surface cracking. Since the model is developed based on data from only one specific site, the regional application is limited.	Moisture and precipitation data for two years of two-lane HMA road in North Texas was used to develop this model
EICM (*40*)	Comprises of three different models	Currently used in Pavement-ME, results are widely accepted	Comprehensive but complex in general for new users	Software
Han et al. model (*29*)	An analytical solution to quantify water balance between surface and drainage layer to estimate pavement infiltration rate	Incorporated surface discontinuities in the model. The final form of the solution is user-friendly	Derivation of expression is complex. Moreover, experimental and field investigation not yet validated	Numerical solution
Hansson et al. (*34*) solution	Numerical code built in Hydrus 2D	Good simulation of water movement in pavement layers, especially with varying rainfall intensity, rain and aperture size (detecting cracks on the surface)	A complex approach requires expertise in model simulation and defining boundary conditions	Software-based

2.5 SUMMARY

This chapter starts with the brief description of various sources causing the moisture change in pavement-unbound layers, particularly infiltration of rainfall through surface discontinuities (cracking and joint sealant damage). It provides discussion on moisture-related damage to the pavements and different procedures adopted for its mitigation. It was found in the literature that the moisture-related damage is significant, especially for the pavements located in areas with higher precipitation levels. This chapter also documents the moisture content modeling techniques found in literature, followed by a discussion on various empirical and analytical models available in the literature. Subsequently, it elaborates the moisture model used in Pavement-ME, which relates the unbound layers stiffness properties to moisture change. Finally, it provides the summary of moisture models along with pros and cons. Moisture variations adversely affect the pavement performance. Based on the literature review, true quantification of moisture variations within pavement unbound layers is warranted.

CHAPTER 3 DATA SYNTHESIS

3.1 SEASONAL MONITORING PROGRAM (SMP) BACKGROUND

Previous research highlighted that moisture variation within unbound layers is one of the leading factors for premature pavement deterioration (*7, 13, 16*). Therefore, the hypothesis of this study is that moisture variation in unbound layers, i.e., base layer, can be related to the amount of surface discontinuities (cracking and joint seal damage) in different climatic zones. To validate this hypothesis, an important challenge was to identify the data set documenting the subsurface moisture levels in the base layer. Only SMP study has TDRs installed at different depths in many pavement sections. In addition, the performance monitoring data were also recorded for those pavement sections. The SMP study was designed to characterize the magnitude and impact of temporal variations in pavement response and material properties due to the separate and combined effect of moisture, temperature and frost/thaw variations. It also includes higher monitoring frequency of deflections, longitudinal profile, and distress surveys on 64 SMP LTPP test sites, which were selected from GPS and SPS studies. In addition to performance data, other measurements—including subsurface moisture, temperature, rainfall, and surface elevations—were also recorded at these sites (*41*). The SMP study has a comprehensive database for subsurface moisture and temperature records. Because of its uniqueness, SMP data were identified as the best available source to quantify moisture damage in flexible and rigid pavements.

3.2 DATA SELECTION CRITERIA

Various data elements from the SMP LTPP sections were reviewed and collected for further analyses to accomplish the objectives of this study. Of the particular interest was the data assessment of SMP sites with an unbound base material having sufficient subsurface in-situ moisture, precipitation, and performance time series data. The SMP sections with at least three years or more subsurface moisture data were identified and used in the subsequent analyses. The timing of pavement maintenance actions was also considered for each section to obtain the amount of unsealed cracking and joint seal damage in a month. Time series of all the desired variables, (i.e., subsurface moisture, precipitation, and fatigue cracking) was considered during data analysis. As mentioned above, the SMP flexible and rigid sections with only unbound base layers were analyzed.

3.3 DATABASE DEVELOPMENT

The required data were obtained from the LTPP database standard release 30.0. All SMP test sections were assigned with a unique ID by combining state code and SHRP ID. Multiple data buckets for desired variables were downloaded using online Infopave® features. The downloaded data elements were organized in various data tables to create a relational database.

3.4 DATA ELEMENTS

The following data elements were identified for the analysis:

- Section inventory
    - Sate code.
    - SHRP ID.
    - Site location.
    - Climatic region
    - Assign date.
    - Construction number.
    - Survey date.
- Pavement structure
    - Layer type.
    - Representative layer thicknesses.
    - Survey width.
    - Survey length.
- Performance data
    - Flexible pavement sections.
        - Alligator cracking.
        - Longitudinal cracking wheel path (WP).
        - Longitudinal cracking non-wheel path (NWP).
        - Transverse cracking.
    - Rigid pavement sections.
        - Longitudinal joint sealant damage.
        - Transverse joint sealant damage.
        - Longitudinal and transverse cracking.
- Climatic data
    - Subsurface moisture content.
    - Subsurface temperature.
    - Precipitation (rainfall and snow).
    - Freezing index.
    - Groundwater table depth.
- Materials data
    - Sieve size analysis.
    - Atterberg limits.
    - Specific gravity.

Table 3-1 provides a summary of data types assessed in this investigation, along with the corresponding LTPP data tables containing the required data elements.

Table 3-1 LTPP data base tables used to extract data elements

Type of data	Data elements chosen	Relevant LTPP tables	Table description
General information	LTPP section inventory	EXPERIMENT_SECTION	The three key fields that define a unique record in this table are STATE_CODE, SHRP_ID, and CONSTRUCTION_NO, which form the primary backbone of relational links within the LTPP database.
		SECTION_LAYOUT	This table contains section layout and location information. This table contains combined data from INV_ID, INV_GENERAL, SPS_ID, SPS_GENERAL, and SPS_PROJECT_STATIONS.
Structure	Layer thickness and material type	SECTION_LAYER_STRUCTURE	It contains a consolidated set of pavement layer structure information for all LTPP test sections.
Material	Sieve size analysis	TST_SS01_UG01_UG02	This table contains the gradation of unbound coarse-grained granular base, subbase, and subgrade materials.
	Atterberg limits	TST_UG04_SS03	This table contains the Atterberg limit test results for the unbound granular base, subbase, and subgrade materials
	Specific Gravity	TST_UNBOUND_SPEC_GRAV	This table contains the specific gravity of unbound base and subgrade materials.
Climate	Subsurface moisture content	SMP_TDR_AUTO_MOISTURE	This table contains the volumetric and gravimetric moisture contents calculated using TDR.
		SMP_TDR_DEPTHS_LENGTHS	This table contains information on the physical characteristics of the TDR probes, including the depth at which the probe is installed, the length of the probe, and its installation date.
	Subsurface temperature	SMP_MRCTEMP_AUTO_HOUR	This table contains the vast majority of subsurface temperature data. It includes average hourly temperatures at a series of depths.
		SMP_MRCTEMP_DEPTH	This table contains the depths at which each temperature probe at an SMP section was installed and the date of installation.
	Freezing index	TRF_ESAL_INPUTS_SUMMARY	Contents of this table include Climate characterizations including average annual precipitation and freeze index, LTPP experimental climate region and the source for this classification.
	Precipitation	CLM_VWS_PRECIP_MONTH	Virtual weather station monthly precipitation statistics and calculated parameters. The fields in this table are populated only when data for 24 or more days are available for a month.
	Water table depth	SMP_WATERTAB_DEPTH_MAN	This table contains manual observations of the distance from the pavement surface to the water table. A null in the WATERTAB_DEPTH indicates that no water was found in the observation piezometer well.
Performance	AC surface distresses	MON_DIS_AC_REV	This table contains distress survey information obtained by manual inspection in the field for pavements with AC surfaces.
	PCC surface distresses	MON_DIS_JPCC_REV	This table contains distress survey information obtained by manual inspection in the field for jointed PCC pavements.

3.4.1 Pavement Performance Data

Monthly surface distress data were obtained for all the flexible and rigid SMP pavement sections. Flexible pavement sections distress data included extent and severity of unsealed alligator, transverse, longitudinal wheelpath (WP) and non-wheelpath NWP cracking. The total cracking length for a flexible pavement section was calculated in feet by using following equation:

$$\mathrm{CRK}_{Total} = WP_{CRK\ length} + LC_{NWP} + TC \quad (1)$$

where;

$WP_{CRK\ length}$ = Unsealed wheel-path cracking length (ft) includes alligator and longitudinal WP

LC_{NWP} = Unsealed longitudinal cracking length outside wheel-path (ft)

TC = Unsealed transverse cracking length (ft)

CRK_{Total} = Total cracking length for a flexible pavement section (ft)

Rigid pavement sections distress data included extent and severity of unsealed longitudinal/transverse cracking and joint sealant damage. It was observed that longitudinal and transverse cracking magnitudes were very low in rigid pavements; therefore, only the length of joint sealant damage was used. While calculating the length of the damaged transverse joint seal, 5%, 25% and 50% of the joint seals were considered damaged for low (less than 10% damage), medium (10% to 50% damage), and high (more than 50% damage) severity transverse joint seal damage, respectively. The total PCC joint sealant damage length in feet was calculated by using Equation (2).

$$\mathrm{JSD}_{Total} = NDJ_{Trans-low} \cdot \mathrm{W}_{\mathrm{Svy}} \cdot 0.05 + NDJ_{Trans-med} \cdot \mathrm{W}_{\mathrm{Svy}} \cdot 0.25 + NDJ_{Trans-high} \cdot \mathrm{W}_{\mathrm{Svy}} \cdot 0.5 + LDJ_{Long} \quad (2)$$

where;

$NDJ_{Trans-low}$ = Number of low severity transverse joints with damaged joint sealant

$NDJ_{Trans-med}$ = Number of medium severity transverse joints with damaged joint sealant

$NDJ_{Trans-high}$ = Number of high severity transverse joints with damaged joint sealant

LDJ_{Long} = Length of longitudinal joints with damaged joint sealant (ft)

$\mathrm{W}_{\mathrm{Svy}}$ = Survey width (ft)

JSD_{Total} = Total length damaged joint sealant (ft)

3.4.2 Subsurface Moisture and Temperature

Time domain reflectometry (TDR i.e., moisture sensors) and thermistors (temperature sensors) were installed in all the SMP pavements sections to measure the in-situ subsurface moisture and temperature data at different depths (*42-52*). Also, the SMP database has volumetric and gravimetric moisture data at different depths (dry densities were used to convert volumetric moisture to gravimetric moisture content) (*41*). In this study, gravimetric moisture data were used for further analysis.

Subsurface moisture and temperature data at the middle of the base layer were estimated from TDRs and thermistors for each site. To obtain the exact depth of subsurface moisture and temperature measurements, unique section IDs were matched with TDR and thermistor numbers. For example, if the base layer mid-depth is at 15 inches from the surface (a=15 inch), then the average moisture content measured using TDRs located within ± 5 inch (b=5 inch) to the reference point was calculated; i.e., moisture content was calculated by averaging the values measured by TDRs between the depths of 10 to 20 inches. However, often only one TDR or thermistor was encountered within base layer for obtaining subsurface moisture and temperature data. This approach represents the moisture and temperature variations within the base layer. Figure 3-1 is showing the schematic of these calculations.

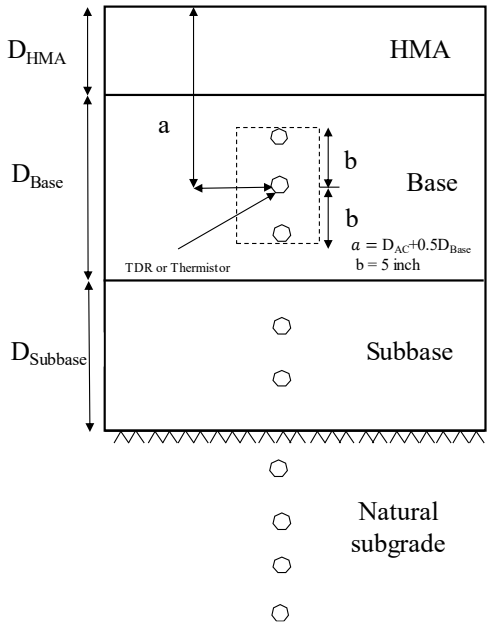

Figure 3-1 Subsurface moisture and temperature measurements

Table 3-2 presents the summary of SMP sections layer structure, subsurface moisture, and temperature depth, and the available number of years for the data elements.

Table 3-2 Layer structure and TDR/thermistors depths

Unique ID	State description	Climatic regions	Base type	Base thickness (inches)	Surface type	Surface layer thickness (inches)	Subsurface moisture availability (years)	Mid of Base (inches)	TDR depth (inches)	Temperature availability (years)	Thermistor depth (inches)
01_0101	Alabama	WNF	GB	7.9	AC	7.4	3	11.3	11.0	4	12.9
01_0102	Alabama	WNF	GB	12.0	AC	4.2	3	10.2	10.0	3	10.2
04_0113	Arizona	DNF	GB	7.5	AC	4.9	3	8.7	8.7	8	9.6
04_0114	Arizona	DNF	GB	12.0	AC	7.3	4	13.3	12.8	8	**Avg (12.4+15.5)**
04_1024	Arizona	DNF	GB	6.3	AC	11.0	4	14.1	13.9	4	**Avg (13.4+16.5)**
08_1053	Colorado	DF	GB	5.4	AC	6.8	3	9.5	7.2	5	9.6
09_1803	Connecticut	WF	GB	12.0	AC	8.9	5	14.9	13.2	4	15.4
10_0102	Delaware	WNF	GB	11.8	AC	5.5	5	11.4	14.2	5	**Avg (11.9+15.0)**
13_1005	Georgia	WNF	GB	8.8	AC	7.6	5	12.0	11.6	4	13.4
13_1031	Georgia	WNF	GB	8.8	AC	11.3	4	15.7	17.1	4	14.5
16_1010	Idaho	DF	GB	5.4	AC	10.9	5	13.6	14.0	5	**Avg (13.7+16.8)**
23_1026	Maine	WF	GB	17.6	AC	9.0	5	17.8	14.7	5	**Avg (14.2+17.2)**
25_1002	Massachusetts	WF	GB	4.0	AC	7.8	5	9.8	9.5	4	10.1
27_1018	Minnesota	WF	GB	5.2	AC	6.4	5	9.0	9.4	5	14.8
27_6251	Minnesota	WF	GB	10.2	AC	9.0	4	14.1	11.4	10	15.2
30_0114	Montana	DF	GB	12.4	AC	7.7	7	13.9	13.2	5	14.9
31_0114	Nebraska	WF	GB	12.0	AC	6.4	5	12.4	13.4	7	14.8
32_0101	Nevada	DF	GB	8.5	AC	7.2	4	11.5	10.8	7	12.7
33_1001	New Hampshire	WF	GB	19.3	AC	10.4	5	20.0	20.4	5	19.5
35_1112	New Mexico	DNF	GB	6.4	AC	6.2	5	9.4	10.0	6	**Avg (8.2+11.1)**
36_0801	New York	WF	GB	8.4	AC	5.0	7	9.2	9.4	10	10.4
46_0804	South Dakota	DF	GB	12.0	AC	9.3	7	15.3	12.9	9	13.6
48_1060	Texas	WNF	GB	12.3	AC	7.5	3	13.7	12.6	5	**Avg (12.8+15.8)**
48_1077	Texas	WNF	GB	10.4	AC	5.0	6	10.2	12.0	5	10.1
48_1122	Texas	WNF	GB	15.6	AC	3.7	5	11.5	9.7	7	**Avg (10.9+13.9)**
49_1001	Utah	DNF	GB	5.8	AC	6.0	5	8.9	10.4	5	**Avg (8.7+11.8)**
50_1002	Vermont	WF	GB	25.8	AC	8.5	7	21.4	**Avg(16.5+20.5)**	9	21.9
51_0113	Virginia	WNF	GB	7.9	AC	4.0	4	8.0	7.1	7	8.4
51_0114	Virginia	WNF	GB	11.9	AC	8.8	6	14.8	12.6	7	11.3
56_1007	Wyoming	DF	GB	6.2	AC	3.5	5	6.6	6.0	5	6.5
83_1801	Manitoba	WF	GB	5.6	AC	4.4	7	7.2	7.9	10	8.9
87_1622	Ontario	WF	GB	6.7	AC	7.6	5	10.9	8.9	5	10.4
04_0215	Arizona	DNF	GB	6.3	PCC	11.0	3	14.1	13.6	8	13.2
13_3019	Georgia	WNF	GB	7.2	PCC	8.9	3	12.5	12.2	7	12.8
18_3002	Indiana	WF	GB	5.5	PCC	11.2	3	13.9	12.6	4	**Avg (10.4+14.8)**
27_4040	Minnesota	WF	GB	6.0	PCC	8.1	3	11.1	10.8	5	11.7
32_0204	Nevada	DF	GB	6.2	PCC	11.8	3	14.9	13.8	3	12.8
37_0201	North Carolina	WNF	GB	9.3	PCC	9.2	5	13.9	11.0	10	14.6
39_0204	Ohio	WF	GB	5.8	PCC	11.1	3	14.0	14.1	3	14.5
42_1606	Pennsylvania	WF	GB	8.6	PCC+AC	10.0+4.3	5	18.5	21.6	8	19.4
53_3813	Washington	WNF	GB	4.5	PCC+AC	8.0+5.2	4	13.9	14.1	4	12.8
83_3802	Manitoba	WF	GB	4.9	PCC+AC	9.8+6.0	3	18.3	17.5	6	19.2
89_3015	Quebec	WF	GB	13.3	PCC+AC	8.2+9.4	8	24.3	22.0	9	22.2

Avg= average of the moisture and temperature data were obtained from all the available TDRs/Thermistors installed within base layer.

3.4.3 Precipitation Data

Pavement performance temporal data were matched to obtain total monthly precipitation amount (i.e., rainfall and snow). Water infiltration followed by snow melting can substantially increase moisture levels within the pavements layers, especially in wet climates. Therefore, total monthly precipitation levels were calculated by adding rainfall and snow.

3.4.4 Ground Water Table Depth

Capillarity action can also cause moisture change within pavements unbound layers. The depth of groundwater table (GWT) was obtained to isolate the effect of capillarity water, traveling

from subgrade to base layer. Further, in the analysis part, GWT depth relationship was assessed with varying base layer moisture levels over time.

3.4.5 Freezing Index

Average annual freezing index (FI) data were obtained to keep a record of freezing and no freezing regions while developing moisture prediction models.

3.4.6 Materials Data

Material data elements were extracted by following the guidelines from the LTPP Information Management System materials module. Site-specific materials data were available for most of the SMP sites. Materials data needed to calculate base layer resilient modulus (MR) were obtained by combining unique ID and layer numbers. Linked SHRP IDs were used to obtain data for those SMP sections with missing site-specific material data. Sieve size distributions, Atterberg limits and specific gravity data elements were extracted by combining various data tables in the database. Sieve size analysis data were used to obtain D_{60} (the grain diameter at 60% passing). Figure 3-2 (a) and (b) show the base material particle size distribution for flexible and rigid pavement sections, respectively. Table 3-3 presents the summary of base layer material properties for flexible and rigid pavement sections.

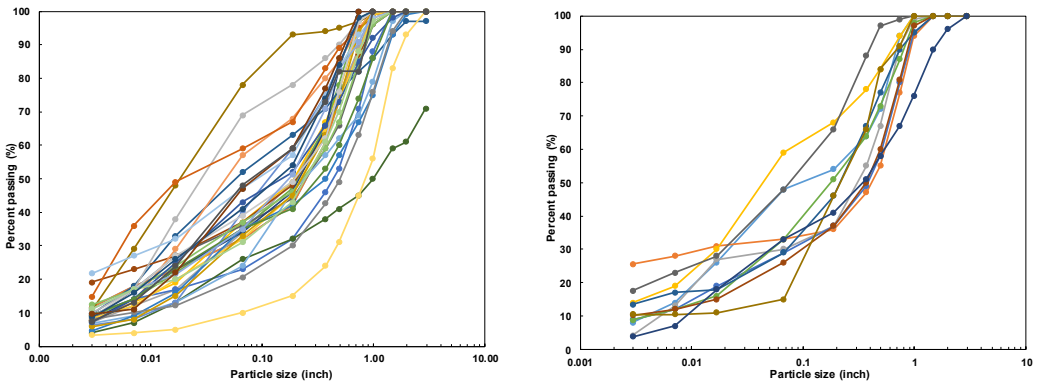

(a) SMP flexible pavement sections (b) SMP rigid pavement sections

Figure 3-2 Base material particle size distribution

Table 3-3 Base layer material properties

Unique_ID	Climatic Regions	Surface Layer	Base type	Percent passing # 200	D_{60} (inches)	PI	Specific Gravity	Material type
01_0101	WNF	AC	GB	11.5	0.4	NP	2.87	303-Crushed Stone
01_0102	WNF	AC	GB	11.5	0.4	NP	2.87	303-Crushed Stone
04_0113	DNF	AC	GB	7.1	0.3	NP	2.72	304-Crushed Gravel
04_0114	DNF	AC	GB	7.6	0.3	NP	2.72	304-Crushed Gravel
04_1024	DNF	AC	GB	9.3	0.6	NP	2.70	304-Crushed Gravel
08_1053	DF	AC	GB	8.9	0.3	NP	2.65	304-Crushed Gravel
09_1803	WF	AC	GB	9.6	0.1	NP	2.65	302-Gravel (Uncrushed)
10_0102	WNF	AC	GB	19.1	0.3	NP	2.85	303-Crushed Stone
13_1005	WNF	AC	GB	7.8	0.4	NP	2.65	308-Soil-Aggregate Mixture (Predominantly Coarse-Grained)
13_1031	WNF	AC	GB	10.7	0.0	NP	2.70	309-Fine-Grained Soils
16_1010	DF	AC	GB	7.8	0.3	NP	2.65	308-Soil-Aggregate Mixture (Predominantly Coarse-Grained)
23_1026	WF	AC	GB	4.0	1.7	NP	2.65	302-Gravel (Uncrushed)
25_1002	WF	AC	GB	6.9	0.4	NP	2.65	304-Crushed Gravel
27_1018	WF	AC	GB	7.7	0.1	NP	2.65	302-Gravel (Uncrushed)
27_6251	WF	AC	GB	9.9	0.1	NP	2.65	302-Gravel (Uncrushed)
30_0114	DF	AC	GB	8.2	0.3	NP	2.65	304-Crushed Gravel
31_0114	WF	AC	GB	6.2	0.2	NP	2.65	303-Crushed Stone
32_0101	DF	AC	GB	12.4	0.4	NP	2.70	304-Crushed Gravel
33_1001	WF	AC	GB	4.6	0.6	NP	2.68	302-Gravel (Uncrushed
35_1112	DNF	AC	GB	14.7	0.1	7	2.55	308-Soil-Aggregate Mixture (Predominantly Coarse-Grained)
36_0801	WF	AC	GB	8.1	0.7	NP	2.83	304-Crushed Gravel
46_0804	DF	AC	GB	5.9	0.3	NP	2.71	303-Crushed Stone
48_1060	WNF	AC	GB	7.1	0.3	NP	2.61	303-Crushed Stone
48_1077	WNF	AC	GB	9.3	0.5	NP	2.60	303-Crushed Stone
48_1122	WNF	AC	GB	21.7	0.2	NP	2.58	308-Soil-Aggregate Mixture (Predominantly Coarse-Grained)
49_1001	DNF	AC	GB	8.6	0.3	NP	2.65	304-Crushed Gravel
50_1002	WF	AC	GB	3.4	1.1	NP	2.65	304-Crushed Gravel
51_0113	WNF	AC	GB	11.0	0.3	NP	2.63	303-Crushed Stone
51_0114	WNF	AC	GB	11.1	0.4	NP	2.63	303-Crushed Stone
56_1007	DF	AC	GB	8.6	0.2	NP	2.65	304-Crushed Gravel
83_1801	WF	AC	GB	9.6	0.2	3	2.65	302-Gravel (Uncrushed)
87_1622	WF	AC	GB	7.4	0.2	NP	2.69	304-Crushed Gravel
04_0215	DNF	PCC	GB	8	0.3	NP	2.71	304-Crushed Gravel
13_3019	WNF	PCC	GB	25.6	0.5	NP	2.61	308-Soil-Aggregate Mixture (Predominantly Coarse-Grained)
18_3002	WF	PCC	GB	4.1	0.4	NP	2.65	303-Crushed Stone
27_4040	WF	PCC	GB	14	0.1	NP	2.65	302-Gravel (Uncrushed)
32_0204	DF	PCC	GB	8.9	0.5	NP	2.65	304-Crushed Gravel
37_0201	WNF	PCC	GB	8.8	0.3	NP	2.76	303-Crushed Stone
39_0204	WF	PCC	GB	13.4	0.3	NP	2.74	303-Crushed Stone
42_1606	WF	PCC+AC	GB	10.2	0.5	6	2.7	304-Crushed Gravel
53_3813	WNF	PCC+AC	GB	17.5	0.1	NP	2.65	308-Soil-Aggregate Mixture (Predominantly Coarse-Grained)
83_3802	WF	PCC+AC	GB	10.5	0.3	NP	2.65	304-Crushed Gravel
89_3015	WF	PCC+AC	GB	3.7	0.5	NP	2.65	303-Crushed Stone

3.5 DATA LIMITATIONS

Since time series of all desired variables (subsurface moisture, cracking, and precipitation) had to be matched on a monthly basis, a considerable amount of data points were not used in further data analysis because either time series did not match or data were not available at required depths. The database was shortened further by eliminating SMP sections with treated bases. Finally, SMP sections with less than two years of temporal data were excluded which further reduced the available number of SMP pavement sections.

3.6 AVAILABLE SMP SECTIONS FOR ANALYSIS

SMP pavement sections, which satisfied the data selection criteria, were reviewed for quality, reasonableness, and availability in the light of supporting the moisture variation impact on long-

term pavement performance. Because of data cleaning, 32 SMP sections were identified with an adequate amount of data for flexible pavements, and 11 SMP sections for rigid pavements. Table 3-4 presents the summary of data elimination process. Figure 3-3 presents the climatic summary of total and available SMP pavement sections considered for this research.

Table 3-4 Number of available SMP LTPP pavement sections

Surface type	Moisture content	Temperature	Precipitation	Freezing index	Performance	Sites with granular base	Time series mismatch/data (less than three years)	Number of available sections
AC	43	43	43	43	43	38	6	32
PCC	21	21	21	21	21	11	0	11

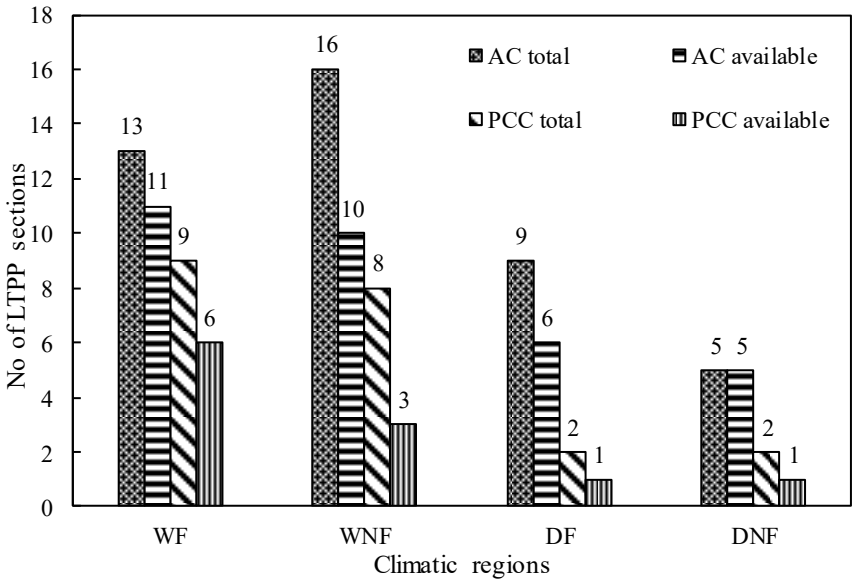

Figure 3-3 Climatic distribution of SMP LTPP sections

3.7 SUMMARY

Seasonal Monitoring Program (SMP) study in the LTPP program primarily was designed to investigate the combined impact of temperature, moisture and frost/thaw variations on pavement material properties, response and performance. Data from SDR 30.0 (the most up to date at the time of this study was conducted) were obtained for this study. Flexible and rigid pavements sections with granular bases and at least three years or more of performance and moisture data were considered for the analysis. In flexible pavement sections, the total length of unsealed cracking was calculated by adding lengths of transverse, longitudinal, and fatigue cracking. All severity levels, i.e., low, medium, and high were added while calculating extents of cracking. In PCC SMP sections, while calculating length of damaged transverse joint seal, 5%, 25% and 50% of the joint seals were considered damaged for low (less than 10%), medium (10% to 50%), and

high (more than 50%) severity transverse joint seal damage, respectively. Total monthly precipitation levels were calculated by adding rainfall and snow. Subsurface moisture and temperature data at the middle of the base layer were obtained from time domain reflectometry (TDR) and thermistors for each pavement section. Exact depths of subsurface moisture and temperature measurements within base layer were estimated by combining unique section IDs with TDR and thermistor numbers, respectively. Pavement construction numbers were also recorded to quantify the exact amount of unsealed cracking/joint seal damage in a month. Material data elements were extracted by following the guidelines provided in the LTPP Information Management System materials module. Materials data needed for base layer MR calculations were obtained by combining unique ID and layer numbers. Site-specific materials data were available for most of the SMP test sections. Linked SHRP IDs were used to calculate data for those SMP sections with missing site-specific material data. Since time series of all desired variables (subsurface moisture, cracking, and precipitation) had to be matched on a monthly basis, a considerable amount of data points were not used in further data analysis because either time series did not match or data were not available at required depths. With data elimination process 32 flexible, and 11 rigid pavement sections were identified with appropriate data for further analysis.

CHAPTER 4 DATA ANALYSIS AND MODELING

4.1 HYPOTHESIS

The past research has defined that moisture variation within pavement unbound layers is one of the leading factors for premature pavement deterioration (*7, 9, 13, 16*). This fluctuation in moisture can be estimated by analyzing the subsurface moisture data available in SMP study. After analyzing the moisture and performance data for few SMP pavements sections, it was hypothesized that variation in subsurface moisture, essentially within base layer, can be related to the extents of surface discontinuities in different climatic zones. Subsequently, by looking at the data and through descriptive statistics, a few other factors that may cause potential moisture change within pavement base layers were identified. These factors affiliated with pavement structure, materials, and climate, were used as covariates while estimating subsurface moisture content. Factors initially considered for the analysis are described below:

- Pavement age
- Surface discontinuities (cracking and joint sealant damage)
- Subsurface temperature
- Precipitation (rainfall and snow)
- Number of wet days
- Moisture depth
- The thickness of pavement structure above the base
- Percent passing sieve number 200
- Freezing index (FI)
- Groundwater table (GWT) depth

Figure 4-1 illustrates the effect of cracking and precipitation on base layer moisture for the SMP section 36-0801 located in WF climate. The data shows that when the pavement section is new with minimal cracking, even with the higher amount of precipitation base layer moisture did not vary much, and only showed a cyclic trend. However, as the cracking extents increased over time, moisture content changed significantly even at lower precipitation levels. This moisture change is accumulative and primarily caused by water infiltration through surface cracks. Fluctuation in groundwater table (GWT) depth may also cause seasonal variations in unbound layers in-situ moisture content. GWT depth records over time were obtained to separate the moisture variations associated with a change in GWT from surface infiltration. Seasonal fluctuations in GWT depth adversely affect deeper layer material properties, essentially up to subgrade and subbase layers, and it will have little effect on the base layer in-situ moisture. GWT and subsurface moisture is plotted for one flexible SMP pavement section located in WF climate as shown in Figure 4-2. It is observed from the relationship that when the pavement is new (initial 3-4 years of service life), the variation in base layer moisture is cyclic, even at times the GWT is very high (i.e., lower GWT depth). On the other hand, when the pavement gets older (7-8 years of service), the variations in moisture are significant for almost same levels of GWT, or even for very low GWT depth (between 6 and 8 years). This evidence supports the hypothesis that main cause of base layer moisture fluctuation is the infiltration though surface discontinuities followed by rainfall.

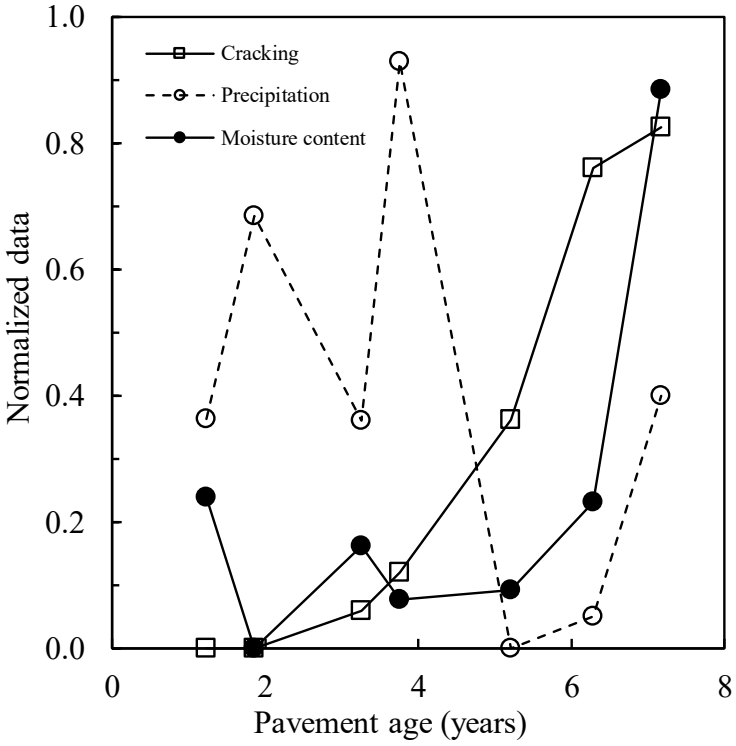

Figure 4-1 Impact of cracking and precipitation on base layer moisture change (36-0801)

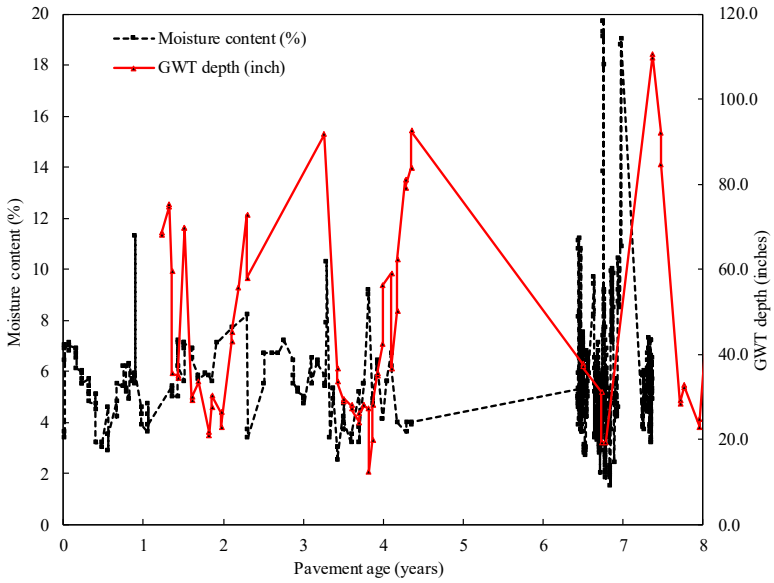

Figure 4-2 Effect of GWT on base layer moisture change (36-0801)

For the same pavement section moisture profile with depth and age is also shown in Figure 4-3. It can be observed that moisture variations are high at the top of pavement structure, i.e., within base and subbase layers, and with an increase in depth, these changes become negligible. A similar trend in moisture change was observed in most of the SMP test sections.

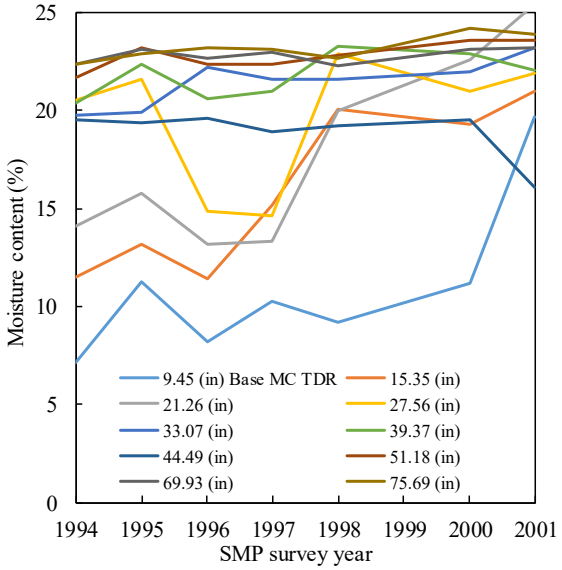

Figure 4-3 Subsurface moisture variations with depth (36-0801)

4.2 METHODOLOGY

As mentioned before, many external and internal sources can cause the subsurface moisture variations in pavement unbound layers (*53*). Surface discontinuities such as cracks or joint openings allow water to infiltrate in sublayers. Bottom-up fatigue is a classic example of through cracking that would allow the surface water to infiltrate into the base layer. However, the amount of water infiltration is expected to be more on locations with higher precipitation levels.
In this study, the amount of surface cracking (joint seal damage in the case of rigid pavements) in flexible pavements over time was related to seasonal moisture levels at different depths of the pavement structure. The primary objective is to identify the additional amount of moisture in the sublayers due to change in surface cracking extent over time in different climates. Subsequently, material properties (i.e., MR) can be related to different moisture levels. The developed models can assist highway agencies in proactive maintenance practices to mitigate moisture-related damage due to surface cracking. The agencies can estimate the maximum cracking extent at which the cracks should be sealed to reduce the water infiltration rate into sublayers.

4.3 DESCRIPTIVE STATICS

Summary of descriptive statics for flexible and rigid SMP LTPP sites is given in Table 4-1. The data extents show that cracking, precipitation, and subsurface moisture levels are very high in wet climates.

Table 4-1 Summary of regional climatic and performance data

Surface type	Climate	Cracking (feet)/Joint seal damage* (feet)		Precipitation (rainfall +snow) (inch)		Temperature (°C)		Gravimetric moisture content (%)		Freezing index	
		Max	Min	Max	Min	Max	Min	Max	Min	Max	Min
AC	DF	699	0	18.1	0	33	-2	12	2	986	215
	DNF	620	0	5.5	0	39	2	14	2	108	1
	WF	1512	0	29.5	2.0	28	-14	19	3	1729	194
	WNF	1175	0	10.6	0	38	4	23	4	76	0
PCC	DF	131	20	1.2	0.5	33	-2	9	8	214	214
	DNF	522	20	1.2	0	39	2	12	11	1	1
	WF	564	13	14.6	1.0	28	-14	28	2	1684	299
	WNF	705	23	12.6	0	38	4	21	4	32	12

* Longitudinal and transverse Joint seal damage in case of PCC pavements.

Figure 4-4 shows cracking progression for flexible pavement sections located in different climates. As compared to DF/DNF, greater cracking extents were observed in WF/WNF regions.

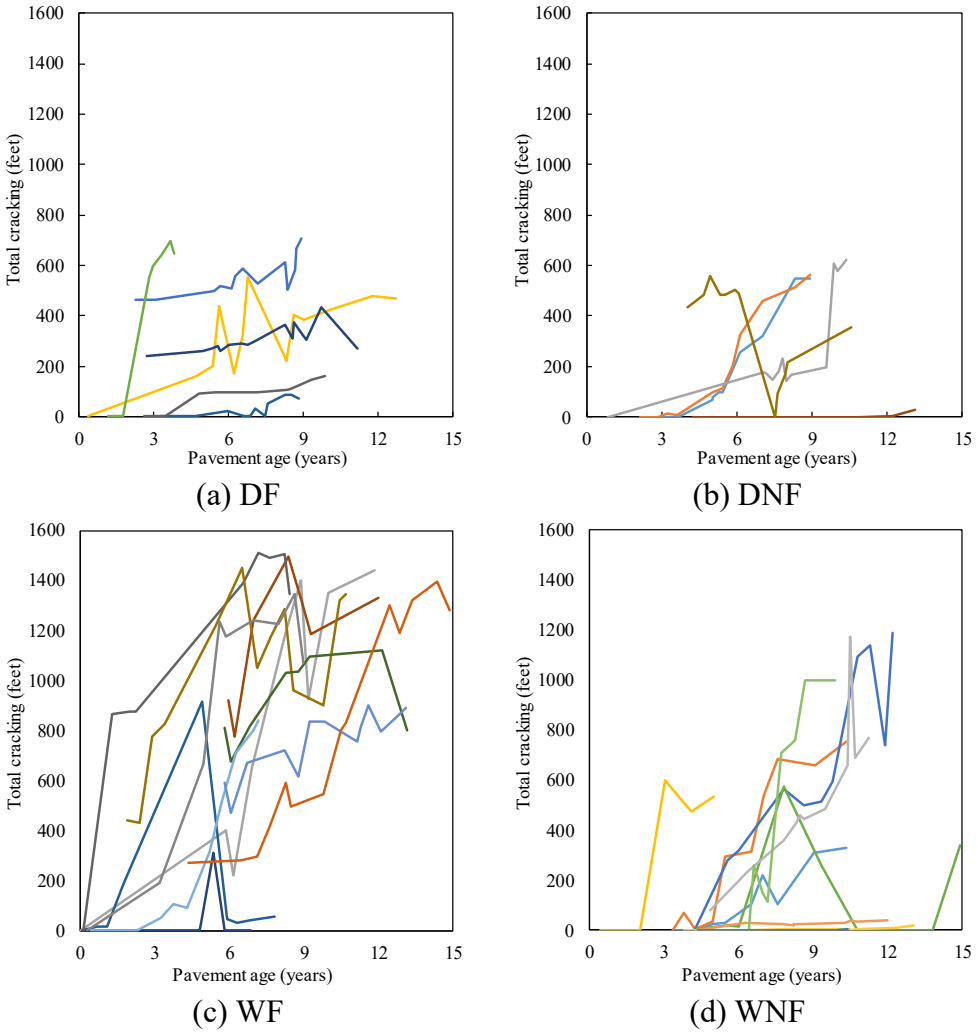

Figure 4-4 Cracking progression with age in flexible pavements sections

Figure 4-5 shows rigid pavements cracking and joint seal damage progression with age in different climates. Due to a limited number of PCC sections, SMP sections located in DF/DNF and WF/WNF regions were combined. As compared to DF/DNF, much greater cracking extents were observed in WF/WNF regions. Additionally, as compared to longitudinal and transverse cracking, the joint sealant damage extents were significantly high.

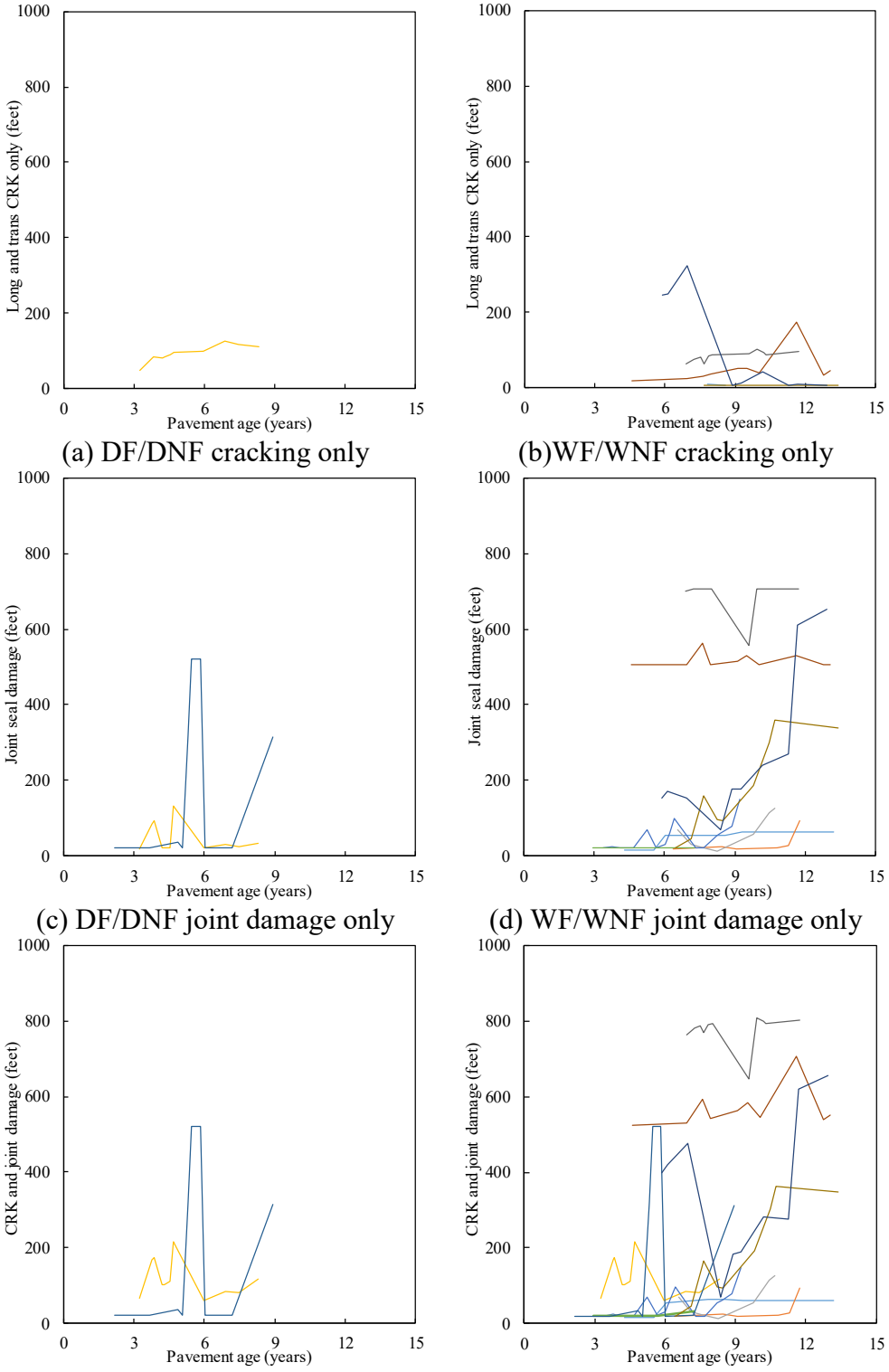

Figure 4-5 Cracking progression with age in rigid pavements sections

Figure 4-6 shows the precipitation extents for flexible and rigid SMP pavement sections located in different climates. As compared to dry climates, higher precipitation levels were observed in wet climates.

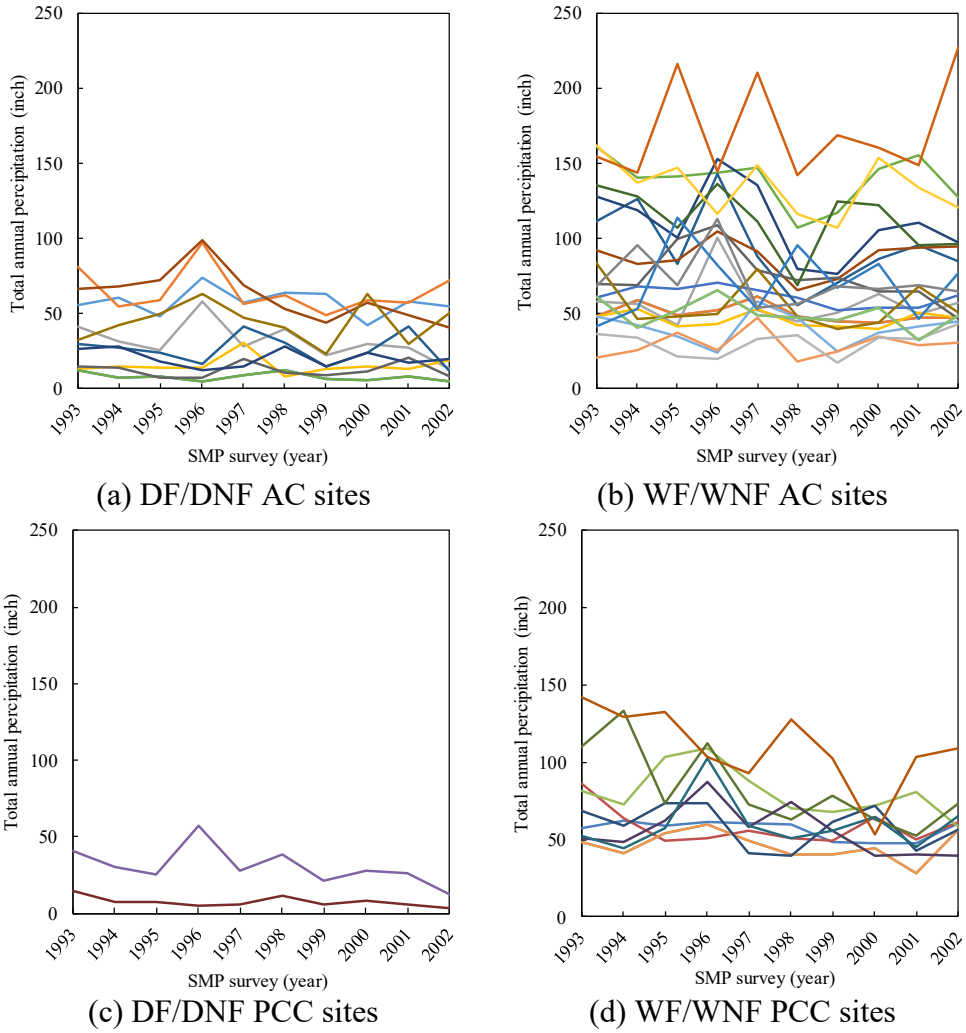

Figure 4-6 Precipitation levels in different climates

Figure 4-7 shows the base layer moisture variations with age for the flexible pavements SMP sections located in different climates. As compared to dry regions, subsurface moisture greatly fluctuated for the SMP sites located in wet climates.

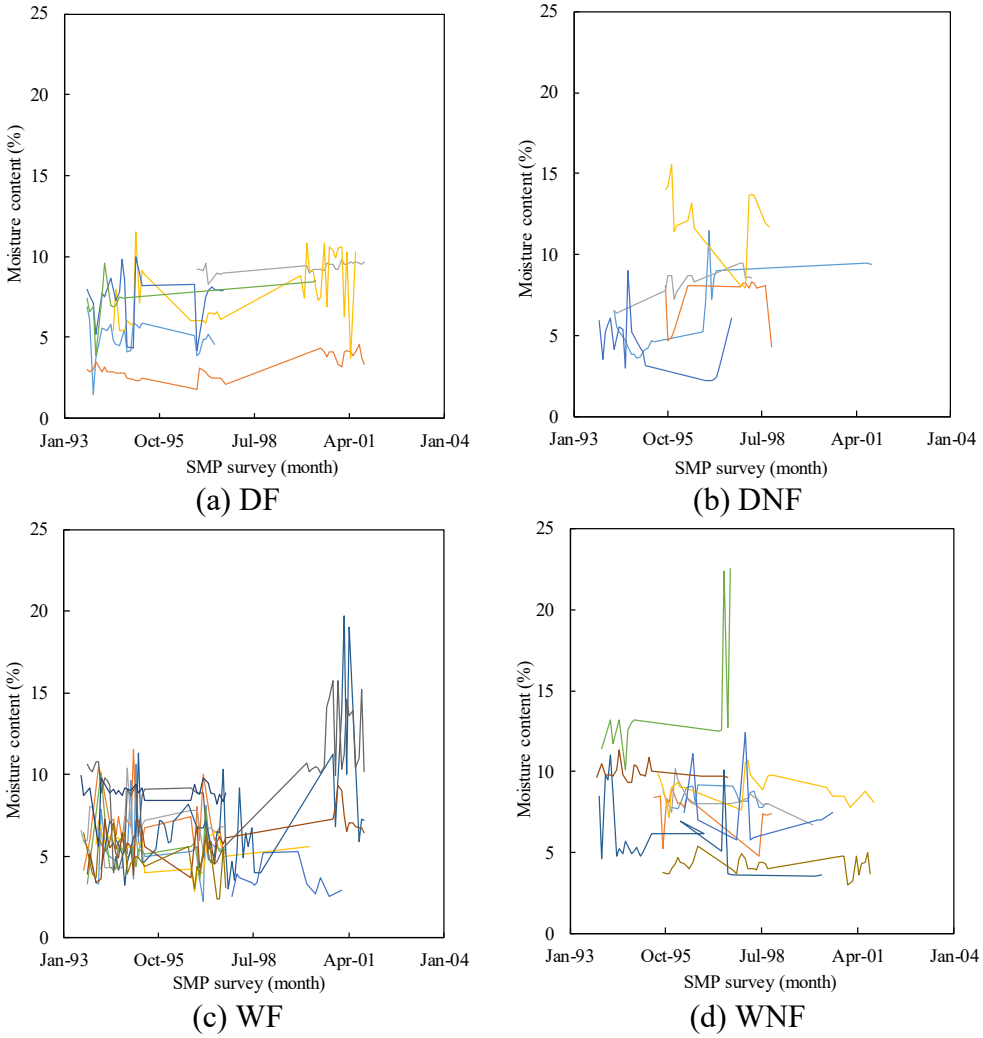

Figure 4-7 Moisture variations in base layer — flexible SMP sections

Figure 4-8 shows the base layer moisture variations with age for the rigid pavements SMP sections located in different climates. Similar to flexible pavements sections, higher moisture fluctuations are observed for the rigid pavements sections located in wet climates.

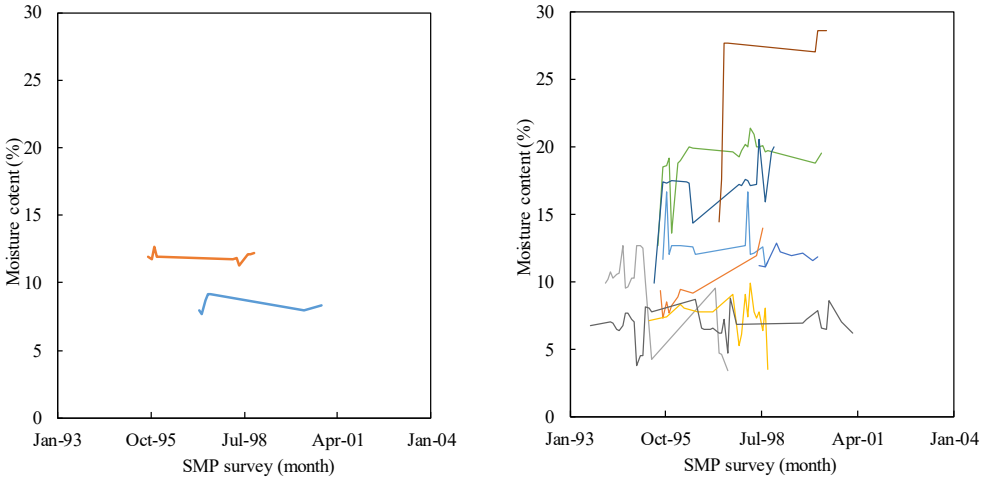

(a) DF/DNF (b) WF/WNF

Figure 4-8 Moisture variations in base layer — rigid SMP sections

4.4 IDENTIFYING SIGNIFICANT VARIABLES

Correlation matrix between different variables in flexible and rigid SMP pavements sections is given in Table 4-2 and Table 4-3, respectively.

Table 4-2 Correlation matrix flexible pavements sections

Pearson Correlation Coefficients, N = 215 Prob > |r| under H0: Rho=0									
	Moisture content	**Age**	**Cracking**	**HMA thickness**	**P200**	**MC depth**	**FI**	**Temp**	**Precipitation**
Moisture content	1	**0.231**	**-0.069**	**-0.069**	**0.172**	**-0.120**	**-0.130**	**0.156**	**0.027**
		0.0006	0.3111	0.3146	**0.0114**	**0.0789**	0.0566	0.0224	0.6931
Age	0.231	1	0.408	0.082	0.076	0.032	0.128	0.041	-0.023
	0.0006		<.0001	0.2314	0.2698	0.6457	0.0617	0.5509	0.7368
Cracking	-0.069	0.408	1	0.100	-0.283	-0.022	0.486	-0.164	0.110
	0.3111	<.0001		0.1441	<.0001	0.7472	<.0001	0.0163	0.1065
HMA thickness	-0.069	0.082	0.100	1	-0.355	0.752	0.026	-0.126	0.145
	0.3146	0.2314	0.1441		<.0001	<.0001	0.7066	0.0661	0.0336
P200	0.172	0.076	-0.283	-0.355	1	-0.281	-0.317	0.176	-0.133
	0.0114	0.2698	<.0001	<.0001		<.0001	<.0001	0.0098	0.0516
MC depth	-0.120	0.032	-0.022	0.752	-0.281	1	-0.093	0.020	0.095
	0.0789	0.6457	0.7472	<.0001	<.0001		0.1734	0.7707	0.1646
FI	-0.130	0.128	0.486	0.026	-0.317	-0.093	1	-0.277	0.267
	0.0566	0.0617	<.0001	0.7066	<.0001	0.1734		<.0001	<.0001
Temp	0.156	0.041	-0.164	-0.126	0.176	0.020	-0.277	1	-0.380
	0.0224	0.5509	0.0163	0.0661	0.0098	0.7707	<.0001		<.0001
Precipitation	0.027	-0.023	0.110	0.145	-0.133	0.095	0.267	-0.380	1
	0.6931	0.7368	0.1065	0.0336	0.0516	0.1646	<.0001	<.0001	

Table 4-3 Correlation matrix rigid pavements sections

Pearson Correlation Coefficients, N = 53 Prob > |r| under H0: Rho=0											
	Moisture content	Age	Joint seal damage	long and trans Cracking	combined cracking and jointdamge	PCC thickness	P200	MC depth	FI	Temp	Precipitation
Moisture content	1	**0.336**	**0.664**	**-0.038**	**0.593**	**0.155**	**0.425**	**0.150**	**-0.184**	**-0.119**	**0.115**
		0.014	<.0001	0.786	<.0001	0.268	0.002	0.285	0.188	0.398	0.411
Age	0.336	1	0.274	-0.038	0.239	0.148	0.280	0.169	0.294	-0.262	0.324
	0.014		0.047	0.786	0.085	0.291	0.043	0.228	0.033	0.058	0.018
Joint seal damage	0.664	0.274	1	0.277	0.973	0.392	0.320	0.285	-0.306	-0.012	0.158
	<.0001	0.047		0.045	<.0001	0.004	0.020	0.039	0.026	0.931	0.260
Long and trans cracking	-0.038	-0.038	0.277	1	0.492	0.558	-0.139	0.462	0.093	-0.050	0.008
	0.786	0.786	0.045		0.000	<.0001	0.320	0.001	0.510	0.722	0.953
Cobined cracking and joint damge	0.593	0.239	0.973	0.492	1	0.490	0.256	0.369	-0.255	-0.023	0.145
	<.0001	0.085	<.0001	0.000		0.000	0.064	0.007	0.065	0.870	0.301
PCC thickness	0.155	0.148	0.392	0.558	0.490	1	-0.409	0.899	0.333	-0.148	0.050
	0.268	0.291	0.004	<.0001	0.000		0.002	<.0001	0.015	0.289	0.720
P200	0.425	0.280	0.320	-0.139	0.256	-0.409	1	-0.427	-0.347	-0.045	0.256
	0.002	0.043	0.020	0.320	0.064	0.002		0.001	0.011	0.749	0.064
MC depth	0.150	0.169	0.285	0.462	0.369	0.899	-0.427	1	0.340	-0.126	-0.029
	0.285	0.228	0.039	0.001	0.007	<.0001	0.001		0.013	0.368	0.835
FI	-0.184	0.294	-0.306	0.093	-0.255	0.333	-0.347	0.340	1	-0.269	0.055
	0.188	0.033	0.026	0.510	0.065	0.015	0.011	0.013		0.052	0.696
Temp	-0.119	-0.262	-0.012	-0.050	-0.023	-0.148	-0.045	-0.126	-0.269	1	-0.701
	0.398	0.058	0.931	0.722	0.870	0.289	0.749	0.368	0.052		<.0001
Precipitation	0.115	0.324	0.158	0.008	0.145	0.050	0.256	-0.029	0.055	-0.701	1
	0.411	0.018	0.260	0.953	0.301	0.720	0.064	0.835	0.696	<.0001	

The correlations of moisture content with independent variables were not very strong. However, by running forward and backward model selection in statistical analysis system (SAS) and then by extensively running the genetic algorithm, following variables were identified for accurate estimation of moisture variation in the base layer.

- Surface cracking
- Moisture depth
- P200
- Precipitation
- FI
- Subsurface temperature

Moisture depth and HMA/PCC layer thicknesses were highly correlated, therefore considering the relationship with subsurface moisture, only moisture depth was included in further modeling. Freezing index was included as an independent variable to keep a record of freeze and no freeze regions.

4.5 DEVELOPMENT OF EMPIRICAL MODELS

As highlighted earlier, the main objective of this study is to investigate the additional amount of moisture in the pavement base layer due to infiltration of water through surface cracks in different climates. SMP data in LTPP is highly scattered due to large variations in climate, material, and pavement structure. With preliminary correlations, significant variables like surface cracking, joint seal damage, precipitation, subsurface temperature, moisture depth, and % passing No.200, were identified which could probably cause a change in base layer moisture content. Different multilinear, nonlinear and polynomial regression techniques were used to develop the relationship between independent variables and subsurface moisture content. However, due to the complexity and great variation within the data, none of these procedures

yielded desired results. Finally, Artificial Neural Network (ANNs) were used to model the data and it gave reasonable results with an acceptable degree of error.

4.6 FLEXIBLE PAVEMENTS MODELING

This section presents the subsurface moisture prediction models developed to estimate base layer in-situ moisture content. It also documents the potential impacts of subsurface moisture variations on base MR. Subsequently, the influence of base MR on long-term pavement performance in terms of predicted cracking are discussed. Based on the results, appropriate crack sealing application timings are recommended to extend the service life of flexible pavements in different climates.

4.6.1 Site-Specific Models for Flexible Pavements

As the first step, data from individual SMP pavements sections were used to develop empirical correlations. The site-specific models gave a good insight of the moisture variation phenomenon in the base layer; however, due to a typical climate and material type these models lacked potential of the universal application. In the beginning, separate models were developed for wet and dry climates. Eureqa (genetic algorithm) (*54*) toolbox was used to establish a relationship for base layer moisture content as a function of surface cracking, precipitation, and subsurface temperatures. Equation (1) shows the model developed for DF/DNF region using data from two SMP sites.

$$MC = 7.57 + 0.338P + 0.00329C + 0.00494T \times P + 0.000458P \times T^2 + \left(\frac{0.000517T^2 - 0.000517T}{P - 0.0691T} \right) \quad (1)$$

where,

MC = Gravimetric moisture content (%)
P = Precipitation (inch)
C = Total monthly Cracking (feet)
T = Average monthly temperature (ºC)

Equation (2) shows the model developed for WF region using data from one SMP section.

$$MC = 6.41 + 0.601P + 0.016C \times P - 0.071T - 0.000708C \times T \quad (2)$$

Figure 4-9 shows the goodness of fit for both the models.

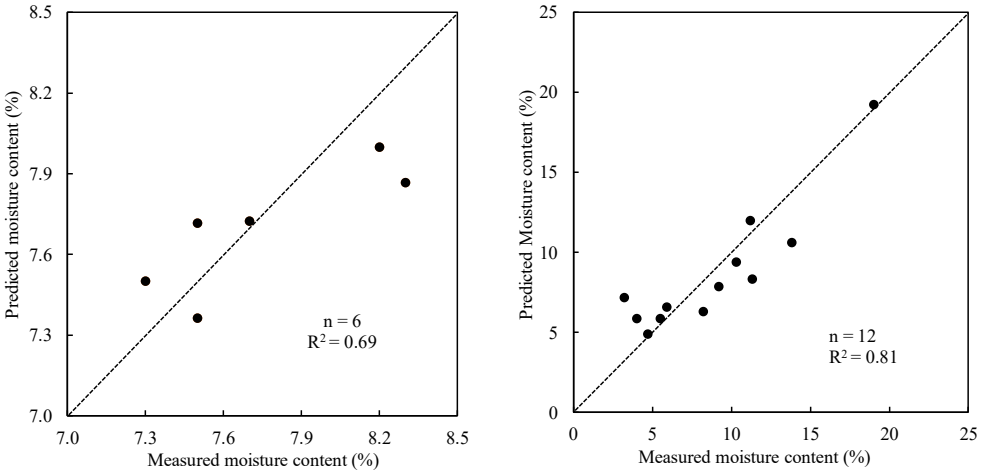

(a) DF/DNF climate (b) WF climate

Figure 4-9 Measured Vs. predicted site-specific models for flexible pavements

Figure 4-9 (a) shows that variation of moisture is very small in dry climates. To address greater variability and limited applicability of site-specific moisture prediction models, the scope of data modeling was expanded by adding data from all available flexible SMP pavement sections for further data analysis and modeling. This was a very challenging task because the variety and extents of climatic, material and pavements structure variations. Finally, five independent variables were chosen for ANN modeling. Subsurface temperature data were not used in further analysis due to its insignificance, and to reduce the number of independent variables.

4.6.2 ANN Modeling Flexible Pavements

ANNs are computational modeling tools that have lately emerged and found extensive acceptance in many disciplines for handling very complex problems. They can be defined as structures consist of tightly interconnected processing elements (called artificial neurons or nodes) operating in parallel (*55, 56*). ANNs are capable of solving non-linear problems by acquiring information and restructuring the relationship between independent variables and response variables even when the information and data are complex, noise-contaminated, and incomplete (*57*). ANN is an information processing system that replicates functioning of a human brain by emulating the functioning and connectivity of biological neurons (*58, 59*). ANN does not need much of detailed description or formulation of the underlying process, and thus widely received by practitioners and researchers, who tend to rely on data. Depending on the network structure, usually, a series of connecting neuron weights are altered to reduce the error between training data outputs and the network predicted outputs (*60*). When a neuron weight is adjusted, it is said that the neuron is learning. The training is the process through which NN learns. Depending on the complexity of the data and intended use, ANN can be composed of one or more hidden layers (*61, 62*). More discussion on ANN training can be found elsewhere (*58*). In the current study, ANN fitting app in MATLAB toolbox was used to establish a relationship for base layer moisture content as a function of surface cracking, precipitation, moisture depth, the percentage passing #200, and freezing index (FI). Since ANN toolbox is equipped with flexible hidden layer and neuron features, very complex trends in the data can be captured by selecting the best layer and neurons combination.

Using LTPP SMP data, multi-layer perceptron (MLP) (single input layer, single hidden layer, and single output layer) feedforward-backpropagation artificial neural network (BPNN) was developed with hidden sigmoid neurons and linear output neurons. A feedforward NN consists of series of layers. The first layer has a connection from the network input. Each subsequent layer has a connection from the previous layer. The final layer gives the network's output. Feedforward networks can be used for any kind of input to output mapping (*63*). ANNs toolbox in MATLAB provides different features and apps to deal with complex nonlinear systems that are not easily modeled with a closed-form equation (*64*).
The main network architecture is the number of hidden layers and number of neurons (NoN). The selection of these parameters largely depends on the complexity of the data inputs used for training. If the NoN are too low, the network may not capture the real trends in the data. If the NoN are too high, it may over fit the data. There is no exact guide for the choice of the NoN, and the optimum model design is often achieved by trial and error (*58, 65*). MATLAB ANN fitting app also provides different options for network training and layer activation functions; those are chosen based on available memory, computational speed, and research needs. The aim of the best suitable training function is to train the network at relatively fast speed with high precision. Levenberg - Marquardt backpropagation (trainlm), Bayesian regularization backpropagation (trainbr), and Scaled conjugate gradient backpropagation (trainscg) are widely used network training functions available in MATLAB ANN toolbox, whereas main transfer functions are, Hyperbolic tangent sigmoid transfer function (tansig), Log-sigmoid transfer function (logsig), and Linear transfer function (purelin).To develop ANN model for this study trainlm was used to train the network, tansig and purelin activation functions were used for the hidden and output layer neurons, respectively. Detail description of training and transfer functions and related algorithms is given elsewhere (*63*).
The layer activation and network training functions used for this study are briefly discussed in subsequent paras.

4.6.2.1 Network Training Function — trainlm

Trainlm is a network training function in MATLAB toolbox that adjusts the weights and bias values according to Levenberg-Marquardt algorithm (LMA) optimization. LMA or just LM, also known as damped least-square (DLS) method is used to address non-linear least square problems. It is often the fastest backpropagation algorithm in the MATLAB toolbox, as is highly recommended as a first choice supervised algorithm, though it requires more memory than other training algorithms(*63*). As opposed to unsupervised training function, a supervised training algorithm requires target (response variable) data (*66*).
Like the quasi-Newton methods (*67*), the LMA was developed to approach second-order training speed without having to compute the Hessian matrix. The Hessian matrix or Hessian is a square matrix of second-order partial derivatives of a scalar-valued function, or scalar field which describes the local curvature of a function of many variables (*68*). LMA uses the Jacobian for calculations, therefore the network trained with this function must use either mean squared error (MSE) or the sum of squared errors (SSE) as performance function. When the performance function is SSE (*63*), as mostly the case for feed-forward networks, then Hessian matrix (H) and the gradient (g) can be estimated as:

$$H = J^T J \tag{3}$$

$$g = J^T e \tag{4}$$

Where J is the Jacobian matrix contains the first derivative of the network errors concerning the weights and biases, and e is the vector of network errors. The Jacobean matrix is computed through a standard backpropagation technique that is much less complex than computing the Hessian matrix. The Levenberg-Marquardt algorithm uses this approximation to the Hessian matrix in the following Newton-like update (*69*):

$$X_{k+1} = X_k - [J^T J + \mu I]^{-1} J^T e \tag{5}$$

When the scalar μ is zero, this is just Newton's method, using the approximate Hessian matrix. When μ is large, this becomes gradient descent with small step size. Newton's method is faster and more accurate near an error minimum, so the aim is to shift toward Newton's method as quickly as possible. Thus, μ is decreased after each successful step (reduction in performance function) and is increased only when a tentative step would increase the performance function. In this way, the performance function is always reduced at each iteration of the algorithm. Further discussion on LMA and its application in NN training is described elsewhere (*70, 71*).

4.6.2.2 Hidden and Output Layer Transfer Function — (tansig and purelin)

Transfer functions are generally allocated to a network layer to first start the input signal, followed by the calculation of appropriate weight for the output signal such that the relationship between the input and target data can be ascertained (*57*). Mathematical expressions for mainly used transfer functions in ANN models given in the following equations:

$$\tan sig\ (n) = \frac{2}{1 + e^{(-2n)} - 1} \tag{6}$$

$$\log sig\ (n) = \left(\frac{1}{1 + e^{-n}}\right) \tag{7}$$

$$purelin\ (n) = n \tag{8}$$

Logsig yields output in the range of 0 to 1, tansig yields output in the range of -1 and +1, and purelin yields output in the range of $-\infty$ to $+\infty$(*58, 72*). Sigmoid transfer functions are usually used in hidden layers, and linear functions are used in the output layer. The hyperbolic tangent sigmoid transfer function (tansig) is mathematically equivalent of tanh(n). In NN, it is widely used as hidden layer activation function; it runs faster than the MATLAB application of tanh(n) with very small numerical differences. This function is a good tradeoff for NN applications, where speed is important, and the exact shape of the transfer function is not (*73, 74*). Linear transfer (purelin) is mainly used as the output layer transfer function for function fitting (or nonlinear regression) problems. Logsig is frequently used in output layer for pattern recognition problems(in which decision is made by the network), where the output range is between 0 and 1 (*63*). Variations in layer activation functions are primarily due to the high ANN sensitivity to the type of data. Likewise, different data inputs would require different activation functions in ANN

architecture. No single network settings can be universally applied to model different types of problem situations effectively (*57*).
Besides many pros, due to the inherent complexity of ANN models, they are not easy to interpret and understand. Optimum settings for the ANN model that was developed using data from 32 flexible SMP sites are given in Table 4-4. However; the best network configuration may vary from case to case and largely depend on input/output data type and complexity. Figure 4-10 shows the schematic of ANN model developed for the flexible pavements sections.

Table 4-4 Optimum settings for the flexible pavements ANN model

Network type	BPNN
No of hidden layer	1
Data entries for training, testing, and validation	151,32,32
Training function	trainlm
Hidden layer transfer function	tansig
Output layer transfer function	purelin
Performance function	MSE
No of hidden neurons	37

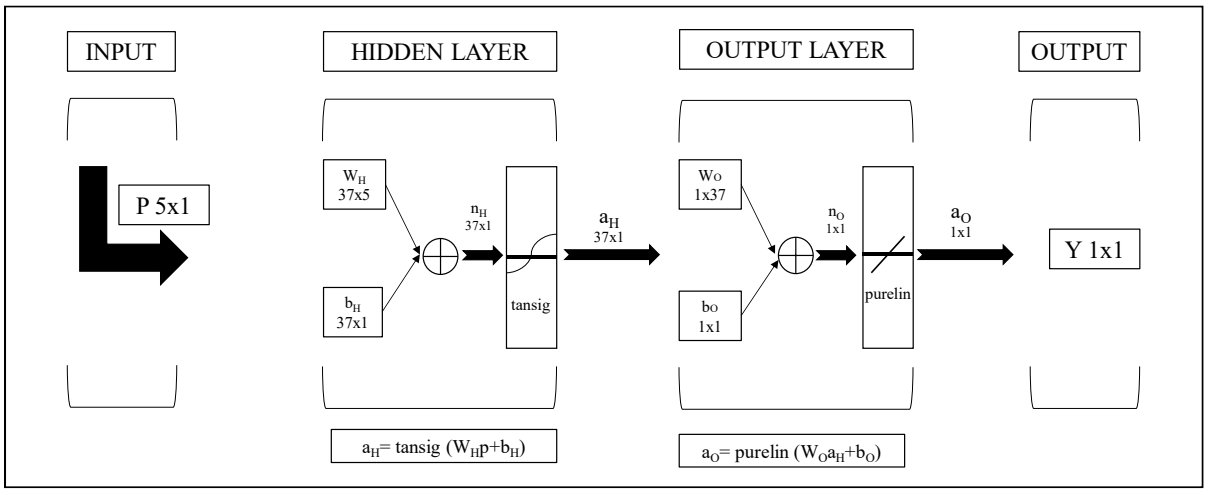

Figure 4-10 ANN model flow for flexible pavements SMP sections

Figure 4-11(a) shows the goodness of fit for ANN model. Figure 4-11(b), (c), and (d) show model sensitivity to different inputs. The results of the ANN model sensitivity show that with an increase in surface cracking, there is an increase in the base moisture levels. This change in moisture is significant in WF/WNF climates with higher precipitation levels [see Figure 4-11(b)]. Higher the percentage passing 200, higher is the moisture, higher the depth of moisture within the base layer, lower is the moisture [see Figure 4-11 (c) and (d)]. It can be seen in Figure 4-11(d) that effect of moisture content depth is minimal. It is worth noting that when the cracking reaches approximately 70 to100 meters in length, moisture content increases exponentially.

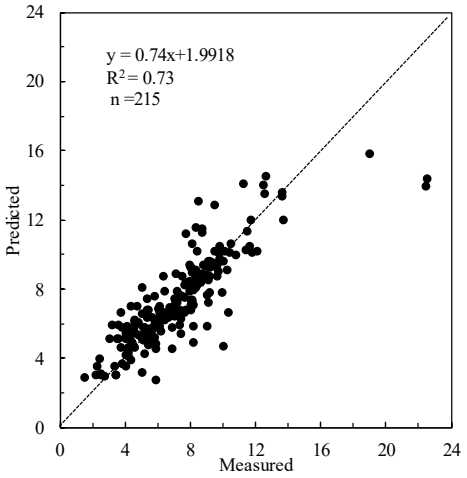

(a) Measured Vs predicted

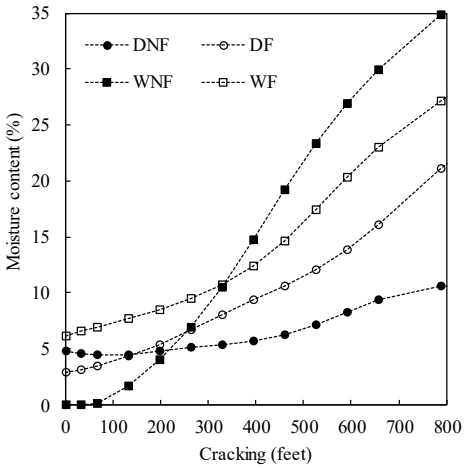

(b) Effect of Precipitation and freezing

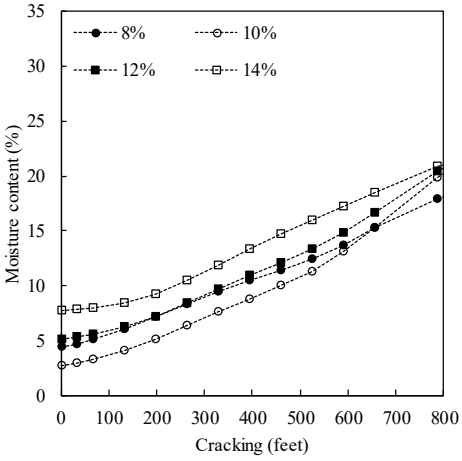

(e) Impact of percent passing 200

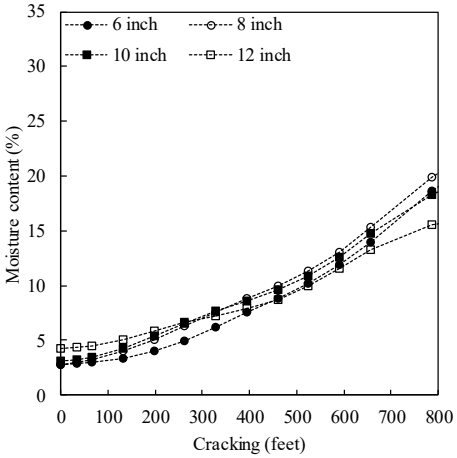

(f) Impact of MC depth

Figure 4-11 ANN model predictions and sensitivity — flexible pavements

To see the effect of precipitation alone, its levels were varied between 0 and 30 inches for ANN predictions in wet regions. The ANN model predictions show that moisture increases with increase in precipitation levels up to a certain limit, and then the effect of precipitation becomes negligibly. This implies that after a certain amount of precipitation base layer reaches saturation and a further increase in precipitation may not cause much moisture variation [see Figure 4-12].

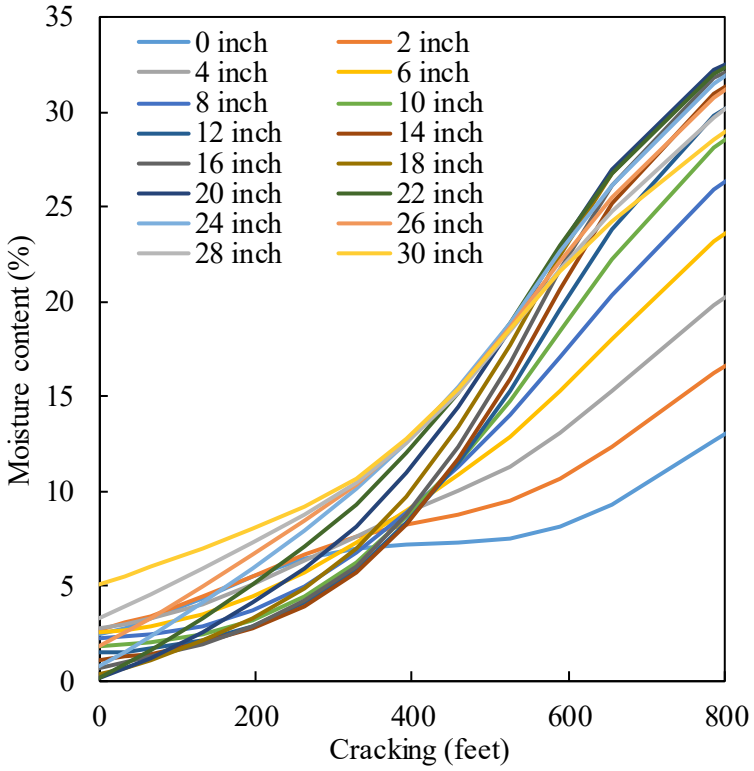

Figure 4-12 Effect of precipitation on moisture variations

Figure 4-13 shows moisture profiles with depth for two SMP sections before and after a considerable amount of cracking. These profiles help to visualize the overall moisture variation in the pavement system for the sites located in wet and dry regions. It is evident from the moisture profiles that change in moisture is more pronounced at the top few inches of the pavement section, i.e., up to base/subbase layers. The relative change in moisture becomes negligible below subbase levels. Figure 4-13 (a) and (b) show moisture variation in base layer for two pavement sections located in WF and DF climates, respectively. More substantial moisture variations in WF climate are mainly because of the higher rainfall and greater extent of cracking for the selected pavement sections. In contrast, the overall change in base layer moisture for the selected site located in DF climate is minimal. It is mainly because of low precipitation in these particular locations [see Figure 4-13 (b)].

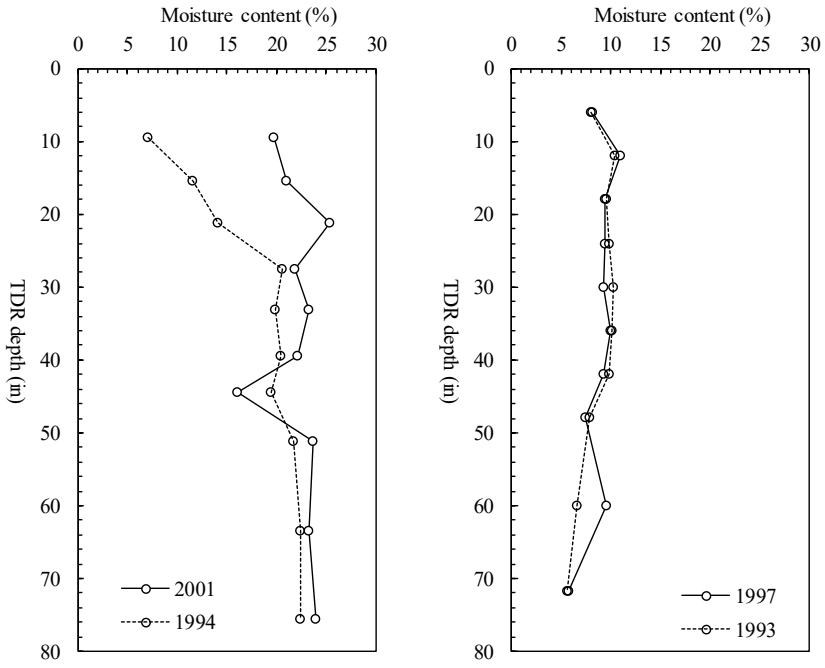

(a) 36-0801 (WF) (b) 56-1007 (DF)

Figure 4-13 Moisture variations with depth in DF/WF region

4.6.3 Impact of Base Moisture on Long-Term Performance

The surface cracks increase the infiltration of water into pavement sublayers. Therefore, the moisture levels will increase in the unbound materials. Moisture variations in base layer will affect the MR of the unbound materials. The SMP sections show that there can be significant variations in base layer moisture, especially in wet climates. The moisture changes can be used to obtain MR of the base material. Subsequently, the calculated MR can be used to predict long-term pavement performance by using the Pavement-ME Design Guide. A brief discussion of these effects is provided next.

4.6.3.1 The Relationship between Base Moisture and Base MR- Flexible Pavements

Witzack model (briefly discussed in Chapter 2) was used to estimate the base layer MR due to variation in in-situ moisture. This model needs several inputs, including % passing 200, LL, PL, D60, and Gs. All the required inputs were obtained from the LTPP database for all the sections. Figure 4-14 shows the relationship between estimated base MR and moisture levels in different climates. The results show that as the moisture content increases, the MR decreases. However, the change is small in DF/DNF regions (approximately 18 to 41% for a particular section) as shown in Figure 4-14 (a) and (b). For the WF/WNF climate, the maximum change in base layer MR can reach approximately 153 to 175% (for a particular section), as shown in Figure 4-14(c) and (d).

Table 4-5 Summary — Change in MR due to moisture variations

Section ID	Climatic region	Minimum MR (psi)	Maximum MR (psi)	Reduction in MR (%)
08_1053	DF	41916.0	42481.6	1%
16_1010	DF	43105.3	44483.2	3%
30_0114	DF	43816.0	44120.6	1%
32_0101	DF	39392.3	41190.8	5%
46_0804	DF	36578.6	43105.3	18%
56_1007	DF	41480.9	43859.5	6%
04_0113	DNF	41451.9	43729.0	5%
04_0114	DNF	40161.0	42032.0	5%
04_1024	DNF	29051.1	41002.2	41%
35_1112	DNF	41364.8	44077.0	7%
49_1001	DNF	42960.3	44352.6	3%
09_1803	WF	40987.7	41829.0	2%
23_1026	WF	42322.1	42974.8	2%
25_1002	WF	41654.9	43322.9	4%
27_1018	WF	40567.1	43670.9	8%
27_6251	WF	43061.8	44120.6	2%
31_0114	WF	42249.6	44323.6	4%
33_1001	WF	42989.3	43772.5	2%
36_0801	WF	16055.7	44135.1	175%
50_1002	WF	41205.3	43845.0	6%
83_1801	WF	32894.6	43917.5	34%
87_1622	WF	43047.3	43816.0	2%
01_0101	WNF	40857.2	41988.5	3%
01_0102	WNF	41654.9	43743.5	5%
10_0102	WNF	39929.0	42032.0	5%
13_1005	WNF	38783.2	40132.0	3%
13_1031	WNF	43134.3	43729.0	1%
48_1060	WNF	13387.0	33822.9	153%
48_1077	WNF	37622.9	43961.0	17%
48_1122	WNF	39203.8	40190.0	3%
51_0113	WNF	41002.2	42728.2	4%
51_0114	WNF	43090.8	43990.0	2%

Note: Results based on approximately 8-9 years of measured SMP LTPP data.

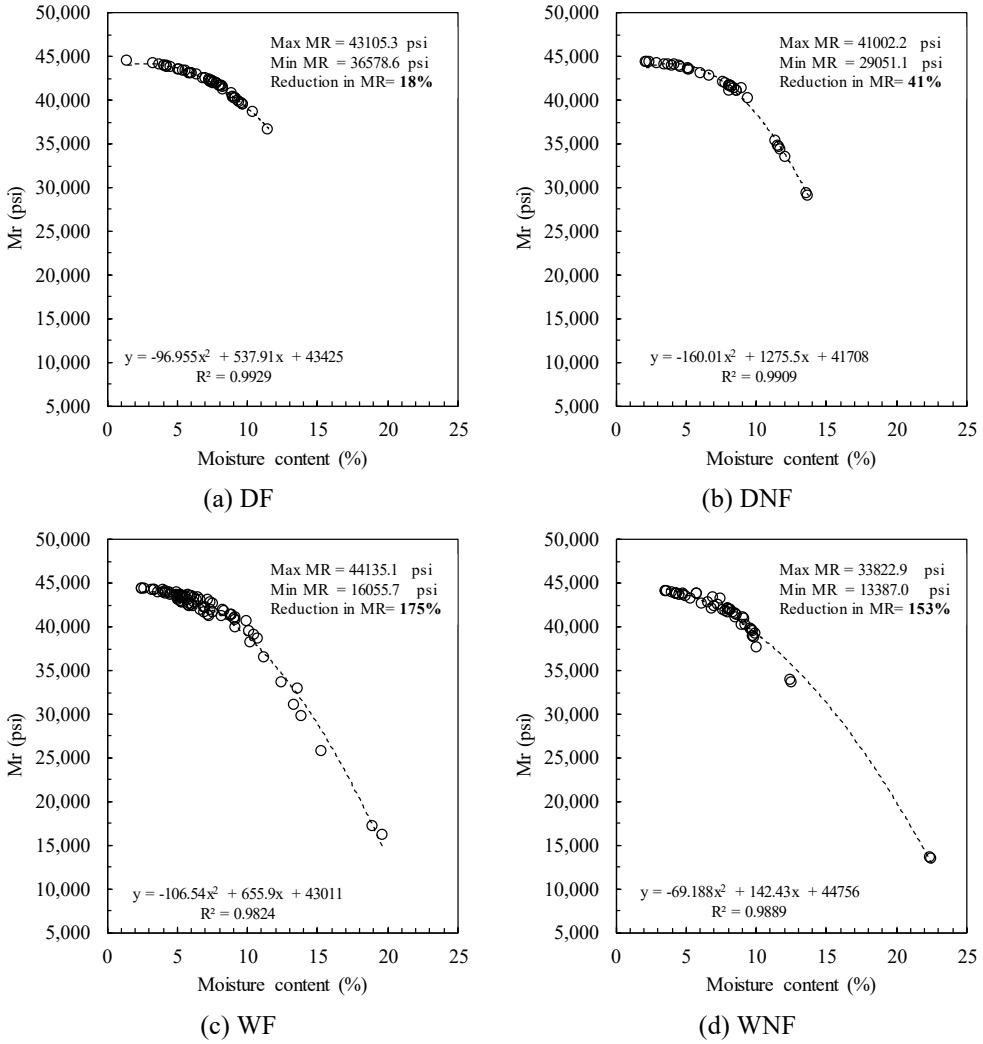

Figure 4-14 Impact of moisture variations on flexible pavements base MR

4.6.3.2 Impact of Flexible Base Resilient Modulus on Long-Term Pavement Performance

The moisture variations and its adverse impact on base MR were quantified for the pavement sections located in different climates. While evaluating the impact of base MR on long-term pavement performance, two flexible pavement sections were considered with the cross-section details as shown in Figure 4-15.

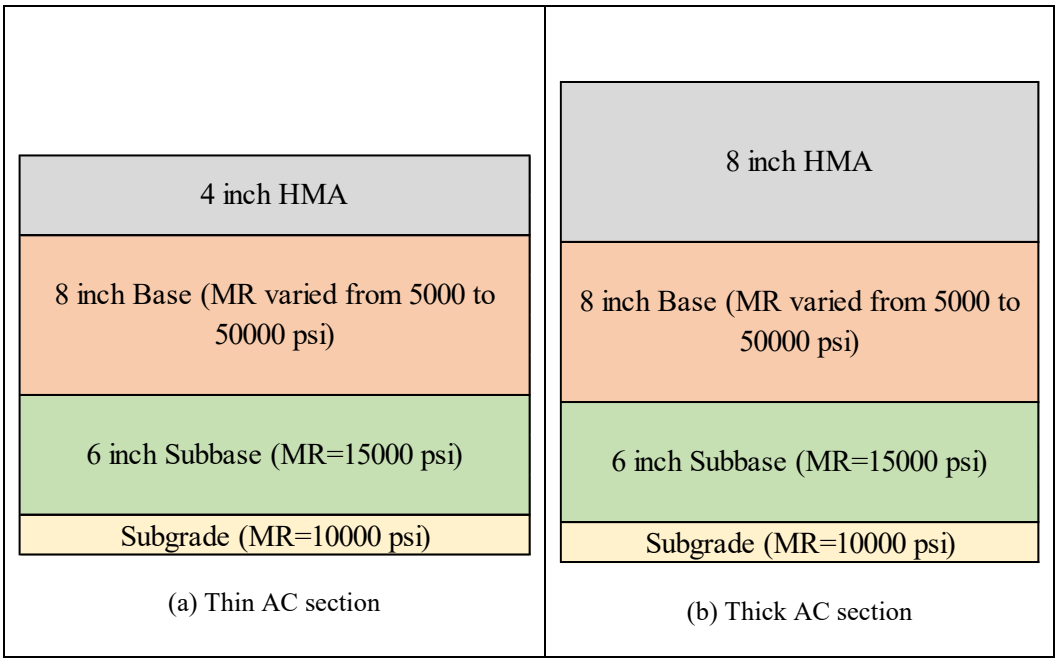

Figure 4-15 Flexible pavement cross sections

The long-term performance was predicted for approximately 14 million ESALs by using the Pavement-ME. Base MR Values were varied from 5000 to 50000 (psi) in the Pavement-ME runs to compare the performance of both the sections. Climatic data from two different weather stations were used to simulate different climates in the Pavement-ME. Weather stations located in Washington and New York were used to simulate DNF and WF climates, respectively. Figure 4-16(a) shows the relationship between total predicted cracking and MR for thin and thick sections located in WF/DNF climates. It can be observed that with a decrease in base MR, amount of surface cracking increased. As compared to dry regions, slightly higher surface cracking extents were observed in wet regions. In addition, much higher levels of surface cracking were observed in thinner section, essentially because of higher traffic. With the decrease in base layer MR values, total surface rutting also increased, this trend is more pronounced for the thin section as compared to thick section, especially for the pavements located in wet climates [see Figure 4-16(b)]. Figure 4-16(c) and (d) show the impact of base moisture on total cracking and rutting in different climates. The results show that for thin HMA sections in wet regions, if the MR is decreased by 175 percent (from 44135 to 16055 psi i.e., the maximum reduction in MR values due to moisture in wet climates), there will be about 102% increase in the long-term total cracking [see Figure 4-16(c)]. Similarly, for thick HMA section in wet regions, the increase in cracking is about 114%. Figure 4-16(d) shows the relationship between predicted rut depths with a change in base MR. In wet climates, a 175% reduction in base MR showed about 17% and 6% increase in surface rutting for thin and thick pavement

sections, respectively. Alike, if the MR is decreased by 41 percent (from 41002 to 29051 psi i.e., the maximum reduction in MR values due to moisture in dry climates), there will be 35% and 38% increase in long-term total cracking and about 6% and 2% increase in surface rutting for thin and thick sections, respectively. Table 4-6 provides the grand summary of measured/ANN predicted moisture data and Pavement-ME performance data.

Table 4-6 Summary measured /predicted moisture data and Pavement-ME performance

Moisture data type used for calculations	LTPP climatic region	Change in measured moisture content			Reduction in MR based on measured moisture			Increase in cracking						Increase in rutting					
								Thick section			Thin section			Thick section			Thin section		
		Maximum moisture (%)	Minimum moisture (%)	Range moisture (%)	Maximum MR (psi)	Minimum MR (psi)	Reduction in MR (%)	Total cracking (feet) at Maximum MR	Total cracking (feet) at Minimum MR	Increase in cracking (%)	Total cracking (feet) at Maximum MR	Total cracking (feet) at Minimum MR	Increase in cracking (%)	Total rutting (in) at Maximum MR	Total rutting (in) at Minimum MR	Increase in rutting (%)	Total rutting (in) at Maximum MR	Total rutting (in) at Minimum MR	Increase in rutting (%)
Measured LTPP	DF	11.5	6	5.5	43105	36579	**18%**	453	538	**18%**	1716	2001	**17%**	0.94	0.94	**1%**	1.30	1.34	**2%**
	DNF	13.7	8.1	5.6	41002	29051	**41%**	440	663	**38%**	1801	2425	**35%**	0.94	0.98	**2%**	1.30	1.38	**6%**
	WF	19.7	3.2	16.5	44135	16056	**175%**	440	922	**114%**	1680	3399	**102%**	0.94	1.02	**6%**	1.30	1.54	**17%**
	WNF	22.5	12.5	10	33823	13387	**153%**	443	1017	**76%**	2146	3635	**69%**	0.94	1.02	**5%**	1.34	1.57	**16%**
	Wet region	19.7	3.2	16.5	44135	16056	**175%**	440	922	**114%**	1680	3399	**102%**	0.94	1.02	**6%**	1.30	1.54	**17%**
	Dry region	13.7	8.1	5.6	41002	29051	**41%**	440	663	**38%**	1801	2425	**35%**	0.94	0.98	**2%**	1.30	1.38	**6%**
ANN model predictions at 300 feet cracking	DF	8.1	2.9	5.2	44237	41394	**7%**	443	472	**7%**	1677	1785	**6%**	0.94	0.94	**0%**	1.30	1.30	**1%**
	DNF	5.4	4.7	0.7	43830	43236	**1%**	446	453	**1%**	1690	1713	**1%**	0.94	0.94	**0%**	1.30	1.30	**0%**
	WF	10.7	6.2	4.5	43482	33069	**31%**	449	591	**32%**	1703	2185	**28%**	0.94	0.98	**2%**	1.30	1.34	**4%**
	WNF	10.5	0.0	10.5	44570	36796	**21%**	436	535	**22%**	1663	1991	**20%**	0.94	0.94	**1%**	1.30	1.34	**2%**
	Wet region	10.7	0.0	**10.6**	44570	33069	**35%**	436	591	**35%**	1663	2185	**31%**	0.94	0.98	**2%**	1.30	1.34	**4%**
	Dry region	8.1	2.9	**5.2**	44237	41394	**7%**	443	472	**7%**	1677	1785	**6%**	0.94	0.94	**0%**	1.30	1.30	**1%**
ANN model prediction sat 200 feet cracking	DF	5.4	2.9	2.5	44237	43352	**2%**	443	449	**2%**	1677	1706	**2%**	0.94	0.94	**0%**	1.30	1.30	**0%**
	DNF	4.8	4.7	0.1	43830	43540	**1%**	446	449	**1%**	1690	1699	**1%**	0.94	0.94	**0%**	1.30	1.30	**0%**
	WF	8.5	6.2	2.4	43482	38638	**13%**	449	509	**13%**	1703	1903	**12%**	0.94	0.94	**1%**	1.30	1.30	**1%**
	WNF	4.0	0.0	4.0	44570	43830	**2%**	436	446	**2%**	1663	1690	**2%**	0.94	0.94	**0%**	1.30	1.30	**0%**
	Wet region	8.5	0.0	**8.5**	44570	38638	**15%**	436	509	**16%**	1663	1903	**14%**	0.94	0.94	**1%**	1.30	1.30	**2%**
	Dry region	5.4	2.9	**2.5**	44237	43352	**2%**	443	449	**2%**	1677	1706	**2%**	0.94	0.94	**0%**	1.30	1.30	**0%**
ANN model predictions at 100 feet cracking	DF	4.3	2.9	1.4	44237	43816	**1.0%**	443	446	**1%**	1677	1690	**1%**	0.94	0.94	**0%**	1.30	1.30	**0%**
	DNF	4.8	4.7	0.1	43830	43540	**0.7%**	446	449	**1%**	1690	1699	**1%**	0.94	0.94	**0%**	1.30	1.30	**0%**
	WF	7.7	6.2	1.5	43482	40074	**8.5%**	449	489	**9%**	1703	1841	**8%**	0.94	0.94	**0%**	1.30	1.30	**1%**
	WNF	1.7	0.0	1.7	44570	44425	**0.3%**	436	440	**0%**	1663	1670	**0%**	0.94	0.94	**0%**	1.30	1.30	**0%**
	Wet region	7.7	0.0	**7.7**	44570	40074	**11.2%**	436	489	**12%**	1663	1841	**11%**	0.94	0.94	**1%**	1.30	1.30	**1%**
	Dry region	4.8	2.9	**1.9**	44237	43816	**1.0%**	443	446	**1%**	1677	1690	**1%**	0.94	0.94	**0%**	1.30	1.30	**0%**

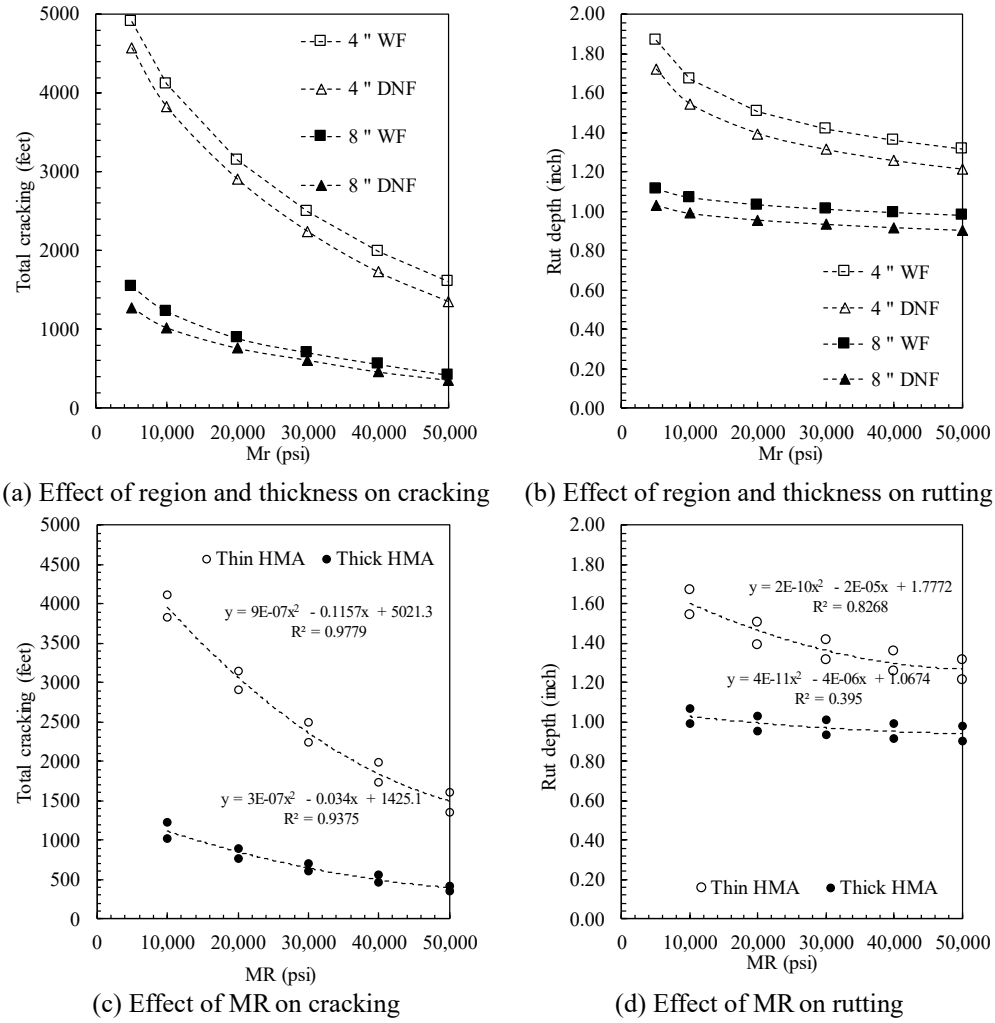

(a) Effect of region and thickness on cracking (b) Effect of region and thickness on rutting

(c) Effect of MR on cracking (d) Effect of MR on rutting

Figure 4-16 Impact of flexible pavements base MR on predicted pavement performance

4.6.3.3 Demonstrative Examples of Crack Sealing Application Timings — Flexible Pavements

The last task of this study was to define optimum timings for effective crack sealing. A few rational assumptions were made based on the data to determine appropriate crack sealing timings. First, the variations in base layer moisture and a corresponding reduction in MR were estimated from the model for a range of cracking—new pavements (at minimal cracking), and old pavements (when surface cracking levels reached 100, 200, and 300 feet) [(for calculations see Table 4-6)]. Figure 4-17 shows the maximum reduction in MR is 7% in dry climates when total surface cracking is 300 feet, for the same level of cracking, the maximum reduction in MR for wet regions is 35%. The results imply that moisture variation severely affects pavements in wet climates, and it is important to seal the cracks when the extent of surface cracking is low (i.e., between 100 to 200 feet). For pavements in dry regions, this cracking extent can be slightly higher i.e., up to 300 feet

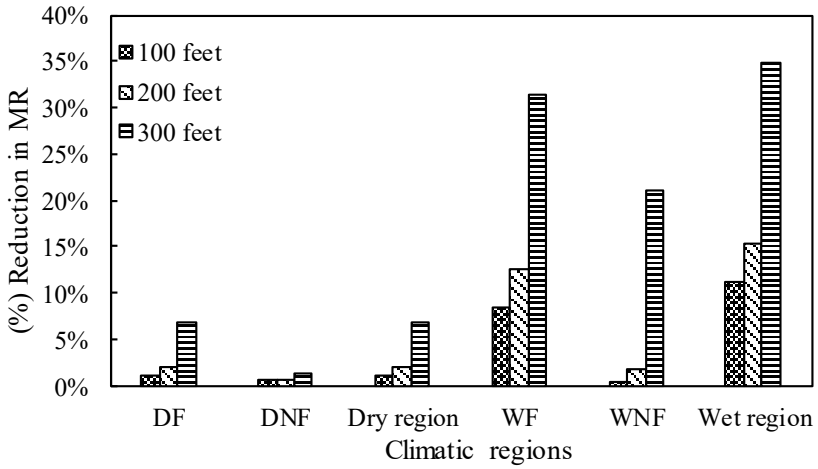

Figure 4-17 Reduction in MR due to increase in moisture at different cracking levels

Since, the develop model uses cracking length (which is calculated based on lengths of different crack types) to predict base moisture, it was important to separate cracks length based on mechanism of cracking (i.e., WP and NWP). Bottom-up fatigue is a classic example of through cracking that would allow the surface water to infiltrate into the pavement unbound layers. Therefore, a second assumption was made about proportion of fatigue cracking length based on the observed cracking data. The observed proportion of WP cracking length (out of total cracking) for all the pavement sections is shown in Table 4-7. Based on the observed data, if on average 50% of the total cracking length is within WP, the optimum crack sealing limits can be estimated in terms of percentage area for fatigue cracking. Based on this assumption, the cracks should be sealed when the WP fatigue is below 6% (average of 4% and 8% corresponds to a total crack length of 100 to 200 feet) and 11% (average of 8% and 13% corresponds to a total crack length of 200 to 300 feet) for the pavements located in wet and dry climates, respectively. Table 4-8 shows the detailed conversions from total cracking length of 100, 200, and 300 feet to percentage area WP fatigue cracking.

Table 4-7 Proportion of observed WP cracking length

Section ID	Climatic region	Pavement age (years)	WP length cracked (feet)	Total cracking length (feet)	Proportion of WP length cracked (%)
08_1053	DF	7.1	480.01	553.50	87%
16_1010	DF	8.6	262.15	581.72	45%
30_0114	DF	6.8	308.74	525.94	59%
32_0101	DF	5.96	23.95	37.73	63%
46_0804	DF	14.2	255.92	693.93	37%
56_1007	DF	9.7	38.06	270.68	14%
04_0113	DNF	8.9	387.81	610.59	64%
04_0114	DNF	9.1	517.41	688.03	75%
04_1024	DNF	10.3	157.16	167.99	94%
35_1112	DNF	7.1	0.00	97.12	0%
49_1001	DNF	16.4	170.28	468.53	36%
09_1803	WF	11.8	117.79	219.50	54%
23_1026	WF	4.9	174.88	917.37	19%
25_1002	WF	15.1	498.71	778.25	64%
27_1018	WF	15.8	436.37	1609.99	27%
27_6251	WF	10.7	494.12	1323.23	37%
31_0114	WF	5.4	313.34	352.71	89%
33_1001	WF	12.1	331.05	881.60	38%
36_0801	WF	13.3	831.08	1345.21	62%
50_1002	WF	15.33	457.04	720.51	63%
83_1801	WF	16.8	852.08	1496.46	57%
87_1622	WF	16.1	1000.71	1573.57	64%
01_0101	WNF	14.1	781.21	829.11	94%
01_0102	WNF	11.9	816.31	843.22	97%
10_0102	WNF	9.4	836.66	1000.71	84%
13_1005	WNF	11.8	219.83	736.91	30%
13_1031	WNF	9.32	0.00	630.61	0%
48_1060	WNF	10.75	38.39	40.03	96%
48_1077	WNF	11.24	268.06	769.72	35%
48_1122	WNF	10.54	5.91	20.67	29%
51_0113	WNF	9.8	908.84	1000.71	91%
51_0114	WNF	13.3	1000.71	1550.27	65%
Average proportion of WP cracking length					**55%**

Table 4-8 Conversions — Total surface cracking length to % area WP fatigue

Length (ft)[1]	Width (ft)[2]	Area (ft²)[3]	WP width (ft)[4]	WP cracking length (%)[5]	Total surface cracking								
					100 feet			200 feet			300 feet		
					Length WP fatigue (ft)[6]	Area (ft²)[7]	Area (%)[8]	Length WP fatigue (ft)[6]	Area (ft²)[7]	Area (%)[8]	Length WP fatigue (ft)[6]	Area (ft²)[7]	Area (%)[8]
500	12	6000	5	50	50[a]	250[b]	4%[c]	100	500	8%	150	750	13%
500	12	6000	5	60	60	300	5%	120	600	10%	180	900	15%
500	12	6000	5	70	70	350	6%	140	700	12%	210	1050	18%
500	12	6000	5	80	80	400	7%	160	800	13%	240	1200	20%
500	12	6000	5	90	90	450	8%	180	900	15%	270	1350	23%
500	12	6000	5	100	100	500	8%	200	1000	17%	300	1500	25%

Note: 1= LTPP section length, 2=Lane width, 3=Total section area, 4=Width of two WP, 5=Assumed WP cracking proportion, 6=Length WP cracking ([a] 0.5*100), 7=Area WP cracking ([b] 50*5), 8= Percentage WP cracking ([c] 250/6000)

Based on the above discussion of results, the effectiveness of crack sealing application timings was incorporated in the Pavement-ME analyses. The crack sealing limits established above were used as guidelines for wet and dry climates to conduct the Pavement-ME analyses. A base MR value of 40,000 psi was assumed as the original material property. Subsequently, to simulate the effect of moisture increase based on the field observations, reduced MR values of 90% and 75% of the original MR value were assumed. The MR values were reduced to characterize the base layer moduli at the time of a particular preservation treatment application. It is also known that preservation treatments cannot restore materials to their original strength. However, they can extend the service life of the pavements by retarding the deterioration rate. Comparisons of the Pavement-ME predicted performances are made by considering the base layer original MR (40,000 psi), 90% of original MR (36,000 psi), and 75% of the original MR (30,000 psi). Figure 4-18 to Figure 4-21 show the predicted long-term pavement performance using the Pavement-ME with the incorporation of multiple crack seal applications. Based on the analysis performed in the previous section the optimum crack sealing limits for fatigue cracking were about 6% and 11% for wet and dry climates, respectively. While developing the preservation plan for wet climates these limits were strictly followed because higher rainfall coupled with higher surface cracking levels can adversely impact the flexible pavements base MR in wet climates.

Figure 4-18 (a) to (d) show an example of a preservation plan for crack seal application timing by using the Pavement-ME for a thick pavement section located in WF. The first crack sealing application was planned as the cracking reached a threshold of 6% in about 8 years of service life [see Figure 4-18(b)]. The treatment application cycle will repeat again, once the pavement reaches the same level of cracking at about 16 years as shown in Figure 4-18(c). The overall effect of crack sealing on cracking progression is shown in Figure 4-18(d). The results show that the pavement life can be significantly extended at a lower level of cracking when crack sealing is applied at the appropriate time (i.e., 6% cracking) for pavement in wet climates.

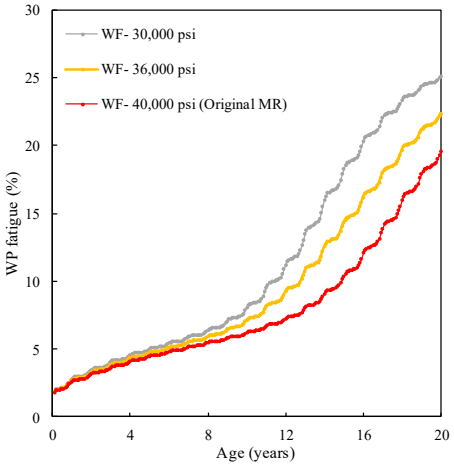

(a) Effect of MR on fatigue cracking (WF)

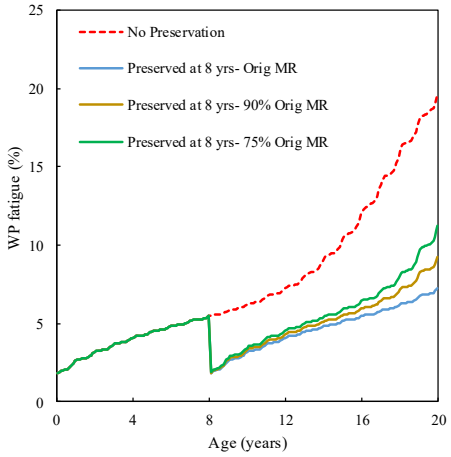

(b) Preservation at 8 years (WF)

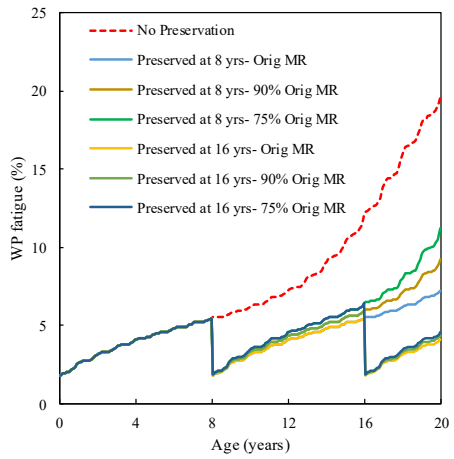

(c) Preservation at 8 and 16 years (WF)

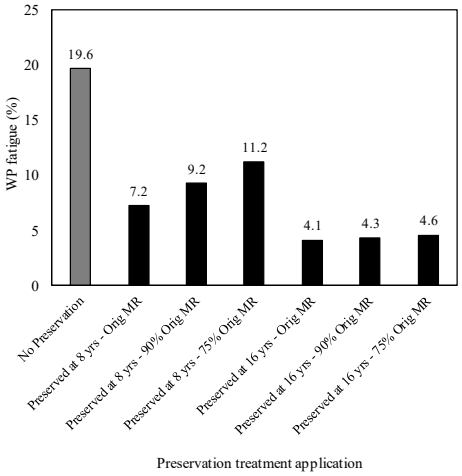

(d) Effect of preservation after 20 years (WF)

Figure 4-18 Preservation treatment plan thick section (WF climate)

Figure 4-19 (a) to (c) show a similar example of a preservation plan for a thick pavement section located in DNF climate. As compared to wet climates, only a single sealing application was planned as the cracking reached a threshold of 11 % in about 11 years of service life [see Figure 4-19(b)]. The WP fatigue threshold in dry climates was between 11 and 12%. This cracking threshold was reached at about 16 years of service life based on the Pavement-ME prediction curve. Theoretically, a sealing application should have been planned at the 16th year of service life. However, it was planned at the end of the 11th year because a pavement can rarely remain in good surface condition after 16 years. The overall effect of crack sealing on cracking progression is shown in Figure 4-19(c). It is evident from the results that proactive maintenance/preservation can considerably enhance pavement service life.

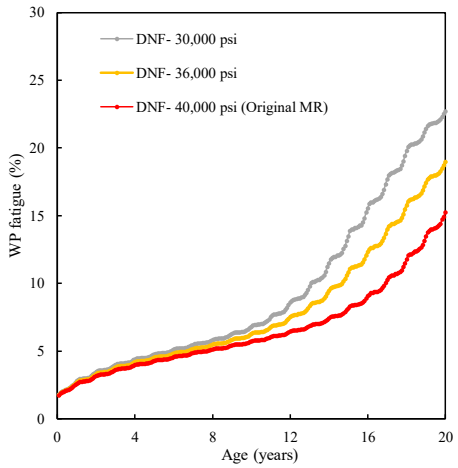

(a) Effect of MR on fatigue cracking (DNF)

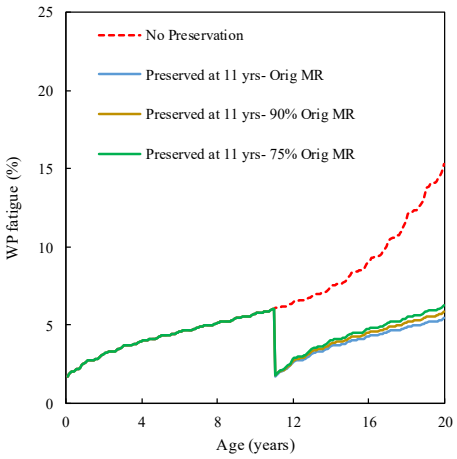

(b) Preservation at 11 years (DNF)

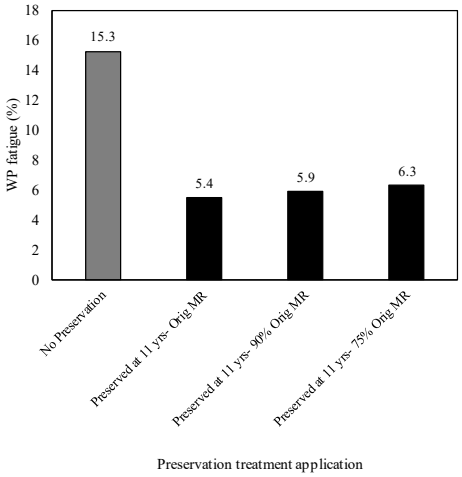

(c) Effect of preservation after 20 years (DNF)

Figure 4-19 Preservation treatment plan thick section (DNF climate)

Figure 4-20 and Figure 4-21 show the suggested preservation plan for thin pavement sections located in WF and DNF climates respectively. For thin pavement sections, more frequent crack sealing applications are needed due to higher levels of fatigue cracking at early ages of pavements service life. In wet climates, the sealing applications were applied every 3 to 4 years to maintain the pavement within the tolerable limit of fatigue cracking [see Figure 4-20 (b) and (c)]. Similarly, sealing applications were planned every 3.5 and 5 years for the thin pavements sections located in DNF climates [see Figure 4-21 (b) and (c)]. The overall effect of crack sealing on cracking progression is shown in Figure 4-20 (d) and Figure 4-21 (d) for thin pavement sections located in WF and DNF climates, respectively.

Pavement-ME is the current state of the art tool for pavement design and analysis, and its farsighted application will enable to plan preservation treatments at the design stage. Preservation plans presented in this study, by using crack seal treatment as an example, can be used as a guideline when moisture variations are only limited to aggregate base material MR. However, to accurately estimate the preservation treatment application timing, stiffness

properties of all pavement layers must be given due importance while predicting the long-term pavement performance. This can be done in future research.

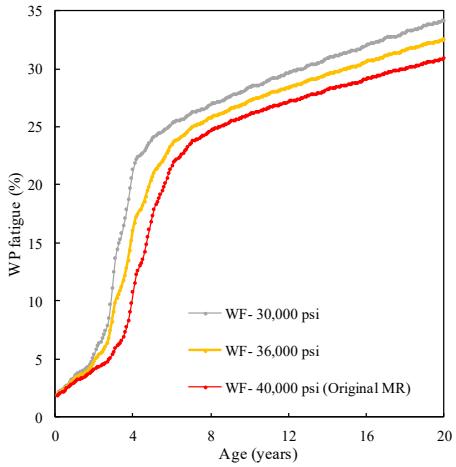

(a) Effect of MR on fatigue cracking (WF)

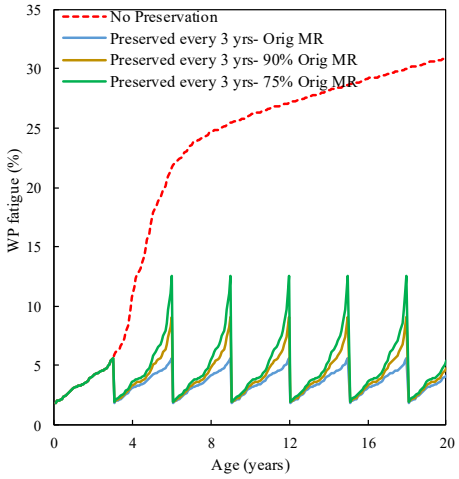

(b) Preservation after every 3 years (WF)

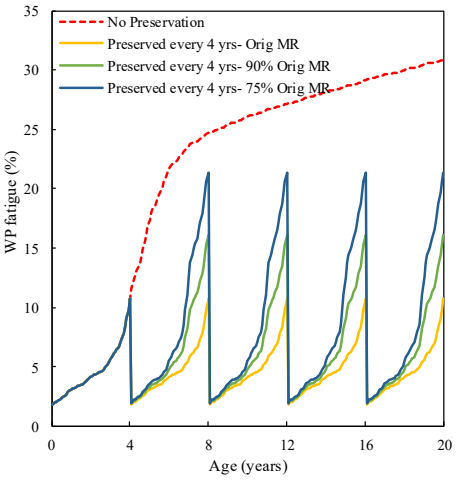

(c) Preservation after every 4 years (WF)

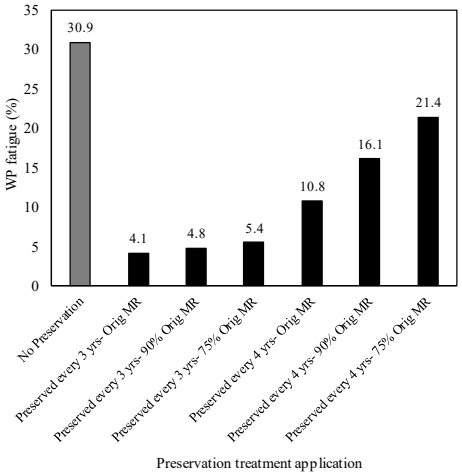

(d) Effect of preservation after 20 years (WF)

Figure 4-20 Preservation treatment plan thin section (WF climate)

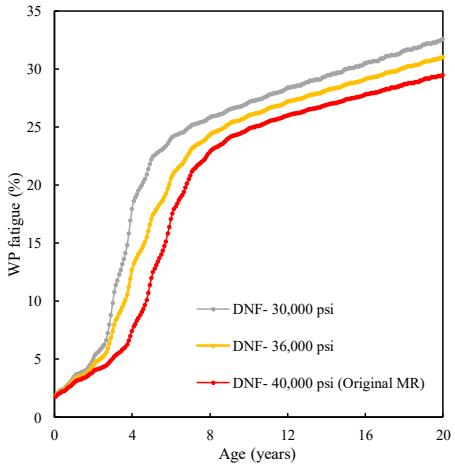

(a) Effect of MR on fatigue cracking (DNF)

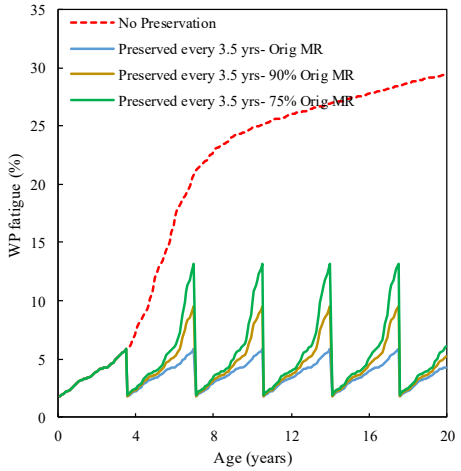

(b) Preservation after every 3.5 years (DNF)

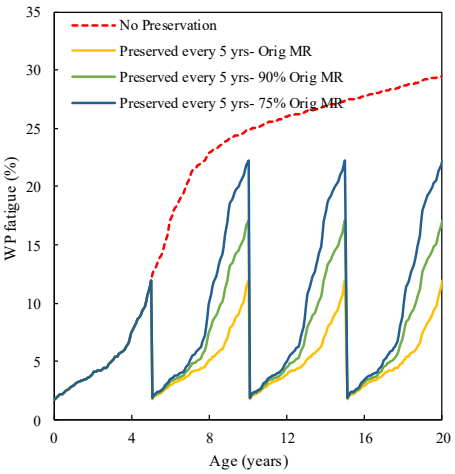

(c) Preservation after every 5 years (DNF)

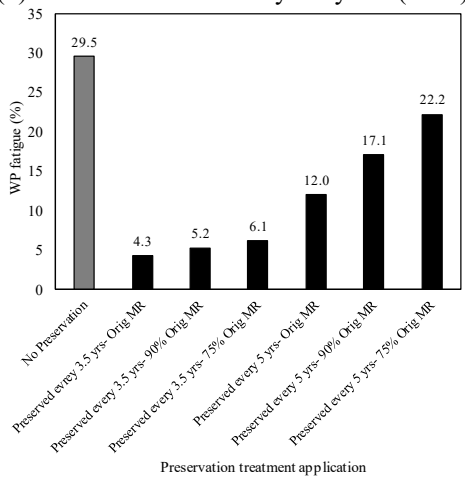

(d) Effect of preservation after 20 years (DNF)

Figure 4-21 Preservation treatment plan thin section (DNF climate)

4.7 RIGID PAVEMENTS MODELING

After quantifying the moisture variations in the flexible pavements base layer and its effect on long-term performance, available rigid pavement sections with granular base layers were also investigated for moisture change. The available number of rigid pavement sections (11 such sections were identified) and data were limited, especially in DF/DNF climate (only two sections). In rigid pavements, same independent variables like flexible pavements were used while developing moisture prediction models, except the total surface cracking, which was replaced with the length of joint seal damage. Initially, total cracking lengths for the rigid SMP sections were ascertained by adding the length of damaged joint sealants and length longitudinal and transverse cracking. It was observed that the lengths of longitudinal and transverse cracking for these sections were very low, as compared to the lengths of damaged joints seals. Base layer moisture content relationship with damaged joints and longitudinal and transverse cracking is shown in Figure 4-22. It can be concluded from these relationships that damage joints are the

primary cause of water infiltration into rigid pavements. Therefore, only lengths of damaged joints were used while developing ANN model for rigid SMP sections.

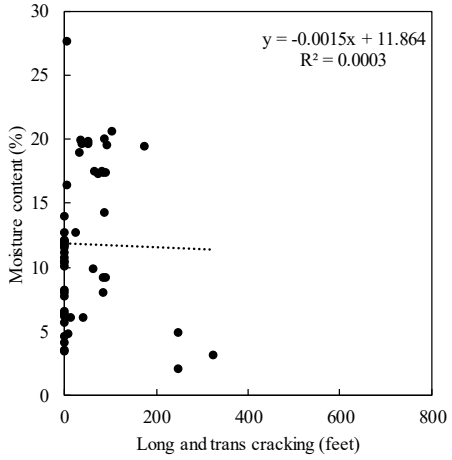

(a) Long/Trans cracking Vs base layer moisture

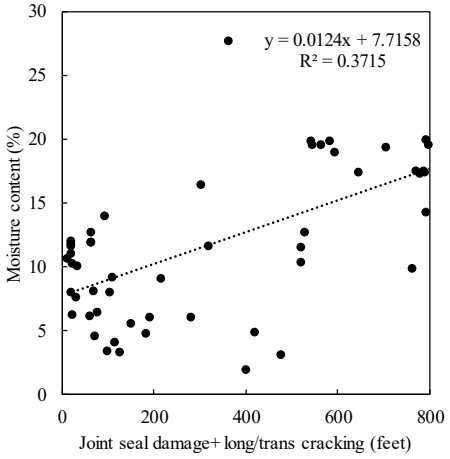

(b) (Joint damage + long/trans cracking) Vs base layer moisture

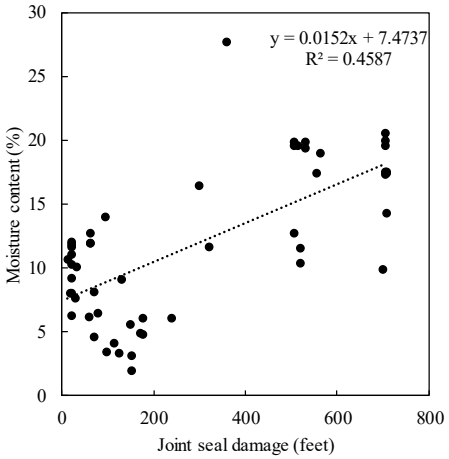

(c) Joint seal damage Vs base layer moisture

Figure 4-22 PCC surface discontinuities relationship with base layer moisture

4.7.1 ANN Modeling Rigid Pavements

Essentially same network settings used earlier for flexible pavements ANN model, were adopted while developing rigid pavements model with minor modifications. In contrast to flexible pavements model, the ANN model developed for the rigid pavements is simple. Also, due to its small size, the data were only used for network training and validation.
Optimum setting for the developed ANN model are given in Table 4-9. Figure 4-23 shows the schematic of ANN model developed for PCC sites.

Table 4-9 Optimum settings for the rigid pavements ANN model

Network type	BPNN
No of hidden layer	1
Data entries for training, testing, and validation	37,0,16
Training function	trainlm
Hidden layer transfer function	tansig
Output layer transfer function	purelin
Performance function	MSE
No of hidden neurons	5

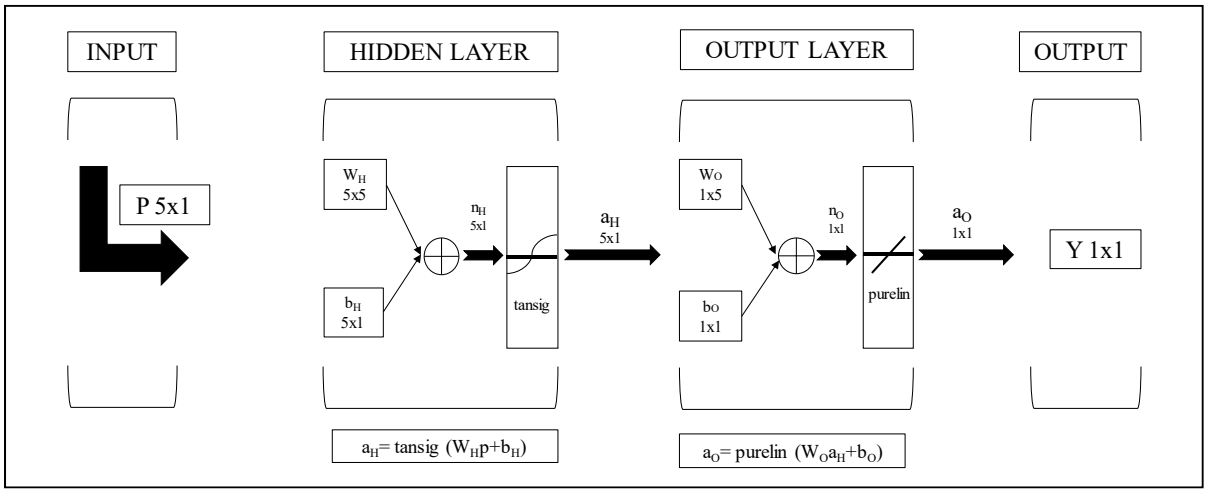

Figure 4-23 ANN model flow rigid pavements SMP sections

Figure 4-24(a) shows the goodness of fit for rigid pavements ANN model. Figure 4-24 (b), (c), and (d) show the ANN model sensitivity to different inputs. The results of the ANN model sensitivity show that with an increase in joint seal damage, there is an increase in the base layer in-situ moisture. Moisture change is significant for higher precipitation levels (wet climate), especially in freezing region [see Figure 4-24(b)]. Higher (%) passing #200, higher is the moisture change, higher the moisture depth within base layer higher is the moisture levels [see Figure 4-24(c) and (d)]. It is worth noting that when the joint seal damage length reached approximately 50m to 75m, moisture increase is substantial. It was observed that rigid pavements ANN model mostly overpredicted the base layer moisture levels. These overpredictions are plausibly caused by, small data size used for the development of ANN model. There could be other potential reasons as well, associated with ANN model settings.

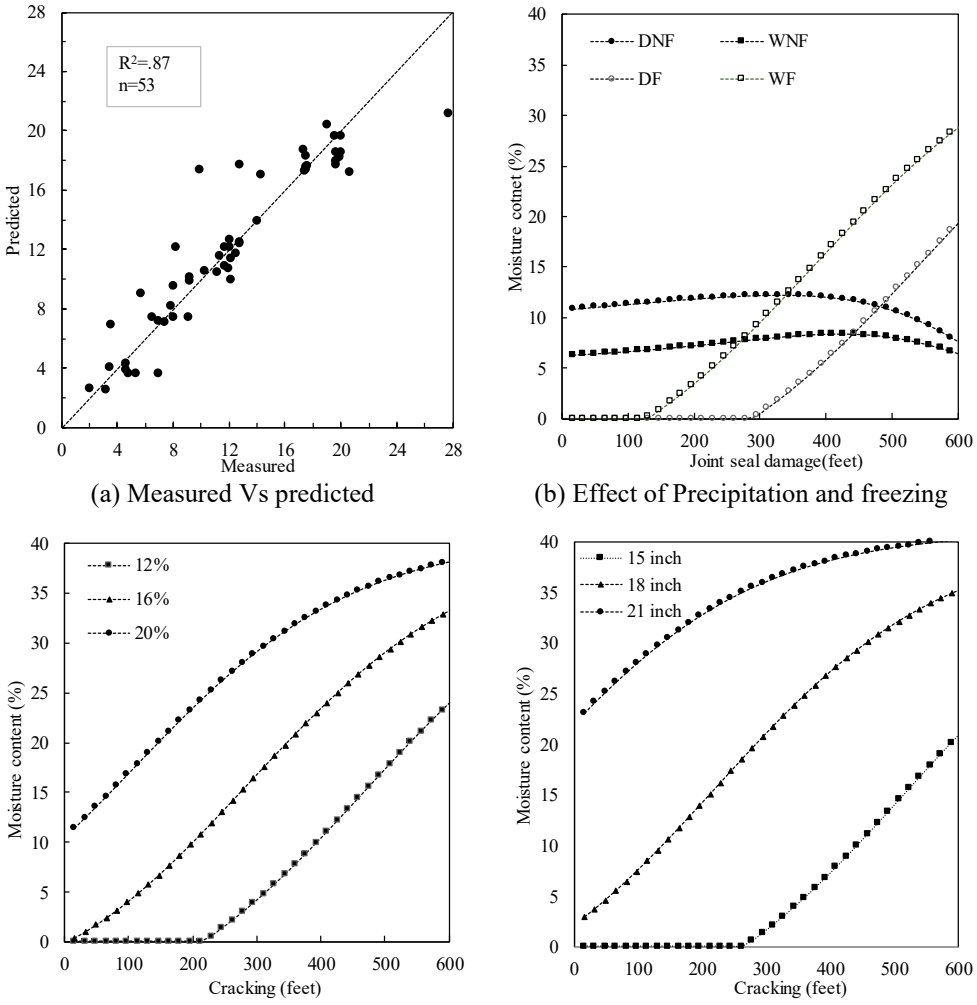

(a) Measured Vs predicted

(b) Effect of Precipitation and freezing

(e) Impact of percent passing 200

(f) Impact of moisture depth

Figure 4-24 ANN model predictions and sensitivity — rigid pavements

4.7.2 The Relationship between Base Moisture and Base Resilient Modulus-PCC Sections

The estimated MR values for base materials with a change in moisture levels based on Witzack model are shown in Figure 4-25. The results show that as the moisture increases, the MR decreases. For the pavement sections located in dry climates, the maximum reduction in base layer MR for a particular section is small, i.e., approximately 10 percent [see Figure 4-25(a)]. The main reasons for the lower change in MR are lower levels of cracking joint seal damage coupled with low precipitation levels in dry climates. For the sections located in wet climates, the maximum reduction in base layer MR for a particular section was approximately 127 percent [see Figure 4-25(b)]. This higher variation in MR can be associated with higher precipitation and cracking/joint seal damage levels in wet climates. Table 4-10 provides the summary of percent

reduction in estimated MR based on all the rigid pavement SMP sections located in different climates.
Due to limited data for rigid pavements, the results may not represent the exact quantifiable moisture variations in these regions.

Table 4-10 Summary — Change in rigid pavements MR due to moisture change

Section ID	Climate region	Minimum MR (psi)	Maximum MR (psi)	Reduction in MR (%)
32_0204	DF	37420	41075	10%
4_0215	DNF	35737	37318	4%
18_3002	WF	28848	41046	42%
27_4040	WF	37101	44208	19%
39_0204	WF	35897	37811	5%
42_1606	WF	15331	32532	112%
83_3802	WF	11487	20595	79%
89_3015	WF	42148	44382	5%
13_3019	WNF	30951	32924	6%
37_0201	WNF	40727	44106	8%
53_3813	WNF	17767	40263	127%

Note: Results based on approximately 8-9 years of measured SMP LTPP data.

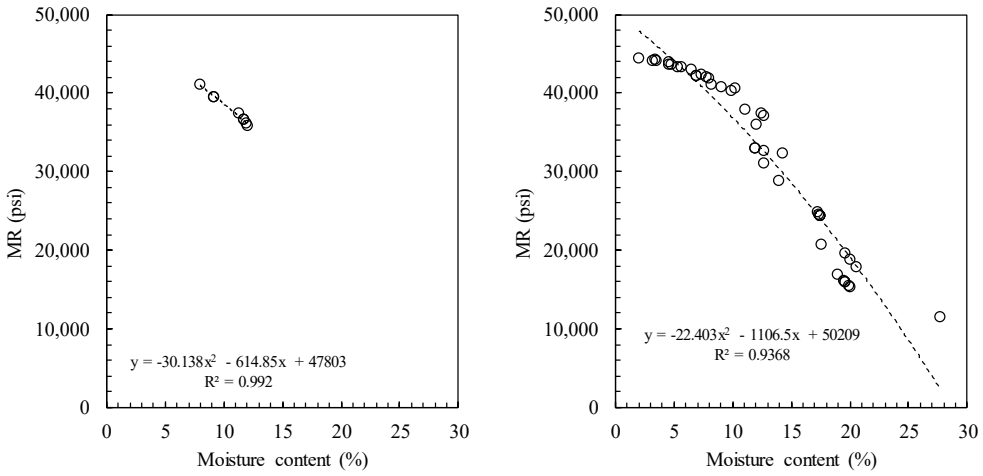

(a) Dry region (b) Wet region

Figure 4-25 Impact of moisture variations on PCC sections base MR

4.7.3 Crack Sealing Application Timings — Rigid Pavements

Based on the rigid pavements sections data analyses results, it can be concluded that PCC joints should be sealed when the length of damaged joints is between 150 to 250 feet. Because within this range the variations in base layer moisture are small and may not significantly affect the stiffness properties of base material [see Figure 4-22 (c) and Figure 4-24 (b)].

4.8 SUMMARY

This section summarizes the data analyses part of rigid and flexible SMP pavements sections, followed by quantification of moisture-related damage and pavement preservation guidelines. The following is a summary of the findings:

- Moisture variation in flexible and rigid pavements base layers significantly impact the pavement performance.
- Higher cracking and greater precipitation levels are the primary reasons for greater moisture change in wet climates.
- GWT can affect seasonal variation in unbound layers moisture content, but the relationship is not very obvious, especially within base layers.
- Subsurface moisture levels significantly vary before and after substantial amount of surface cracking levels.
- As compared to dry climates, moisture variations are very high for the pavement sections located in Wet climates, because of higher precipitation levels and greater cracking extents in these regions.
- Site-specific moisture prediction models highlight the effect of precipitation and cracking on base layer moisture change.
- Factors including surface cracking, precipitation, percentage-passing # 200 sieve, and moisture depth, and freezing index can be used to predict base layer moisture levels with reasonable accuracy.
- The artificial neural network (ANN) models were developed using SMP data for flexible and rigid pavement sections. The results show that higher levels of cracking and joint openings will lead to an increase moisture levels within base layer. Also, the moisture content increases with higher percentage passing # 200 sieve (P_{200}), and higher precipitation levels, especially in wet climates.
- Moisture significantly affected the base layer MR. The observed reduction in MR was up to 41% and 175% for the flexible pavement sections sites located in dry and wet climates, respectively.
- Pavement-ME calculated long-term pavement performance results show that with a reduction in base layer MR, surface cracking, and rutting increased significantly.
- In wet climates, 175% reduction in base MR showed about 114% and 102% increase in cracking, and 6% and 17% increase in surface rutting for thick and thin sections, respectively.
- In dry climates, 41% reduction in base MR showed about 38% and 35% increase in cracking, and 2% and 6% increase in surface rutting for thick and thin sections, respectively.
- Timely and effective preservation can substantially enhance the pavements service life.
- PCC SMP sites data analysis showed that magnitude of transverse and longitudinal cracking is the minimal and primary cause of moisture variation is damaged joint sealant length.
- Moisture variations significantly affected the PCC base layer MR. The observed reduction in MR was up to 10 % and 127% for the PCC sites located in dry and wet climates, respectively,

- Based on the data analysis results it can be concluded that joint seal damage is the main cause of moisture variation in PCC pavements sections.
- Pavement-ME is the current state of the art tool for pavement design and analysis, and its farsighted application will enable us to plan preservation right at the design stage. Preservation plans presented in this research serve as a guideline for the researchers and essentially based on the reduction of base layer moduli only. To accurately estimate the preservation treatment and time, stiffness properties of entire pavement structure must be given due importance while predicting long-term performance.

CHAPTER 5 CONCLUSIONS AND RECOMMENDATIONS

5.1 SUMMARY

Highway agencies have learned that if preservation treatments are applied at an appropriate time, those can help in improving and slowing the deterioration rates for the existing pavements. While pavement preservation is not expected to substantially increase the structural capacity of the existing pavement, it generally leads to improved pavement performance and longer service life. However; still, there are challenges in adoption of such practices. Selection of preservation treatments depends on the pre-existing conditions and other factors contributing to the deterioration of existing roadways. One of the most influential factors affecting pavement performance is the moisture variations within the pavement system, essentially caused by infiltration of rainfall water through surface discontinuities. The SMP study in the LTPP was designed to investigate and quantify the moisture variations, and related damage in flexible and rigid pavements (*75*).

Therefore, the main objectives of this research study were to (a) evaluate the effect of cracking and joint openings on the moisture content in unbound layers, (b) quantify the impact of infiltration and moisture on the stiffness properties of unbound layers, (c) predict long-term pavement performance based on the unbound material properties to evaluate the impacts of preservation treatments, and (d) develop guidelines for optimum crack sealing applications timings for different environmental conditions.

This study presents LTPP data analyses for quantifying the effect of moisture infiltration through surface discontinuities (cracks and joint openings) on flexible and rigid pavement performance. Previous research highlighted that moisture variation within unbound layers is one of the leading factors for premature pavement deterioration (*7, 9, 13, 16*). Therefore, the hypothesis of this study was that moisture variation in unbound layers, i.e., base layer, could be related to the amount of surface discontinuities (cracking and joint seal damage) in different climatic zones. To validate this hypothesis, an important challenge was to identify the data set documenting the subsurface moisture levels in the base layer. Only SMP study used TDRs; those were installed at different depths to record moisture variations within the entire pavement structure. While quantifying the moisture related damage, SMP moisture and performance data from 32 flexible, and 11 rigid pavement sections with granular base layers were used in this study.

The Pavement-ME software provide methodologies for the analysis and design of flexible and rigid pavements. However, these methodologies and related performance prediction models focus on new structural design and rehabilitation of existing pavements and do not explicitly consider the contributions of pavement preservation treatments to the overall pavement performance. Thus, research was needed to identify approaches for considering the effects of preservation on pavement performance and developing procedures that facilitate incorporation of pavement preservation treatments in the Pavement-ME analysis process. The procedures and guidelines documented in this study will help the pavement engineers and agencies to ensure that the contributions of preservation treatments to expected performance and service life are appropriately considered in the analysis and design processes.

5.2 CONCLUSIONS

Based on the results of the analyses performed, the following conclusions were drawn:

1. Moisture variation in flexible and rigid pavements base layers significantly impact the pavement performance.
2. The SMP data can be used to investigate the moisture variations in pavement layers and impact of different climates on moisture variations can be quantified.
3. The rigid and flexible pavements SMP sections data analysis show that there can be significant variations in granular base layer in-situ moisture content.
4. Subsurface moisture levels considerably vary before and after the substantial onset of surface cracking.
5. For wet climates, moisture variations in base layers were very high. Higher cracking and greater precipitation levels are the primary reasons for greater moisture variations for the pavement sections located in wet climates. Relatively, lower cracking and precipitation levels are the primary reasons for small moisture variations for the pavement sections located in wet climates.
6. The artificial neural network (ANN) models were developed using SMP data for flexible and rigid pavement sections. The results show that higher levels of cracking and joint openings will lead to an increase moisture levels within base layer. Also, the moisture content increases with higher percentage passing # 200 sieve (P_{200}), and higher precipitation levels, especially in wet climates.
7. Moisture related damage was very high in WF/WNF climates (153 to 175 percent reduction in MR). It is critical to prevent the unbound layers from moisture related damage due to infiltration, especially before the MR reduction becomes significantly high.
8. Subsurface moisture variations showed relatively less impact on the sites located in DF/DNF climates (18 to 41 percent reduction in MR). For the pavement sites in DF/DNF climates, damage associated with other factors like high temperature is more critical.
9. Pavement-ME predicted long-term pavement performance results show that with a reduction in base layer MR, surface cracking and rutting levels were increased significantly.
10. In wet climates, a 175% reduction in base MR (i.e., maximum MR reduction in wet climates) showed about 114% and 102% increase in cracking, and 6% and 17 % increase in total rutting, for thick and thin flexible pavements sections, respectively.
11. In dry climates, a 41% reduction in base MR (i.e., maximum MR reduction in wet climates) caused 38% and 35% increase in cracking, and 2% and 6% increase in total rutting, for thick and thin flexible pavements sections, respectively.
12. Rigid SMP sections data analysis show that moisture significantly affected the PCC base layer MR. The observed reduction in MR was up to 10 % and 127% for the PCC sites located in dry and wet climates, respectively.
13. Based on the data analysis it was concluded that damaged joint sealant length is the main cause of moisture variation in PCC pavement sections base layers. Therefore, damage joints should be sealed when the extents are between 150 to 250 feet.

5.3 RECOMMENDATIONS

The following are the recommendations based on the findings of this study:

1. Moisture variation severely affects the flexible pavements performance in wet climates. Therefore, in wet climates, it is essential to apply preservation treatment when the fatigue cracking extent is below 6 to 7 percent.
2. For flexible pavements in dry climates, this extent can be tolerated to slightly higher levels of surface cracking, i.e., may be up to 10 to 11 percent.
3. To prevent moisture related damage in rigid pavements, the joints should be resealed when the damaged joint sealant length exceeds 150 to 250 feet. The current Pavement-ME performance models for rigid pavements do not predict damaged joint sealant length. It is recommended for future that damaged joint sealant length may accounted for by indirectly relating it to some other performance measures like joint faulting or IRI.
4. The crack sealing guidelines and moisture predictions models presented in this study can be further improved by including more data to improve pavement preservation practices and, the accuracy of the models.
5. Pavement-ME is the current state of the art tool for pavement design and analysis, and its farsighted application will enable us to plan preservation right at the design stage. Preservation plans presented in this research serve as a guideline for the researchers and essentially based on the reduction of base layer moduli only. To accurately estimate the preservation treatment and time, stiffness properties of entire pavement structure must be given due importance while predicting long-term performance.

REFERENCES

1. Munnell, A. H., "Policy watch: infrastructure investment and economic growth," *The Journal of Economic Perspectives*, vol. 6, pp. 189-198, 1992.
2. Geiger, D. R., "Pavement preservation definitions," *FHWA Memorandum*, 2005.
3. Davies, R. M. and J. Sorenson, "Pavement preservation: Preserving our investment in highways," *Public Roads*, vol. 63, 2000.
4. Galehouse, L., J. S. Moulthrop, and R. G. Hicks, "Principles of pavement preservation: definitions, benefits, issues, and barriers," *TR News*, 2003.
5. Dan, H.-C., J.-W. Tan, Z. Zhang, and L.-H. He, "Modelling and Estimation of Water Infilteration into Cracked Asphalt Pavement," *Road Materials and Pavement Design*, vol. 18, pp. 590-611, 2017.
6. Espinoza-Melendrez, J., S. Tamari, and A. Aguilar-Chavez, "Simulation of Water Infiltration Below a Damage in the Pavement Surface Course," *Ingenieria Hidraulica en Mexico*, vol. 20, pp. 77-95, 2005.
7. Salour, F., "Moisture Influence on Structural Behaviour of Pavements: Field and Laboratory Investigations," KTH Royal Institute of Technology, 2015.
8. Mallela, J., G. Larson, T. Wyatt, J. Hall, and W. Barker, "User's Guide for Drainage Requirements in Pavements–DRIP 2.0 Microcomputer Program," 2002.
9. Witczak, M., D. Andrei, and W. Houston, "Resilient modulus as function of soil moisture–Summary of predictive models," Appendix DD-1, 2000.
10. Petry, T. M., Y.-P. Han, and D. N. Richardson, "Systems Approach for Estimating Field Moisture Content," presented at Transportation Research Board 85th Annual Meeting, 2006, pp.
11. Officials, T., *AASHTO Guide for Design of Pavement Structures, 1993*, vol. 1: AASHTO, 1993.
12. Cedergren, H. R., "America's pavements: world's longest bathtubs," *Civil Engineering*, vol. 64, pp. 56, 1994.
13. "NCHRP 1-37A Guide for Mechanistic Empirical Design Part-3,Design Analysis ", pp. 32, 2004.
14. Hall, K. and S. Rao, "Predicting subgrade moisture content for low-volume pavement design using in situ moisture content data," *Transportation Research Record: Journal of the Transportation Research Board*, pp. 98-106, 1999.
15. Rao, S., "Analysis of In-situ Moisture Content Data for Arkansas Subgrades," 1997.
16. Hedayati, M. and S. Hossain, "Data based model to estimate subgrade moisture variation case study: Low volume pavement in North Texas," *Transportation Geotechnics*, vol. 3, pp. 48-57, 2015.
17. Fredlund, D. G., H. Rahardjo, and M. D. Fredlund, *Unsaturated soil mechanics in engineering practice*: John Wiley & Sons, 2012.
18. Gu, F., X. Luo, Y. Zhang, R. Lytton, and H. Sahin, "Modelling of Unsaturated Granular Matrerials in Flexible Pavements," *E-UNSAT 2016*, 2016.
19. Lekarp, F., U. Isacsson, and A. Dawson, "State of the art. I: Resilient response of unbound aggregates," *Journal of transportation engineering*, vol. 126, pp. 66-75, 2000.
20. Salour, F. and S. Erlingsson, "Investigation of a pavement structural behaviour during spring thaw using falling weight deflectometer," *Road Materials and Pavement Design*, vol. 14, pp. 141-158, 2013.

21. Nguyen, Q., D. G. Fredlund, L. Samarasekera, and B. L. Marjerison, "Seasonal pattern of matric suctions in highway subgrades," *Canadian Geotechnical Journal*, vol. 47, pp. 267-280, 2010.
22. Hedayati, M., M. S. Hossain, A. Mehdibeigi, and B. Thian, "Real-time modeling of moisture distribution in subgrade soils," presented at Geo-Congress 2014: Geo-characterization and Modeling for Sustainability, 2014, pp. 3015-3024.
23. Broun, R. and G. F. Menzies, "Life cycle energy and environmental analysis of partition wall systems in the UK," *Procedia Engineering*, vol. 21, pp. 864-873, 2011.
24. Lytton, R., D. Pufahl, C. Michalak, H. Liang, and B. Dempsey, "An integrated model of the climatic effects on pavements," 1993.
25. OECD, "Water in Roads,"Prediction of Moisture Content in Road Subgrades," Orgnization of Economic Corporation and Developpment,Paris,France," 1973.
26. Swanberg, J. and C. Hansen, "Development of a Procedure for the Design of Flexible Bases," presented at Highway Research Board PROCEEDINGS, 1947, pp.
27. Navy, U., "Airfield Pavements, Bureau o Yards and Docks, Technical Publication," NAVDOCKS TP-PW-4 1953.
28. Kersten, M. S., L. Palmer, and W. Campen, "Progress Report of Special Project on Structural Design of Nongrid Pavements: Subgrade Moisture Conditions Beneath Airport Pavements," presented at Highway Research Board Proceedings, 1946, pp.
29. Petry, T. M., Y.-P. Han, and D. N. Richardson, "A systems Approach for Estimating Field Moisture Content," *TRB 2006*, pp. 20, 2006.
30. Jiang, Y. J. and S. D. Tayabji, "Analysis of time domain reflectometry data from LTPP seasonal monitoring program test sections," 1999.
31. Kodikara, J., P. Rajeev, D. Chan, and C. Gallage, "Soil moisture monitoring at the field scale using neutron probe," *Canadian Geotechnical Journal*, vol. 51, pp. 332-345, 2013.
32. Fredlund, D. G. and A. Xing, "Equations for the soil-water characteristic curve," *Canadian Geotechnical Journal*, vol. 31, pp. 521-532, 1994.
33. Ridgeway, H. H., "Infiltration of Water through the Pavement Surface (Abridgement)," *Transportation Research Record*, 1976.
34. Hansson, K., L.-C. Lundin, and J. Šimůnek, "Part 3: Pavement: Subsurface Drainage and Reliability in Design and Performance: Modeling Water Flow Patterns in Flexible Pavements," *Transportation Research Record: Journal of the Transportation Research Board*, vol. 1936, pp. 131-141, 2005.
35. Van Genuchten, M. t., "A Closed Form Equation for Predicting the Hydraulic Conductivity of Unsaturated Soils," *Soil Science Society of America Journal*, vol. 44, pp. 892-898, 1980.
36. Mualem, Y. A., "A New Model for Predicting the Hydraulic Conductivity of Unsaturated Porous Media," *Water Resources Research*, vol. 12, pp. 513-522, 1976.
37. Freeze, R. A. and J. A. Cherry, "Groundwater," *Prentice Hall,Englewood Cliffs,N.J*, 1979.
38. Gu, F., H. Sahin, X. Luo, R. Luo, and R. L. Lytton, "Estimation of resilient modulus of unbound aggregates using performance-related base course properties," *Journal of Materials in Civil Engineering*, vol. 27, pp. 04014188, 2014.
39. Lytton, R., "Foundations and pavements on unsaturated soils," presented at Proceedings of the First International Conference on Unsaturated Soils/UNSAT'95/Paris/France/6-8 September 1995. Volume 3, 1996., 1996, pp.

40. "Guide for Mechanistic-Emperical Design of New and Rehablitated Pavement Structures,Appendix DD-1; Resiliant Modulus as Function of Soil Moisture- Summary of Predictive Models," 2000.
41. Elkins, G. E., P. Schmalzer, T. Thompson, and A. Simpson, "Long-term pavement performance information management system pavement performance database user reference guide," 2003.
42. Haider, S. W. and M. M. Masud, "Effect of moisture infiltration on flexible pavement performance using the AASHTOWare Pavement-ME," in *Advances in Materials and Pavement Performance Prediction*: CRC Press, 2018, pp. 31-35.
43. Haider, S. W. and M. M. Masud, "Accuracy Comparisons Between ASTM 1318-09 and COST-323 (European) WIM Standards Using LTPP WIM Data," presented at Proceedings of the 9th International Conference on Maintenance and Rehabilitation of Pavements—Mairepav9, 2020, pp. 155-165.
44. Haider, S. W. and M. M. Masud, "Use of LTPP SMP Data to Quantify Moisture Impacts on Fatigue Cracking in Flexible Pavements [summary report]," United States. Federal Highway Administration. Office of Research … 2020.
45. Haider, S. W., M. M. Masud, and K. Chatti, "Influence of moisture infiltration on flexible pavement cracking and optimum timing for surface seals," *Canadian Journal of Civil Engineering*, vol. 47, pp. 487-497, 2020.
46. Haider, S. W., M. M. Masud, and G. Musunuru, "Effect of Water Infiltration Through Surface Cracks on Flexible Pavement Performance," 2018.
47. Haider, S. W., M. M. Masud, O. Selezneva, and D. J. Wolf, "Assessment of Factors Affecting Measurement Accuracy for High-Quality Weigh-in-Motion Sites in the Long-Term Pavement Performance Database," *Transportation Research Record*, vol. 2674, pp. 269-284, 2020.
48. Masud, M. M., "IRF GLOBAL R2T Conference," 2019.
49. Masud, M. M., *Quantification of Moisture Related Damage in Flexible and Rigid Pavements and Incorporation of Pavement Preservation Treatments in AASHTOWare Pavement-ME Design and Analysis*: Michigan State University, 2018.
50. Masud, M. M. and S. W. Haider, "Long-Term Pavement Performance: International Data Analysis Contest, 2017–2018 Graduate Category: Use of LTPP SMP Data to Quantify Moisture Impacts on Fatigue Cracking in Flexible Pavements," 2020.
51. Masud, M. M. and S. W. Haider, "Estimation of Weigh-in-Motion System Accuracy from Axle Load Spectra Data," in *Airfield and Highway Pavements 2021*, 2021, pp. 378-388.
52. Masud, M. M., S. W. Haider, O. Selezneva, and D. J. Wolf, "Impact of WIM systematic bias on axle load spectra–A case study," in *Advances in Materials and Pavement Performance Prediction II*: CRC Press, 2020, pp. 64-67.
53. Han, Y.-P., T. Petry, and D. Richardson, "Part 2: evaluation of subgrade resilient modulus: resilient modulus estimation system for fine-grained soils," *Transportation Research Record: Journal of the Transportation Research Board*, pp. 69-77, 2006.
54. Dubčáková, R., "Eureqa: software review," *Genetic programming and evolvable machines*, vol. 12, pp. 173-178, 2011.
55. Hecht-Nielsen, R., "Theory of the backpropagation neural network," in *Neural networks for perception*: Elsevier, 1992, pp. 65-93.

56. Basheer, I. A. and M. Hajmeer, "Artificial neural networks: fundamentals, computing, design, and application," *Journal of microbiological methods*, vol. 43, pp. 3-31, 2000.
57. Ismail, H. M., H. K. Ng, C. W. Queck, and S. Gan, "Artificial neural networks modelling of engine-out responses for a light-duty diesel engine fuelled with biodiesel blends," *Applied Energy*, vol. 92, pp. 769-777, 2012.
58. Karadurmus, E., M. Cesmeci, M. Yuceer, and R. Berber, "An artificial neural network model for the effects of chicken manure on ground water," *Applied Soft Computing*, vol. 12, pp. 494-497, 2012.
59. Alba, R. D. and R. M. Golden, "Patterns of ethnic marriage in the United States," *Social forces*, vol. 65, pp. 202-223, 1986.
60. Haykin, S. and N. Network, "A comprehensive foundation," *Neural networks*, vol. 2, pp. 41, 2004.
61. Seitllari, A. and M. E. Kutay, "Use of Soft Computing Tools to Predict Progression of Percent Embedment of Aggregates in Chip Seals," 2018.
62. Hornik, K., M. Stinchcombe, and H. White, "Multilayer feedforward networks are universal approximators," *Neural networks*, vol. 2, pp. 359-366, 1989.
63. Guide, M. U., "ANN 7.11. 0.584," *R2010b). MathWorks*.
64. Guide, M. U. s., "Neural network toolbox," *The MathWorks*, 2002.
65. Grossberg, S., "Nonlinear neural networks: Principles, mechanisms, and architectures," *Neural networks*, vol. 1, pp. 17-61, 1988.
66. Sathya, R. and A. Abraham, "Comparison of supervised and unsupervised learning algorithms for pattern classification," *International Journal of Advanced Research in Artificial Intelligence*, vol. 2, pp. 34-38, 2013.
67. Wedderburn, R. W., "Quasi-likelihood functions, generalized linear models, and the Gauss—Newton method," *Biometrika*, vol. 61, pp. 439-447, 1974.
68. Hiriart-Urruty, J.-B., J.-J. Strodiot, and V. H. Nguyen, "Generalized Hessian matrix and second-order optimality conditions for problems withC 1, 1 data," *Applied mathematics and optimization*, vol. 11, pp. 43-56, 1984.
69. Kişi, Ö. and E. Uncuoğlu, "Comparison of three back-propagation training algorithms for two case studies," 2005.
70. Moré, J. J., "The Levenberg-Marquardt algorithm: implementation and theory," in *Numerical analysis*: Springer, 1978, pp. 105-116.
71. Hagan, M. T. and M. B. Menhaj, "Training feedforward networks with the Marquardt algorithm," *IEEE transactions on Neural Networks*, vol. 5, pp. 989-993, 1994.
72. Bouabaz, M. and M. Hamami, "A cost estimation model for repair bridges based on artificial neural network," *American Journal of Applied Sciences*, vol. 5, pp. 334-339, 2008.
73. Version, M., "7.2. 0.232 (R2006a). The MathWorks," *Inc. www. mathworks. com*, 2006.
74. Vogl, T. P., J. Mangis, A. Rigler, W. Zink, and D. Alkon, "Accelerating the convergence of the back-propagation method," *Biological cybernetics*, vol. 59, pp. 257-263, 1988.
75. Rada, G. R., G. Elkins, B. Henderson, R. Van Sambeek, and A. Lopez, "LTPP seasonal monitoring program: instrumentation installation and data collection guidelines," 1995.